STUDY OF THE SUBSTRATE-RELATED FACTORS AFFECTING SUSTAINABLE PRODUCTION AND UTILIZATION OF HIGH RECALCITRANT FOOD-WASTE AROMATICS IN REDUCTIVE CATALYTIC FRACTIONATION PROCESS

RABIA JALIL KHAN

PhD

The Hong Kong Polytechnic University

2024

The Hong Kong Polytechnic University
Department of Civil and Environmental Engineering

Study of the Substrate-related Factors Affecting Sustainable Production and Utilization of High Recalcitrant Food-Waste Aromatics in Reductive Catalytic Fractionation Process

Rabia Jalil Khan

A thesis submitted in partial fulfillment of the requirements for the degree of Doctor of Philosophy

April 2024

CERTIFICATE OF ORIGINALITY

I hereby declare that this thesis is my own work and that, to the best ofmy knowledge and belief, it reproduces no material previously published or written, nor material that has been accepted for the award of any other degree or diploma, except where due acknowledgment has been made in the text.

Signature: _________________

Name of Student: Rabia Jalil Khan

Abstract

Aromatic compounds are essential fuels and key chemical precursors for organic chemical synthesis; however, their production predominantly relies on fossil resources, leading to carbon emissions. Lignin, a complex polymer abundant in biomass, has gained recognition as a promising alternative to conventional aromatics. To advance research, development, and economic viability of the lignin valorization process, this thesis focuses on in-depth investigations of substrate-related factors and explores sustainable methodologies for the production and utilization of highly recalcitrant food waste, with the specific objective of enhancing monomer production. Particular emphasis is on unexplored lignin structures and their potential functions, highlighting the breakthroughs in lignin-first pretreatment, catalytic lignin depolymerization, and the production of high-value products benchmarked against modern aromatics. Given that, the reductive catalytic fractionation (Anderson, #118) process is highlighted as a favorable strategy and has been adopted to generate lignin oil and transform the lignin-rich biomass into high-value products.

In the realm of biomass resources, the inedible components of nuts and stone fruits emerge as an economically viable and lignin-rich feedstock for the sustainable production of aromatic chemicals, surpassing the potential of agricultural and forestry residues. However, the depolymerization performances on food-related biomass remain unclear, owing to the broad physicochemical variations from the edible parts of the fruits and plant species. The monomer production potentials of ten major fruit and nutshell biomass were investigated with comprehensive numerical information derived from instrumental analysis, such as plant cell wall chemical compositions, syringyl/guaiacyl (S/G ratios, and contents of lignin substructure linkages (β−O−4, β−β, β−5). A standardized one-pot

RCF process was applied to benchmark the monomer yields, and the results were statistically analyzed. Among all the tested biomass, mango endocarp provided the highest monolignol yields of 37.1% per dry substrate. Positive S-lignin (70-84%) resulted in higher monomer yield mainly due to more cleavable β–O–4 linkages and less condensed C–C linkages. Strong positive relationships were identified between β–O–4 and S-lignin and between β–5 and G-lignin. The analytical, numerical, and experimental results shed light on the process design of lignin-first biorefinery in food-processing industries and waste management works.

Next, we investigated the influence of process design and control on biomass pre-treatment and RCF in relation to the quality and yield of lignin. We compared different pre-treatment methods (organosolv, biphasic, and staged organosolv) with the one-pot RCF process to enhance lignin accessibility and reactivity. The results revealed that direct RCF yielded more lignin monomers, while biphasic and staged pre-treatments preserved crucial β–O–4 linkages, enhancing lignin reactivity. The insights gained from this work are of critical importance for optimizing the process parameters in a lignin-first biorefinery. Consequently, these findings establish a connection between the earlier chapters and the subsequent discussions on techno-economic evaluation.

Furthermore, the potential retrofitting of conventional petroleum refineries for lignin-based products is discussed as a means to progressively transition the industry towards carbon neutrality. The application of obtained lignin is also explored, particularly in the field of wastewater treatment. Woody waste-derived organosolv lignin nanoparticles (LNPs) with uniform colloidal spherical morphology and optimized particle size are synthesized via a simple and facile anti-solvent nanoprecipitation technique. These LNPs are then used to fabricate ultrafiltration nanocomposite membranes with enhanced properties. The lignin-enabled membranes exhibit high permeation flux and excellent removal efficiencies for cationic and anionic dyes, making them suitable for real-world wastewater treatment applications.

To guide research efforts towards commercialization, the thesis concludes with a techno-economic evaluation of lignin-first biorefineries utilizing RCF. The economic feasibility and sustainability of the concepts discussed throughout the study are assessed, providing a comprehensive view of the lignin-first biorefinery concept. This evaluation facilitates the transition towards a more sustainable and value-driven biorefinery industry. Overall, this thesis contributes to the development and utilization of lignin as a renewable resource, promoting a more environmentally friendly and economically viable approach to aromatic compound production.

PUBLICATIONS ARISING FROM THE THESIS

Published journal articles

1. **Khan, R.J.,** Lau, C.Y., Farid, M.U., Islam, M.K., An, A.K., Yi, J. and Leu, S.-Y., 2024. Woody biomass derived nano lignin-enabled membrane with high structural stability for efficient wastewater treatment. *Process Safety and Environmental Protection*, 182, pp.595.

2. **Khan, R.J.,** Guan, J., Lau, C.Y., Zhuang, H., Rehman, S. and Leu, S.-Y., 2023. Monolignol Potential and Insights into Direct Depolymerization of Fruit and Nutshell Remains for High Value Sustainable Aromatics. *ChemSusChem*, p.e202301306.

3. **Khan, R.J.,** Lau, C.Y., Guan, J., Lam, C.H., Zhao, J., Ji, Y., Wang, H., Xu, J., Lee, D.J. and Leu, S.-Y., 2022. Recent advances of lignin valorization techniques toward sustainable aromatics and potential benchmarks to fossil refinery products. *Bioresource Technology*, 346, p.126419.

4. Rehman, S., Yang, Y.S., Patria, R.D., Zulfiqar, T., Khanzada, N.K., **Khan, R.J.,** Lin, C.S.K., Lee, D.J. and Leu, S.-Y., 2023. Substrate-related factors and kinetic studies of Carbohydrate-Rich food wastes on enzymatic saccharification. *Bioresource Technology*, 390, p.129858.

5. Farid, M.U., Kharraz, J.A., Sharma, S., **Khan, R.J.,** Khanzada, N.K., Deka, B.J., Nallapaneni, M.K., Chopra, S.S., Leu, S.-Y., Hasan, S.W. and Hilal, N., 2023. Technological advancements in water heating approaches for membrane distillation desalination process: From bulk to localized heating. *Desalination*, p.117235.

Manuscript to be submitted upon this dissertation

6. **Khan, R.J.,** Khan A. and Leu S.-Y., 2023. Waste Management in Climate Change and Sustainability Perspectives: Lignocellulosic waste. Taylor and Francis group.

Conference papers

7. **Khan, R.J.,** Lau, C.Y. and Leu, S.-Y. (2023). Waste Wood-derived Lignin Nano-enabled Membrane for High-efficiency Wastewater Treatment. SDEWES2023, September 2023.

8. **Khan, R.J.,** Guan, J. and Leu, S.-Y. (2023). One-Pot Fractionation of Endocarp Waste for Sustainable High Value-added Products. Proceedings of the International Conference on Solid Waste 2023: Waste Management in Circular Economy and Climate Resilience (ICSWHK2023), Hong Kong, 31 May – 3 June 2023.

9. **Khan, R.J.,** Lau, C.Y., Guan, J. and Leu, S.-Y. (2022). Future of lignin based aromatics: Sustainability assessment and downstream processing of lignin feedstock into value-added products. ICAE 2022 Energy Proceedings, August 2022.

10. Islam, M. K., Rehman, S., **Khan, R. J.,** Yeung, C.S. and Leu, S.-Y. (2020). Pentanol-water biphasic pretreatment facilitates energy-efficient fractionation of lignocellulose. ICAE 2020, Dec.

Acknowledgments

All praises and glory to the Almighty for giving me the opportunity, strength, determination, and patience to complete my Ph.D. degree.

This significant milestone would not have been achieved without the unwavering support and assistance of numerous individuals throughout this period. I would like to seize this moment to express my deepest gratitude and appreciation to each and every one of them. Foremost, I am profoundly grateful to my Ph.D. supervisor, **Prof. Shao-Yuan (Ben) Leu**, for allowing me to work within his esteemed research group. Dr. Leu's continuous guidance, encouragement, and unwavering support have been instrumental in enabling me to complete my degree in a comprehensive manner. I am truly indebted to his invaluable suggestions and contributions. I would also like to sincerely thank my lab mates, for their generous assistance and support throughout this journey.

A special mention of appreciation is due to my family, whose boundless love, understanding, comfort, and support have been my rock during this demanding study period. This thesis is dedicated to them as a testament to their steadfast belief in me and their constant encouragement. Furthermore, I would like to express my sincere gratitude to the Department of Civil and Environmental Engineering for providing me with the opportunity to be a part of their community. Last but not least, I am grateful to the Research Grants Council (RGC) of Hong Kong for their generous funding, which has enabled me to pursue my studies and contribute to the field of research.

Rabia Jalil Khan
May 2024

Table of Contents

List of Figures

List of Tables

List of Abbreviation

3D	Three-dimensional
BDO	1,4-butanediol
CFs	Carbon fibers
CUB	Catalytic upstream biorefining
DA	Dilute acid
DMF	2,5-dimethylfuran
ECN	Effective carbon number
EDX	Energy-dispersive X-ray spectroscopy
FT	Flow-through systems
FTIR	Fourier transform infrared spectroscopy
GHG	Greenhouse gas
GPC	Gel-permeation chromatography
GVL	γ-valerolactone
HDO	Hydrodeoxygenation
HMF	Hydroxymethylfurfural
LA	Levulinic acid
LACs	Lignin activated carbons
LCA	Lifecycle assessment
LCFs	Lignin-based carbon fiber
LNPs	Lignin nanoparticles
MB	Methylene blue
MESP	Minimum ethanol selling price
MO	Methylene orange
MSP	Minimum selling price
NMP	1-methyl-2-pyrrolidone
PDI	Polydispersity index
PES	Polyethersulfone
pNMR	Pulsed nuclear magnetic resonance
POM-IL	Polyoxometalate ionic liquid

PSD	Pore size distribution
PTFE	Poly(tetrafluoroethylene)
PVP	Polyvinylpyrrolidone
RCF	Reductive catalytic fractionation
ROS	Reactive oxygen species
SAF	Sustainable aviation fuel
SEM	Scanning electron microscope
TE	Tracheary element
TEA	Techno-economic analysis
TEM	Transmission electron microscope
THF	Tetrahydrofuran
TMS	Triethylammonium methanesulfonate
TOC	Total organic carbon.
UF	Ultrafiltration
UV	Ultraviolet
WCA	Water contact angle
ZP	Zeta Potential

Chapter 1. Introduction

1.1 Background

The global demand for aromatic compounds is continuously rising, and the substantial utilization of such fossil-based aromatics has led to an utter shortage of energy and significant environmental degradation. As a result, there is a growing global emphasis on the utilization of abundant and renewable energy sources to produce value-added products as alternatives to fossil-based consumption (Balat & Ayar, 2005). Researchers are focusing on overcoming the deficiency of petrochemical sources by creating cost-effective, environment-friendly, and energy-efficient techniques for converting the renewable resources into high-value aromatics and fuels (Yang et al., 2023). The aim is to overcome the dependence on fossil resources and provide sustainable alternatives that meet the increasing global demand for aromatic compounds.

Biorefineries have been foreshadowed as a possible substitution of oil refineries as well as for valorization of the entire biomass into fuel, energy, and high value-added products. Like crude oil, biomass also can be refined into a wide spectrum of products, but its feasibility has long been challenged due to direct competition with crude oil economy, while the technologies have not yet considered "green" especially when completely utilization of whole biomass cannot be achieved. Efforts are therefore now being put to generate green aromatics from the renewable and abundantly available biomass feedstock to restrict use of depleting fossil fuels. As a consequence, the vision of biomass as a surrogate for petroleum is now a central tenet of national biomass valorization strategies all over the world.

One of the most promising resource, the lignocellulosic biomass has pulled in wide interest for its essential qualities, such as sustainability, renewability, cost-effectiveness, and plenitude in the occurrence (Pang, 2019). Lignocellulosic biomass refers to the copious plant-based matter that is composed of three major components. These include cellulose (40-60% by wt.), hemicellulose (10-40% by wt.), and lignin (15-30% by wt.) (Schutyser et al., 2018). The intricate arrangement of these basic components found within the cell wall of plant makes the extraction and conversion of lignocellulosic biomass into valued products a complex process. Most of the lignocellulose type biomass valorization techniques focus on one component and in return making it quite intriguing to ensure the quality of the remaining components (Zhang et al., 2017). However, productively employing all the lignocellulosic parts still remains a challenge due to lignin's recalcitrance and its complex molecular structure (Chundawat et al., 2020). The recalcitrance is dealt with using pretreatment techniques to eliminate the lignin and expose the underlying cellulose and hemicellulose for hydrolysis or fermentation processes. Advances in pretreatment methods, enzyme technology, and biorefining processes are continuously being developed to enhance the economic viability and also the sustainability of utilizing lignocellulosic biomass (Khan et al., 2022; Pang, 2019; Rehman et al., 2023). These efforts aim to optimize the utilization of all components within lignocellulosic biomass for a more efficient and sustainable bio-based industry.

The valorization of lignin has gained significant momentum due to its status as the largest source of aromatics. However, conventional extraction processes often lead to substantial structural alterations in lignin, that negatively affect the subsequent lignin conversion to chemicals. Therefore, to achieve sustainable fuel and chemicals production from lignin, it is crucial to carefully isolate lignin from the biomass without affecting its structure. Over the past several decades, researchers have attempted to break open the recalcitrant nature of lignin to unlock the second largest renewable carbon source for chemical and fuel production. However, despite much devotion, there are still minor technological gaps exist within each research domain. The conventional pretreatment methods used to isolate lignin often result in low selectivity, complex product mixtures, and inefficient utilization of lignin and thus limit their effectiveness and hinder the development of modern biorefineries. In this context, reductive catalytic fractionation (RCF emerges as a promising approach to overcome these limitations. RCF aims to extract lignin from biomass through solvolytic extraction followed by depolymerization and then stabilization in the presence of catalyst and hydrogen. The process yields uncondensed lignin oil that consists of monomers, dimers and oligomers while the carbohydrate rich pulp remains intact. Thus, RCF offers great potential for selective depolymerization of lignin into valuable monomeric and oligomeric products, which can be further utilized for the production of high-value chemicals, materials, and biofuels.

1.2 Outline

The conversion of lignocellulosic biomass into biofuels and chemicals is an emerging topic as new generation biorefinery process. This dissertation focuses on exploiting the potential of lignin, a renewable and abundant biomass component, in producing high-value aromatic hydrocarbons. I explore the concept of a lignin-first biorefinery which prioritize the monolignol production from fractionation, depolymerization, to lignin upgrade. By optimizing these processes, my research aims to develop efficient and economically viable methods for converting lignin into valuable aromatic compounds. The summary of each chapter has been provided as follows:

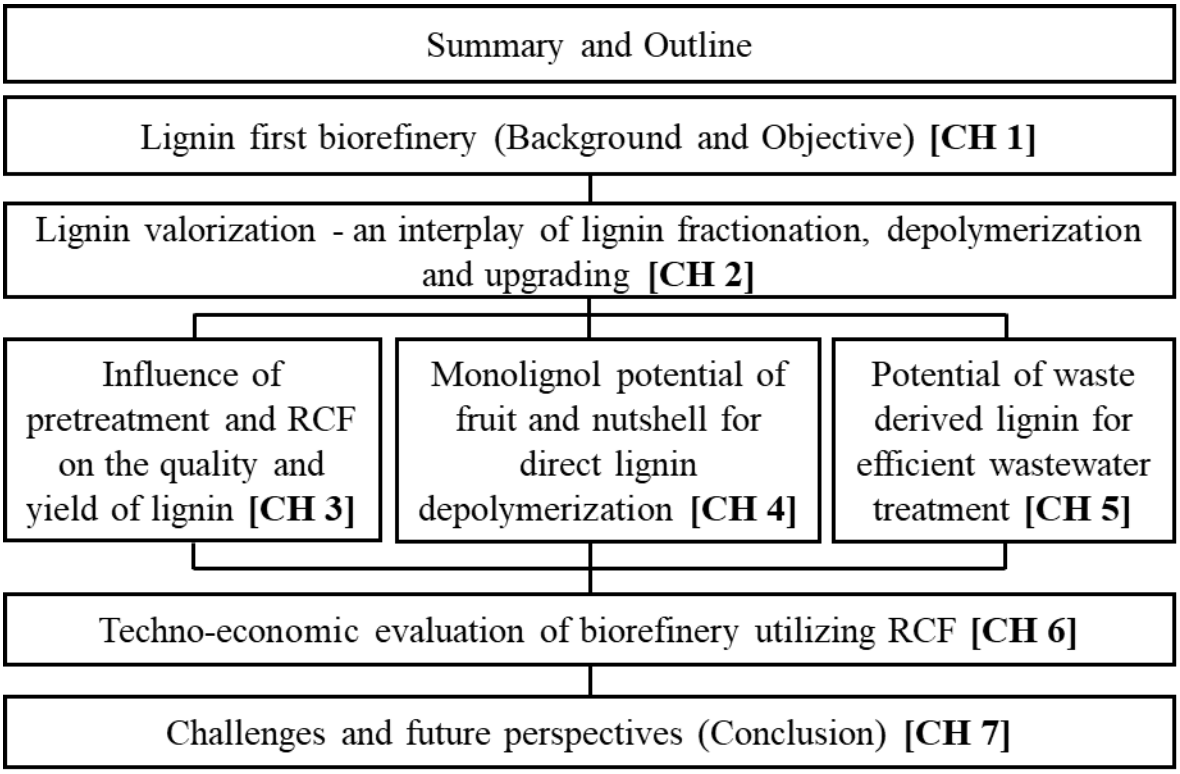

[Chapter 1] Introduction and research gap about lignin valorization

Lignocellulosic biomass is composed of a few major building block chemicals including lignin, cellulose, hemicellulose, and other compounds. The compositions and linkages among those components exhibits significant variation in its physiochemical structure among plant species, organs, parts, and the growing environment. However, the inherent complexity and heterogeneity of lignin have posed significant challenges in developing efficient and selective valorization processes. This chapter introduces the key compositions, functions, and basic structures affecting the recalcitrant of biomass to biological and chemical attacks.

[Chapter 2] Literature review for an interplay of lignin fractionation, depolymerization and upgrading.

This chapter delves into the technical aspects of lignin valorization and discusses how efficient fractionation, depolymerization, and upgrading of lignin are integral to its effective conversion into valuable products. By understanding the interplay between these processes, the efficiency and selectivity of lignin valorization can be maximized. A comprehensive overview of the modern biorefinery techniques, including the lignin-first pretreatment, lignin depolymerization, and the applications of the high value products and creates a foundation for the methods and technologies discussed in the subsequent chapters.

[Chapter 3] Influence of process design and control of biomass pretreatment and RCF on the quality and yield of lignin.

The relationship between process conditions and their effect on the main biomass constituents is very crucial to steer or modify the biorefinery process towards an economic application. Continuing with the theme of practical implementation, this chapter studies the effects of pretreatment methods and RCF on the yield and quality of lignin. Different pretreatment methods (organosolv, biphasic and staged organosolv) were investigated to enhance the accessibility and reactivity of lignin, facilitating its subsequent fractionation and conversion, and were compared with the one-pot RCF process. The insights gathered here are critical for optimizing the process parameters in a lignin-first biorefinery, therefore connecting the previous chapters with the later discussions on techno-economic evaluation.

[Chapter 4] Monolignol potential of fruit and nutshell for direct lignin depolymerization.

This chapter investigates the untapped potential of a specific source of lignin-fruit and nutshell waste for direct lignin depolymerization, considering their unique monolignol profiles. This exploration provides a link between the technical aspects of lignin valorization and the practical aspects of feedstock selection. In this chapter, the monomer production potentials of ten major fruit and nutshell biomass were investigated with comprehensive numerical information derived from instrumental analysis, such as plant cell wall compositions, syringyl/guaiacyl (S/G) ratios, and contents of lignin substructure linkages (β−O−4, β−β, β−5). A standardized one-pot RCF process was applied to benchmark the monomer yields, with mango endocarp resulting in highest yields of 37.1% per dry substrates. The results showed samples with positive S-lignin (70-84%) resulted in higher monomer yield mainly due to more cleavable β–O–4 linkages and less condensed C–C linkages.

[Chapter 5] Potential of waste derived lignin for efficient wastewater treatment.

The application of renewable and functional group-enriched lignin has recently gained huge popularity in the applications of wastewater treatment. Herein, waste wood-derived organosolv lignin nanoparticles (LNPs) with average particle size (~150 nm) were synthesized and used for the fabrication of ultrafiltration nanocomposite membrane which resulted in a thinner surface layer, high pore density (83.2 ± 0.9 %), wider and well-connected internal macrovoids with higher sub-layer porosity, and a higher negative surface charge (-29.8 mV). These structural features contributed to high stable permeation flux (92.3 L m-2 h-1) and higher removal efficiencies (> 95 %) for treating dyes over a wide range of pH conditions. By demonstrating the efficacy of waste-derived lignin in this role, the chapter further enhances the economic viability of a lignin-first biorefinery.

[Chapter 6] Techno-economic evaluation of biorefinery utilizing RCF.

To guide research towards commercialization, cost and sustainability must be considered. This chapter presents a techno-economic evaluation of a biorefinery utilizing RCF and assesses the economic feasibility of the concepts discussed in the previous chapters, thereby providing a holistic view of the lignin-first biorefinery concept and facilitating the transition towards a more sustainable and value-driven biorefinery industry.

[Chapter 7] Conclusion and future perspective.

This chapter summarizes the key findings and highlights the significance of lignin valorization towards the production of high-value sustainable aromatics. It also outlines the future prospects and research directions, identifying areas that warrant further investigation for the advancement of lignin valorization, and promoting its integration into a circular economy.

Chapter 2. Lignin Valorization-An Interplay of Lignin Fractionation, Depolymerization and Upgrading

2.1 Lignocellulose composition

Lignocellulosic biomass is a promising alternative to petroleum, given its abundance and sustainability, and has significant potential in reducing global carbon emissions (Liao et al., 2020). To that end, the biorefineries are an attractive means to convert and optimally utilize the lignocellulosic biomass into value-added products that are helpful in achieving sustainable goals of society leading to circular economy (Ubando et al., 2020). However, as the compositions of biomass varies among plant species, the conventional (sugar-platform) biorefinery processes focus on the conversion of polysaccharides has shown its limitation mainly in bioeconomy, and not suitable for all the biomass feedstock. The design principle of new generation biorefinery technologies needs to emphasize the selection and production of most valuable products among its three main components. Lignocellulosic biomass is composed of three main biopolymers, i.e. cellulose, hemicellulose, and lignin(Fengel & Wegener, 2011; Liu et al., 2022c). Cellulose and hemicellulose are sugar-based biopolymers which can be valorized via biochemical conversion (Patria et al., 2022). Cellulose is a linear polymer made up of a series of glucose units and is the most abundant element in lignocellulosic biomass. It establishes fibrils within the plant cell walls, offering structural rigidity and basic strength. It is a beneficial substrate for enzymatic hydrolysis to produce sugars, that can then be fermented to produce biofuels and some other similar bio-based products (Balasubramanian et al., 2023). Hemicellulose is a branched polymer comprised of various sugar units, including xylose, mannose, arabinose, and galactose. It surrounds the cellulose fibrils and works as a matrix, attaching cellulose and lignin together. Hemicellulose sugars can also be hydrolyzed into simple sugars and further be utilized in the bioconversion processes (Balasubramanian et al., 2023). Lignin is a complex phenylpropanoid polymer and is the most abundant source of renewable aromatic carbon and can be an alluring platform for sustainable chemicals (Khan et al., 2022). Effective utilization of lignin has become a critical subject to enhance the cost-effectiveness and economic viability of the lignocellulose biorefinery(Islam et al., 2020). It is estimated that 150 billion tons of lignin is produced worldwide on an annual basis (Hu et al., 2018). Lignin derived from paper and pulp industry has been considered as a by-product, which contributes to 50 million tons per year, out of which only 2% is converted to lignin-based products and the remaining is either burnt for energy or disposed of in landfills. At present, the market size of lignin and its products is accelerating at a growth rate of 2.28% annually from $599 million in 2014 to $704 million by 2022 (Garlapati et al., 2020). While the greater energy density, high C:H ratio (above 10:1), and exclusive aromatic monomers favors its utilization in biorefinery, the complexity and heterogeneity of lignin makes challenging its valorization and application.

Lignin structure is substantially heterogeneous and can hence vary among diverse plant species and within the various parts of the same plant species. However, lignin, in general, consists of three main forms of phenolic compounds, which are p-hydroxyphenyl (represented by H-lignin), guaiacyl (represented by G-lignin), and syringyl (represented by S-lignin) subunits, as shown in **Figure 2.1**. In some species, the Catechyl lignin (C-lignin) subunits may also be found. However, these are very rare. These subunits are further derived from three distinct monolignols (monomer of lignin): p-coumaryl alcohol

(H units), coniferyl alcohol (G units), and sinapyl alcohol (S units) (Bugg et al., 2011). The overall structure of lignin is principally composed of aromatic rings that are linked together by numerous types of bonds. The stronger the bonding, the harder it is to depolymerize the lignin into its constituent aromatics. The highly common types of bonds found in lignin structure are β–O–4, α–O–4, β–5, β–β, and C–C linkages with side chains. The most ubiquitous and most important linkage in this whole structure is the β–O–4 bond. It connects two adjacent phenolic units via oxygen atom, hence, forming a connection between the aromatic rings (Jindal et al., 2023b).

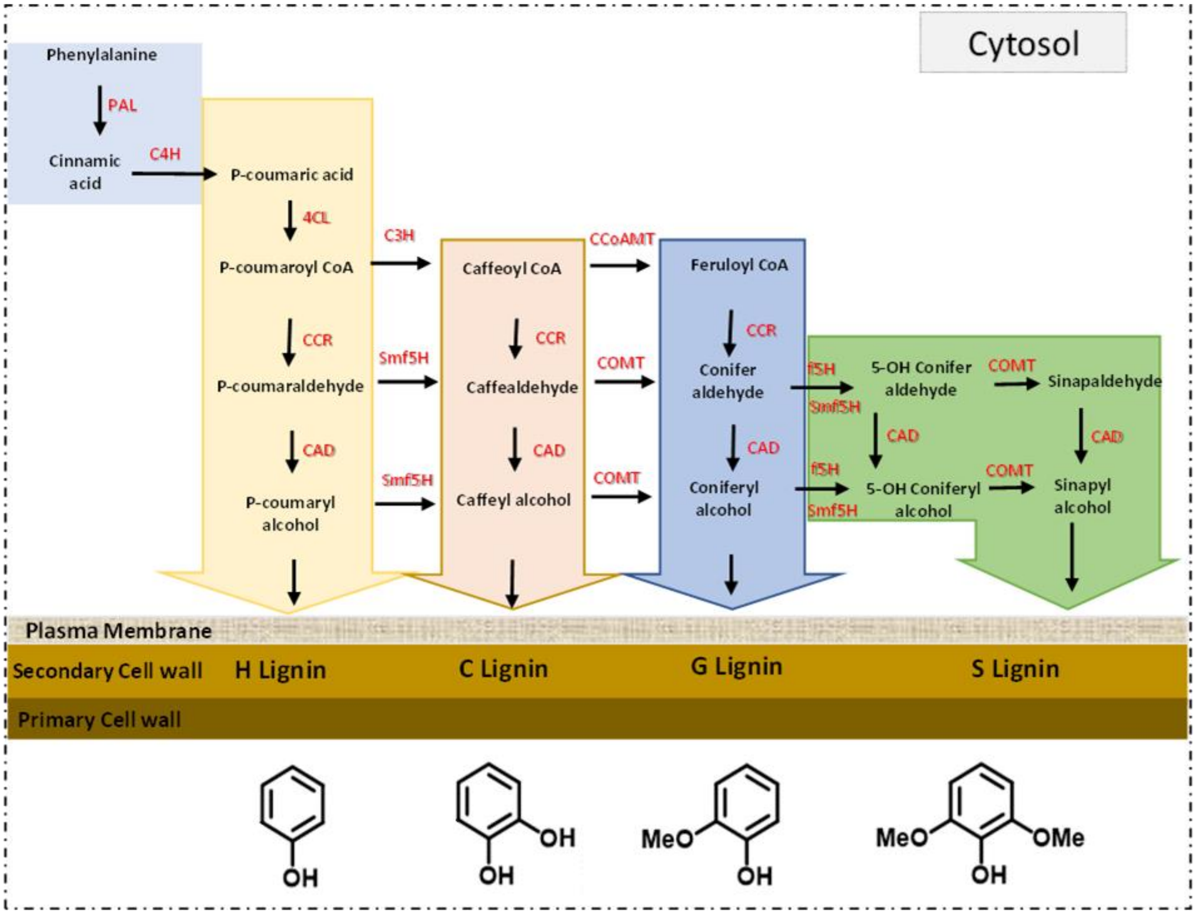

Figure 2.1: Schematic presentation of lignin synthesis pathway.

Lignin structure in various plant species, i.e., softwoods, hardwoods, and herbs, varies significantly. The percentage of H, G and S type subunits vary in each type of lignin (Rumpf et al., 2021). Softwoods (21-29wt%) compared to hardwoods (18-25wt%), and herbaceous crops (15-24wt%) typically have the higher lignin concentration. Softwood lignin is more reactive than hardwood lignin, for example, in the production of stabilised lignin fibers, and softwood lignin is anticipated to be more uniform among different wood types due to structural similarity with lignin comprising of only one prevalent type of monolignol as their building block (Gellerstedt, 2015). There are also significant differences in these classes' relative distributions of precursor monolignols. Hardwood lignin comprises both types of units, S and G, as opposed to softwood lignin, which is nearly entirely made up of G–type units. Herbaceous plants do contain all three H, G, and S units, although the quantity of 'real' H–type units is minimal.

Numerous additional phenolic compounds, in addition to the three classic monolignols, are also included in the structure of lignin (Vanholme et al., 2012). The relative H, G and S units' distribution determines the structure of lignin. S–type units are unable to establish 5–5 bonds and β–5 interunit bonds on essential coupling during the lignification process because they lack free ortho-position. As a result, lignin from hardwoods has fewer stable C–C bonds as compared to lignin from softwoods (Ragauskas et al., 2014). The theoretical maximal monomer yield is almost proportional to the relative concentration of cleavable cross-unit ether linkages' square because the C–C linkages cannot be easily split during the conventional catalytic fractionation process (Rinaldi et al., 2016b). Aside from the element of overall monomer production, the point that softwood lignin is only made up of G–type units reduces the range of catalytic fractionation products, making downstream purification easier (Schutyser et al., 2018). In addition to the three main components already discussed in detail, woody biomass also contains extractable substances like resins and minerals. Wood extracts are quite important in utilizing wooden products, and their main constituents include fatty acids, resin acids, fatty acid esters, and phenols. The proportion of extracted substances vary between 1% and 20% of the total woody mass, dependent on the wood type, location in the tree, and position of the wood (Pang, 2019).

2.2 Chemical and structural characteristics of lignin

Lignin is biosynthesized through various enzymatic oxidation and dehydrogenation process from phenylalanine and the three basic building blocks. The high variability of phenolic hydroxyl groups introduced the high functionality for promotion of rigidity and turgidity in various parts of woody plantations. Different functional groups are responsible for introducing functions such as enhanced stiffness, surface-activeness, high thermal stability and anti-oxidative abilities into the lignin chains. These features made lignin a potential material for replacing the conventional synthetic products as summarized follow **(Figure 2.2a)**:

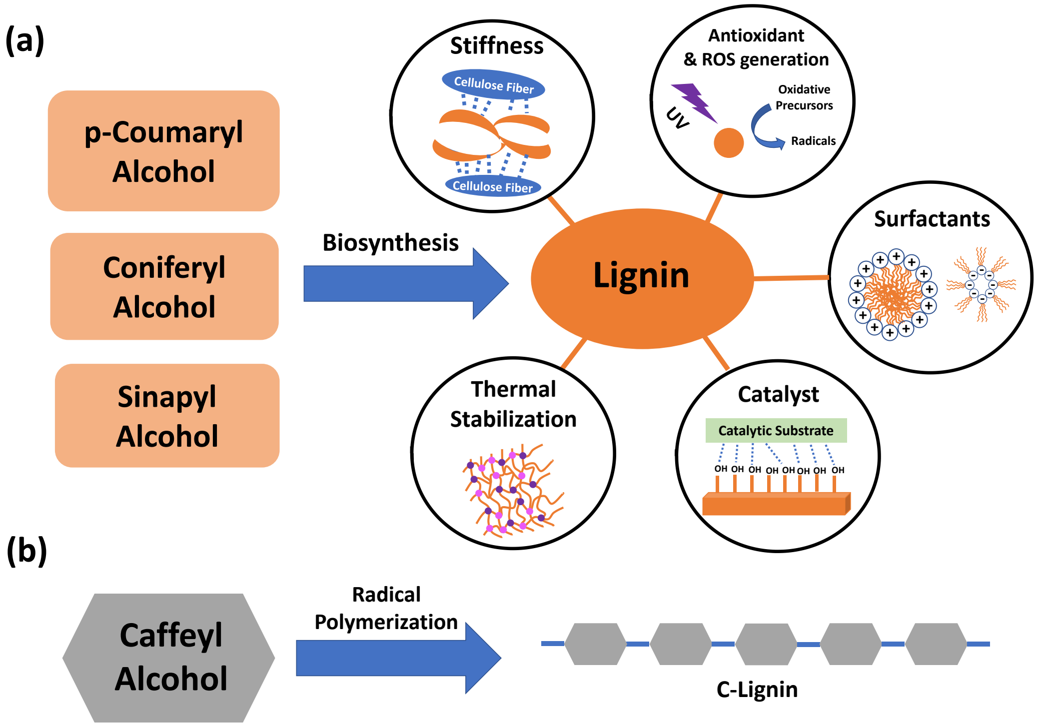

Figure 2.2: Formation of (a) hetero- and (b) homo- lignin polymers and their key properties for valorization

2.2.1 Stiffness

Lignin is known to enhance the rigidity and stiffness of woody biomass. It also provides resistance against physical corrosions like bending through the strong adherences with cellulosic fibers. The stiffness of lignin can be accounted for the high abundance of van der Waals' interactions between cellulose and lignin, which increase with the molecular weights and amounts of phenolic groups of the lignin (Youssefian & Rahbar, 2015). The strength and modulus of lignocellulosic biomass can also be further promoted by the presence of hydrogen bonds in between the hydroxyl groups of cellulose and lignin (Jiang et al., 2020).

2.2.2 Surface chemistry

Lignin is a macromolecule which consists of a large phenolic network linked together mainly by different ether bond linkages. This network and the presence of many fat-soluble groups like methoxy groups (-OCH_3) can account for the high hydrophobicity of lignin (Li et al., 2018c). The highly hydrophobic nature can be of great potential in the development of green lignocellulosic biomass-derived surfactants if hydrophilic heads are attached on the lignin. Lignosulfonates has gained its attention as surfactant as the sulfite treatment is amongst the most common and major process in pulping industry (Cai et al., 2017). Lignosulfonate consists of hydrophilic sulfonate groups supported by a giant hydrophobic aromatic ring structure, making it proper surfactants and flocculants (Xu et al., 2019). In addition to lignosulfonate, recent studies have also introduced other cationic/anionic groups or polymers on lignin, so it can further reduce the surface tension on the air/water interface and oil/water interface, and hence enhance the removal of organic and hydrophobic wastes from water (Guo et al., 2021). As lignin is also a natural and biodegradable polymer, it will be more environmentally friendly compared with the conventional ionic surfactants like cetylammonium bromide and soap less detergents. Due to the hydrophobic nature of the large covalent network, lignin based surfactants has been used and incorporated in enhancing the encapsulation and drug control-release strategies (Li et al., 2017b).

The large number of hydroxyl groups in lignin have also made this macromolecule a potential catalyst on the ring-opening and nucleophilic addition of certain molecules, like epoxides can exhibit high amount of dimeric hydrogen bonding. The intermolecular hydrogen bonds can reduce the activation energies of the molecules and weaken the chemical bonds in molecules like epoxides and carbon dioxide (Guo et al., 2019), which increase the tendency for the nucleophile to attack the molecules. The aromatic three-dimensional (3D) interpenetrating polymer network is also vital for being an excellent catalyst support. Lignin with high sulfonate group content has shown to be an excellent candidate for the conversion of monosaccharides like glucose, fructose and xylose to hydroxymethylfurfural (HMF) or furfural (Gan et al., 2019; Li et al., 2020).

2.2.3 Structural heterogeneity

The various kinds of linkages, such as β–O–4, α–O–4, β–β, and many other linkages introduce structural heterogeneity to the lignin macromolecules **(Figure 2.3)**. Studies have shown that structural heterogeneity can enhance the variability of lignin macromolecules formed, which can be utilized in various parts of woody biomass (Polo et al., 2020). However, heterogeneity also introduces a large variability of crosslinks and intermolecular forces in different lignin chains and hence enhances the difficulty in reproducibility of bond and crosslinks breakages during valorization. The difficulty in formulation and uniformity of lignin valorizations and applications is further increased due to the variation of aliphatic and phenolic hydroxyl groups in the structure. In order to enhance the functionality and reproducibility of lignin-derived materials, recent research has been focusing on the development of c-type lignin. C-type lignin is a type of benzodioxane homopolymer which is made up of only one monomer, *i.e.*, caffeyl alcohol **(Figure 2.2b)**. Caffeyl alcohol is classified into the hydroxycinnamyl alcohol group and the catechol groups are linked together by β–O–4 bonds. C-lignin proved to have a higher thermal and chemical stability than ordinary hetero-polymeric lignin due to the difference in the attachment of hydroxyl groups on benzyl groups instead of the usual methoxy groups (Li et al., 2018b). The post-radical coupling reaction is allowed for the re-aromatization of the intermediates on the benzodioxane ring production, which can in turn protect the reactive hydroxyl groups on the benzyl ring (Berstis et al., 2016). C-lignin chains have high uniformity and homogeneity due to the unique repeating unit in the group. Therefore, it enhances the repeatability and reproducibility of lignin-derived products. These properties have shown that c-lignin can be a potential material for adopting in various applications which may bring better performance than conventional hetero-polymeric lignin chains like photosensitizers and dyes. Studies have also extended further into the production of genetically modified lignin, which can control the S, G, and H ratio of lignin in a woody biomass. The control of various repeating units on lignin can reduce the possibility of condensation reaction during the pretreatment process and hence enhance the enzymatic digestibility of cellulose and chemical digestibility, delignification and depolymerization of lignocellulosic biomass and lignin chains.

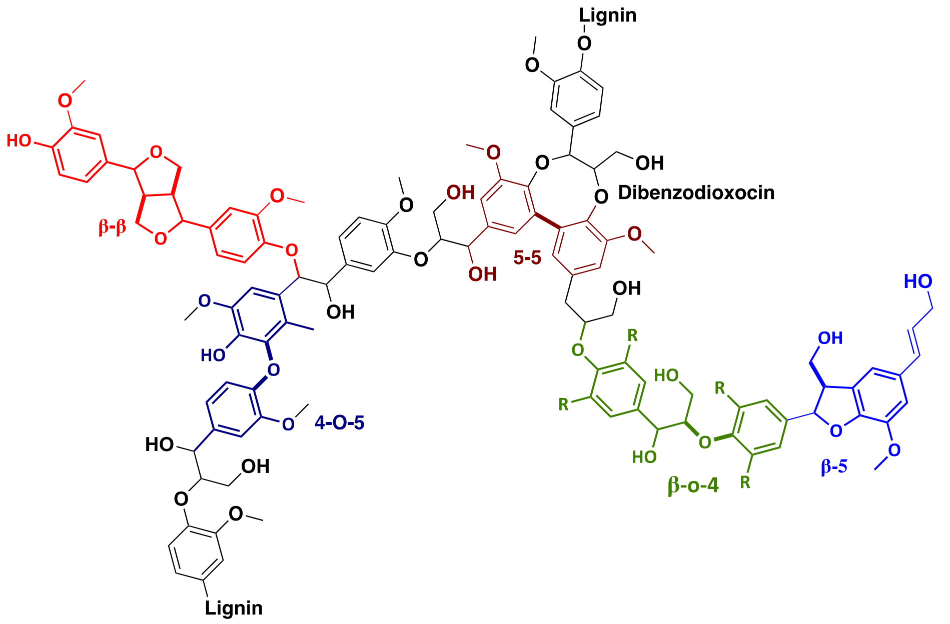

Figure 2.3: Common lignin linkages.

2.2.4 Thermal stability

The extra stability provided among the conjugated aromatic rings and the ether linkages in the 3D covalent network of lignin increase the activation energies for the bond-breaking process. Hence the thermal stability of lignin can be exploited to enhance the structural integrity of synthetic biomaterials. Recent studies have shown that the incorporation of lignin has significantly improved the thermal stability of cellulose nanofibers (Zhang et al., 2019a). Lignin has also been incorporated into vulcanized rubber and showed an increase in the stability of thermosetting plastics under high temperatures (Barana et al., 2016). Adopting various functional groups into lignin chains will affect the ability to withstand high temperatures. Phenolated sulfuric acid lignin, of which the lignin treated with p-toluenesulfonic acid, has showed higher thermal stability than aliphatic sulfonated lignin and sulfuric acid lignin (Taleb et al., 2020). Lignin treated with P_2O_5

introduces the flameproof ability due to the addition of phosphate and phosphonate groups on lignin chains (Prieur et al., 2017; Zhang et al., 2018c).

2.2.5 Antioxidant activity

The high phenolic hydroxyl groups linked together by β–O–4, β–β, α–O–4 allowed lignin to be a potential antioxidant which can serve as a quencher for mild oxidants or scavengers for various reactive oxygen species (ROS) like hydroxyl radical ($OH^{\cdot}$), superoxide radical (O_2^{-}.). Recent research has revealed that shorter lignin chains with higher abundance of phenolic hydroxyl groups showed a higher ability on resisting antioxidant attacks (Gordobil et al., 2018). Lignin also has excellent ultraviolet (UV) radiation absorbing property due to the presence of conjugated systems like carbon-carbon double bonds, aromatic groups and carboxyl groups. Depending on the degree of conjugation, lignin chains can have the ability to absorb various electromagnetic radiations like deep UV radiations or near-visible light radiations. The presence of auxochromes like methoxy ($-OCH_3$) and carbonyl groups ($-C=O$) also enhances the UV absorption and hence reduce the probability of ROS formation. However, the antioxidant ability decreases as the degree of lignin condensation increases (Piccinino et al., 2021). This shows that lignin from certain pretreatment methods like acid-catalyzed pretreated lignin may not be suitable for antioxidant usage. This property allowed the extension of lignin application in healthcare or cosmetic product as UV radiation and absorption agent.

2.3 Types and sources of lignin

Lignin polymers are deemed as the most recalcitrant components of biomass and can be extracted only via employing some pretreatment strategy (Vuppaladadiyam et al., 2023). To harvest the needed functional groups, various extraction methods were therefore adopted to obtain lignin chains for further valorization and functionalization (Table 2.1). The extraction step is a technically sound process that greatly influences the quality of fractionated lignin. Based on the extraction mechanism, there are four different types of lignin, namely Kraft Lignin, Soda Lignin, Organosolv Lignin, and Lignosulfonate (Rumpf et al., 2021).

Table 2.1. Concentrations of key functional groups in lignin after different pretreatment

Feedstock	**Extraction method**	**Aliphatic OH (mmol/g)**	**Phenolic OH (mmol/g)**	**Carboxylic (mmol/g)**	**Average MW (Da)**	**Ref.**
Poplar	Acid	3.25	3.04	0.05	2871	Wang et al. (2021a)
Poplar Wood Chip	Acid/Organosolv	4.55	1.56	0.08	9400	Wang et al. (2020c)
Poplar Wood Chip	Acid/Organosolv	1.11	3.05	0.15	3400	Wang et al. (2020c)
Poplar	Alkali/Organosolv	1.61	1.69	0.32		Li et al. (2021)
Masson Pine	Alkali/Organosolv	1.29	1.57	0.51		Li et al. (2021)
Softwood	Alkali/Organosolv	2.50	1.53	0.28	3603	Zhong et al. (2020)
Eucalyptus	Organosolv	1.92	2.32		8500	Dong et al. (2019)
Sugarcane Bagasse	Acid/Ionic liquid	0.79	2.84	0.23	956	Ji et al. (2021)
Reed	Ionic liquid	6.59	4.68	048	3962	Zhang et al. (2021b)

2.3.1 Kraft lignin

Kraft lignin is a type of industrial lignin derived from Kraft pulp, accounting for approximately 85% of the overall lignin production worldwide. The Kraft pulp technique is the most common method for turning coniferous wood to pulp; it produces more pulp than other alkaline pulping processes. In the Kraft cooking process, around 90-95% of the lignin is dissolved in the cooking fluid, which contains sodium hydroxide and sodium sulphide (Tolbert et al., 2014). During the pulping process, the lignin macromolecules are fragmented, the molecular weight is reduced, and the lignin is dissolved in an alkaline solution, which turns the solution dark brown. Kraft lignin is being produced globally around 130 million tonnes per year, and it is mostly utilized for heat recovery by burning, resulting in a low-value utilization (Rinaldi et al., 2016a) . Apart from being utilized as a biofuel, kraft lignin may be utilized via polymerization to polyurethane and employed in phenolic resins (Jönsson, 2016).

2.3.2 Lignosulfonate

Lignosulfonate comes principally from the conventional sulfite pulping and modified sulfite pulping methods (Chen, 2015). The sulfite process is like the Kraft process, except that the alkaline system is replaced by an acidic medium at temperatures ranging between 130 and 160°C (Hu et al., 2018). Pulping takes place in aqueous sulphur dioxide and a base for 3-7 hours, allowing for two reaction routes depending on the pH: at lower pH (1-1.6), the sulphurous acid process takes precedence, while at higher pH (1.8-3.1), the acid sulfite pathway prevails. The acidic environment cleaves the alkyl-aryl-ether (β–O–4; α–O–4) bonds and introduces sulfonic acid into the α-carbon. The lignosulfonic acids may then be extracted from the black liquid, which is often not burnt in comparison to the Kraft process, leaving the lignin accessible as lignosulfonates (Kai et al., 2016). One drawback in compared with Kraft lignin is the large number of contaminants, since lignosulfonates include up to 25% carbohydrates, ash, and other inorganic elements (Macfarlane et al., 2014).

2.3.3 Organosolv lignin

Organosolv lignin is the type of lignin extracted using organic solvents. The organosolv method dissolves lignin by acid-catalyzed solvolysis of its β–ether bonds. The acid is either added or created in situ by deacetylating hemicellulose, which releases acetic acid into the reaction mixture. The external acid increases acidolysis of β–ethers, resulting in cellulose pulp with decreased lignin concentration. In situ acid production produces lignin with more β–ether bonds than native lignin. Organosolv lignin's quantity of β–ether connections is comparable to kraft lignin with similar delignification. At greater acidity, lignin fragments condense into higher molecular weight polymers due to the creation of formaldehyde from the removal of γ–CH2OH. As a result, optimising the procedure to maximise cellulose quality reduces lignin quality, and vice versa (Shrotri et al., 2017). Organosolv lignin fractionation uses solvents such ethanol (Parchami et al., 2022), methanol (Weerasai et al., 2021), butanol (Rivas et al., 2021), ethylene glycol (Wei et al., 2021), formic acid, γ–valerolactone (GVL) (Raj et al., 2021), and tetrahydrofuran) (Zhao et al., 2022). Among these, ethanol appears to be one of the most popular solvents for the organosolv process due to its low cost, low toxicity, and ease of recovery. The processing temperature varies from 140 to 220°C, while solvent concentrations in water vary from 40% to 80%. One of the primary benefits of this method is that it produces sulfur-free lignin, as opposed to kraft lignin and lignosulfonates. It also has excellent purity, quality, and chemical reactivity, making it ideal for direct usage or conversion into high-value compounds (Liu et al., 2022b)

2.3.4 Soda lignin

Soda lignin is produced during the soda pulping technique. Compared to Kraft lignin and lignosulfonates, soda lignin is sulfur-free and pure. The soda pulping technique is mostly used to prepare annual crops such as straw, bagasse, and hardwood. In truth, the alkaline delignification process in soda pulping is quite similar to the Kraft technique, with the exception of sulphur content. Sodium hydroxide is used to create an aqueous alkaline media. The delignification process in hot alkaline solution can change lignin inter-units, including β–O–4 and β–5 connections (Liu & Abu-Omar, 2021). An effort to boost efficiency is the use of anthraquinone, which increases the breaking of ether bonds while minimizing the degradation of carbohydrates, resulting in a considerable decrease in cooking time (Schutyser et al., 2018).

2.4 Lignin fractionation and depolymerization

Biomass fractionation technology plays a decisive role in biorefineries as it determines the fate of different components of lignocellulose, thus influencing the range of downstream valorization options. Various fractionation methods have been developed, each resulting in a specific type of lignin product, such as solid residue, lignin precipitate, or depolymerized product mixture. These methods induce structural changes in native lignin, which affect its reactivity towards depolymerization, often evaluated through measuring the content of β–O–4 linkages. While β–O–4 linkage content is an important factor, other structural characteristics like molecular weight, OH-group content, and certain impurities can also impact lignin reactivity (Boudet, 2000; Phongpreecha et al., 2017). The type of biomass and the fraction of the prevalent β–O–4 bonds also influence the reactivity of lignin. In addition, the different source of biomass such as hardwood, softwood, and the herbaceous feedstocks exhibit significant structural and compositional variations, which further influence the fractionation efficiency (Achyuthan et al., 2010; Boudet, 2000). Consequently, making generalized comparisons between isolated lignins is challenging due to the multitude of variables involved, including the fractionation method, analysis techniques, and biomass source.

During biomass fractionation, lignin is liable to structural distortion, thus resulting in a decrease in ether bond content and a subsequent increase in the carbon-carbon bonds compared to the native lignin structure. As most depolymerization techniques are not able to cleave C-C bonds, an increase in carbon-carbon bonds reduces the potential for depolymerization and reactivity. To mitigate this reactivity loss, one approach is to perform lignin depolymerization absolutely on native lignin within the lignocellulosic substrate, combining fractionation and depolymerization simultaneously. However, traditional fractionation processes often produce large amounts of degraded lignin units, which offer opportunities for depolymerization into valuable chemicals. Alternative techniques for fractionation are being developed to produce reactive separated lignin with a high content of β–O–4 linkages. Therefore, the depolymerization of detached lignin, whether it is reactive or moderately degraded, is a significant research area in the perspective of lignin valorization.

2.4.1 Lignin depolymerization

The feasibility of lignin valorization rests in our ability to depolymerize it into the smaller aromatic unit. This section devotes to summarize the latest strategies of lignin valorization, which is divided into three stages: isolation, depolymerization, and recovery. The effort to achieve efficient depolymerization of lignin has sustained decades of research in the renewable chemicals and fuel community (Van et al., 2018). Different degradation protocols, such as thermal, chemical, and biological routes, or a combination of those, have been studied extensively (Song et al., 2021). These methods include thermochemical (pyrolysis, gasification, hydrothermal liquefaction, and microwave-assisted), chemical (acid/base- catalysed, IL-, sub-, or supercritical fluid- assisted, oxidative, hydroprocessing, and bioinspired/biomimetic), and biological (bacterial, fungal, or enzymatic) processes (Klinger et al., 2020). Several reviews were recently published to address the advances in lignin conversion and upgrading (Wong et al., 2020). Various depolymerization strategies based on their redox properties and temperature ranges have been summarized in **Figure 2.4**.

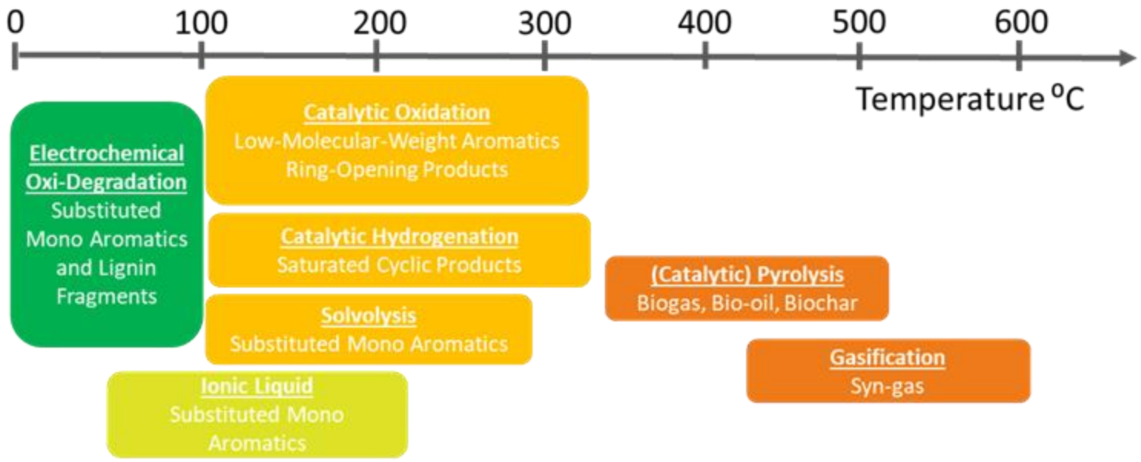

Figure 2.4: An overview of lignin conversion methods

2.4.1.1 Hydrogenolysis

In the hydrogenolysis process, hydrogen or other hydrogen sources have been used to thermally reduce lignin. Through the hydrogenation treatment, depolymerized lignin, phenols and other chemicals with high added value can be obtained, as well as low molecular weight hydrocarbon fuels can also be prepared. The main types of reactions involved in the hydrotreating process of lignin include hydrogenolysis, hydrodeoxygenation, hydrogenation, and integrated hydrogen-processing. Those thermal catalytic processes include a broad consideration of the application of a catalyst at an elevated temperature in a pressurized setting. They often include the design of solvent systems too. For the most part, hydrogenolysis by reductive catalytic depolymerization has received more attention than the oxidative approach because of the preservation of the linkages, such as β–O–4, during the lignin isolation process. An increasing number of research articles have also demonstrated convenient one-pot lignin isolation and depolymerization in a reductive environment (Renders et al., 2017). The strategy has resulted in a newly found "lignin-first" concept (discussed in section 2.5), where lignocellulosic biomass undergoes an in-tandem depolymerization-stabilization treatment while having the β–O–4 bonds preserved for further treatment, which can produce higher-value chemicals (Renders et al., 2017).

2.4.1.2 Solvolytic treatment

The use of an organic solvent to solubilize lignin at elevated temperature can also promote lignin depolymerization. Solvent choices can be protic (water or alcohols) or aprotic organics (*e.g.*, dioxane, acetone, tetrahydrofuran, and tetralin) or a combination of both. The degree of substitution of the products can be influenced by the reaction temperature. In general, a lower temperature would favour the alkylated phenols and guaiacols, whereas a higher temperature could favour the less substituted phenols or catechols. One of the advantages of solvolytic treatment is that it would allow researchers to fine-tune the chemical reactivity by adjusting the solvent system strategically. For example, Lewis-based solvents, such as methanol, has shown to preserve the aromaticity of the depolymerized product by suppressing hydrogenation. However, solvent recovery through distillation methods can be energy-intensive and solvent loss during the recovery has shown to be one of the most sensitive operating cost expenditures of large-scale lignin depolymerization (Kouris et al., 2018). An innovative approach could be sought by considering a higher boiling point solvent systems, for instance, IL, to promote the boiling point differences between the solvent and the solutes.

2.4.1.3 Ionic liquid

Although often criticized for its environmental toxicity, IL exhibits some remarkable chemical activities towards lignin degradation and transformation. IL can offer a high extraction yield and minimal structural alteration in extraction, which makes it more suitable for aromatic feedstock production (Ji & Lv, 2020). Other ILs have demonstrated the conversion of commercial lignin into speciality chemicals, namely homovanillic and vanillic acid, using the combination of [EMIM][Triflate] and triethylammonium methanesulfonate (TMS) with water and H_2O_2 (Dier et al., 2017). However, some of the ILs are known to induce additional chemical changes. For example, alkali and sulphate-based IL could lead to a decrease in β–O–4 bond cleavage while promoting more stable C–C bond formation, which leads to less depolymerization. The uses of ILs require comprehensive considerations. For example, the production of byproduct waste and odour from the amine- or sulphate-based ILs could make the process environmentally unfavourable. If the depolymerization aims to produce aromatic fuel additive of BTEX, any nitrogen-based or sulphur-based IL may require additional purifications to minimize residual hetero-atom contaminant, as they may induce NOx or SOx formation during combustion.

2.4.1.4 Thermal treatment

Thermal treatment of lignin concerns the transformation of solid lignin into liquid or gas products by supplying thermal energy. Depending on the temperature profile and the reaction environment, the degree of lignin fragmentation can be adjusted. Pyrolysis and gasification are the two most common examples in the category. Pyrolysis of biomass is typically performed in an oxygen-free environment, and the temperature can rise from room to 400-600°C in several seconds. The rate of heating, final temperature, and the residences time scan be used to control the resulting product. Compared to chemical-based fragmentation, pyrolysis is a low-cost method to achieve lignin depolymerization efficiently, but the resulting liquid products, such as bio-oil, typically exhibit multiple phase separation issues and may contain highly reactive carbonyl groups that are prone to uncontrolled polymerization. The chemical instability of the product requires additional hydro-stabilization treatment before the bio-oil can be used for further upgrading or stored (Lam et al., 2020). Meanwhile, the lignin based bio-oil has high oxygen content, leading to significant deficiencies in heating value, which has also become a bottleneck problem in the practical application of the technology. It is essential to add a suitable catalyst during the pyrolysis process to control the degree of lignin pyrolysis and product distribution, which will be discussed in Section 4.2.

2.4.1.5 Electrochemical depolymerization

Electrochemical depolymerization of lignin has recently gained increasing attention because of its unique advantages to achieve chemical redox mildly at below water-boiling temperature and atmospheric pressure. Moreover, electrocatalysis offers a direct connection between the renewable electricity harnessed from intermittent sources and chemical transformation, enabling a renewable-energy powered electrified biorefinery. Several recent reviews have discussed the advancement of electrocatalysis to valorize lignin for fuel and chemicals production (Garedew et al., 2021). Electrochemical depolymerization of lignin is typically achieved in a strongly alkaline aqueous environment, which provides conductivity and improves lignin solubility. Electrochemical degradation often occurs in oxidative environments, while electrochemical hydrogenation are usually applied toward upgrading the degraded aromatic units (Garedew et al., 2019; Lam et al., 2020). Cai et al. (2018) demonstrated the production of mono-aromatic specialty chemicals, such as vanillin, syringaldehyde, guaiacol, trans-ferulic acid, syringaldehyde, and acetosyringone, but the overall yield remains low due to a few reasons. First of all, the reaction medium must be conductive, and the electrolyte recovery can be an energy-intensive process (Tu et al., 2021). The reaction rate is dictated by the current flow, and electrochemical reactions operate on a low current flow to avoid side reaction, such as water oxidation. Future works must develop high surface area electrodes to compensate for the low current density and develop specific electrocatalytic surface to improve adsorption. Over-oxidation of the product can be another issue because of the indiscriminative nature of electrocatalysis; the development of a membrane reactor may protect the products from undesired additional redox reaction (Bawareth et al., 2019).

2.4.2 Catalysts for and from thermochemical processes

The thermochemical methods for the conversion of lignin can be divided into three major ways **(Figure 2.5)**, *i.e.*, catalytic pyrolysis in an inert atmosphere, catalytic hydrogenolysis in a reducing atmosphere such as hydrogen (Type I), and catalytic oxidation in an oxidizing atmosphere or in the presence of an oxidant (Type II). At the same time, lignin as a carbon source can be used as a raw material for the preparation of carbon-based catalysts (Type III).

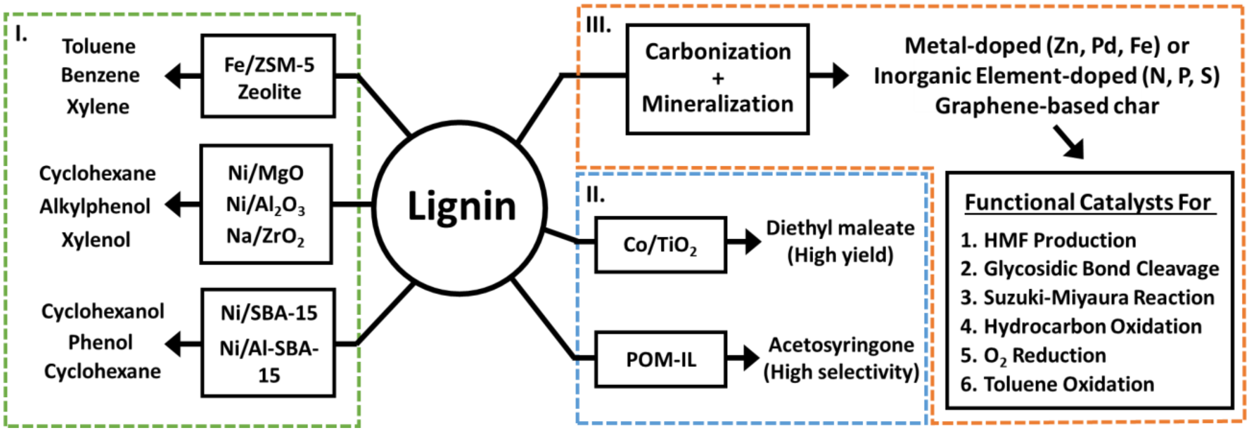

Figure 2.5: Three thermochemical approaches and the related products of lignin valorization. Type I – Reductive depolymerization (Si et al., 2019; Zhang et al., 2018b). Type II – Lignin derived catalysts (Li et al., 2020). Type III – Oxidative depolymerization (Cai et al., 2019a)

2.4.2.1 Catalytic pyrolysis of lignin

Zeolite is a typical catalyst for the catalytic pyrolysis of lignin. Zeolite has a huge pore volume and specific surface area, which is beneficial to promote the pyrolysis of lignin and reduce the energy consumption of the process. Generally, zeolite with higher acidity and larger pore size shows higher activity, while non-acidic zeolite preferentially resulted in oxygenated aromatics, such as guaiacyl units. In the pyrolysis of lignin, the activity of zeolite catalysts will be reduced or even deactivated due to carbon deposits. Therefore, the used catalysts need to be calcined in an aerobic environment to remove the carbon deposits to restore catalytic activity. Y-zeolite and BETA zeolite catalysts were used for the conversion of phenol intermediates (Kim et al., 2020). Y-type zeolite was the most effective catalyst for monocyclic aromatic hydrocarbons production and BETA zeolite was the most effective catalyst for naphthalene products. Doping other metal elements such as Ni, Zn, Fe, Mo, Ga, etc. in the zeolite can improve the activity, selectivity and carbon deposition resistance of the catalyst. For example, when Fe-modified ZSM-5 zeolite catalyst was used for lignin catalytic pyrolysis, the product selectivity of BTX and the yield of upgraded bio-oil were improved (Zhang et al., 2018b). In addition to the optimization of reaction conditions such as reaction temperature, heating rate, and reaction time, pretreatment can also increase the efficiency of lignin depolymerization and pyrolysis. Microwave-assisted heating technology has also been applied in lignin pyrolysis. Studies have shown that microwave-assisted technology is an effective way to shorten the reaction time and increase the yield of the target product (Ma et al., 2017).

Metals or metal oxides are also commonly used catalysts in chemical reactions. The surface of metal or metal oxides has a variety of adsorption reaction centers and high activity. Various chemical reactions proceed on the surface of the catalyst at the same time, and hence reduce the selectivity of the product. Cu/C, Pd/C, Pd-Ag catalysts can reduce the temperature required for larch sawdust pyrolysis to produce phenol-rich bio-oil. Different catalysts exhibit different catalytic performance. Among them, the proportion of phenols (GC-area) increased from 25.28% to 35.11% in the presence of Pd/C catalysts (Wang et al., 2018b). Ru@N-doped carbon catalysts with homogeneously dispersed Ru nanoparticles and defect-rich carbon supports were synthesized by a two-stage pyrolysis method and used in lignin pyrolysis, resulting in 30.5% yield of aromatic monomers at 300°C (Li et al., 2019a). Metal or metal oxide can also regulate the composition of pyrolysis gas. Nickel oxide derived from nickel plating slag was applied in the pyrolysis of woody biomass for the improved hydrogen production (Guo et al., 2020). Metal doping is an effective method for the preparation of catalysts with enhanced selectivity towards different products. Hendry et al. (2020) used ZrO_2 as a carrier to load Na, Ce, NiCe, MgCe, Fe and FePd for lignin pyrolysis and reported improved production of monomeric phenolics and alkyphenols when the Na/ZrO_2 to lignin ratio is 3:1 at 500°C.

Metal salts have been also used as catalysts for the pyrolysis of lignin. The lignin and the metal salt undergo pyrolysis after being mixed or impregnated, and the metal salt can promote the reaction through complexation with the reactant. Fan et al. (2020) studied the effect of K_2CO_3 for the catalytic pyrolysis of pinewood, peanut shell, rice straw in a fixed-bed reactor. It was found that the addition of K_2CO_3 lead to a decrease in liquid product yield, while the gas yield increased obviously. Ketones and phenols were the main components in the liquid products. Yin et al. (2020) used KCl, KOH and K_2CO_3 in catalytic pyrolysis process and demonstrated the important role of anions deployed in two lignin-related polymers. They found that KOH and K_2CO_3 can reduce the thermal stability of lignin polymers and effectively promote the breaking of C_β–O bonds, but the effect of KCl is very limited.

2.4.2.2 Catalysts used in hydrogenolysis process

Hydrogenation is a chemical reaction that uses hydrogen atoms to saturate or reduce organic compounds. C=C bonds, C≡C bonds, and C=O bonds become saturated during the hydrogenation process, increasing the content of hydrogen atoms in the product. The hydrogenation can be selectively controlled by applying appropriate catalysts and reaction conditions. Various Ni based catalysts have been developed for lignin hydrogenolysis. Ni/C showed high thermal stability during lignin hydrogenolysis and produce arenes and phenols in high yield (Gao et al., 2016). Ni/MSN-Al prepared by the immobilization of Ni clusters in the channel of mesoporous aluminum silica nanospheres showed much higher activity than the Ni-γ-Al_2O_3 in the hydrogeneolysis of lignin C-O linkages (Si et al., 2019). Platinum group metal-based catalysts were also used in lignin hydrogenolysis. Zhang et al. (2021a) found that the synergy of Pt nanoparticles and basic sites in hydroxyapatite supported Pt catalysts facilitate the production of monomers in high yield in the catalytic hydrogenolysis of alkaline lignin. Hu et al. use isopropanol as hydrogen donor to study the lignin hydrogenolysis with different catalysts include Pd/C, HZSM-5, Pt/TiO_2 and Re/TiO_2 under different reaction conditions such as hydrogen, temperature and pretreatment. They found that PtRe/TiO_2 showed higher activity on the cleavage of C-O bond than the other catalysts (Hu et al., 2019). Finally, hydrodeoxygenation (HDO) process can remove oxygen from phenolic molecules and is an important method of bio-oil upgrading. Mukundan et al. (2021) developed a solvent-free HDO process for the conversion of softwood lignin to aromatics with carbon-ZrO_2 supported Ni/MoS_2 catalyts. The highest deoxygenation of 82.2% was achieved with a 69.1% yield of monomer after optimization. The catalysts Fe_2P, Co_2P, and WP have been applied to the HDO reaction of lignin and lignin derived products. Compared with noble metal catalysts, these metal phosphide catalysts can improve the products selectivity and exhibit good stability.

2.4.2.3 Catalytic oxidation of lignin

The catalytic oxidation of lignin has milder reaction conditions and shorter reaction time than pyrolysis and hydrogenation. In the lignin oxidation process, oxygen is introduced into the side chain or aromatic ring, which reduces the electron density and increases the steric hindrance between the lignin aromatic rings, making the lignin structural units easier to dissociate. Therefore, catalytic oxidation of lignin is a very promising method for lignin utilization. The lignin catalytic oxidative depolymerization catalysis can be divided into homogeneous catalysis and heterogeneous catalysis reactions, in which transition metals and precious metals catalysts such as Pt and Pd are widely applied. Kumar et al. (2020) prepared a series of catalysts by supporting cobalt on TiO_2, CeO_2 and ZrO_2 for the oxidative depolymerization of prot lignin (a commercial lignin) and alkali lignin. Results showed that high bio-oil yield was obtained when Co/CeO_2 was used as the catalyst, and high selectivity of acetosyringone was achieved with Co/TiO_2 as catalysts. Cabral Almada et al. (2021) loaded Au and Pt particles on TiO_2 for the oxidative depolymerization of Kraft and ethanol organosolv lignins, and showed that Au-TiO_2 can further oxidize the aromatic hydrocarbons produced by the depolymerization of lignin, resulting in a lower yield of the target product, while Pt-TiO_2 can promote the conversion of lignin into high value-added aromatic hydrocarbons.

Walch et al. (2021) used $VO(acac)_2$ and $Cu(OAc)_2$ as homogeneous catalysts for the oxidative depolymerization of Kraft lignin to high-value aromatics with oxygen. A 50% bio-oil yield and increased production of aromatic monomers were achieved by the use of both catalysts, suggesting the favorable combined effect. Cai et al. (2019b) applied polyoxometalate ionic liquid (POM-IL) catalysts in the oxidative cleavage of lignin aromatic unit. The high yield of diethyl maleate was attributed to the combined catalytic effect with acidic and redox active sites from the POM and IL. Das et al. (2017) tested the catalytic performances of $CoCl_2 \cdot 6H_2O$, $CuSO_4$, $MnN_2O_6 \cdot 4H_2O$, $CrKO_8S_2 \cdot 12H_2O$, and $NiCl_2 \cdot XH_2O$ in the catalytic oxidative depolymerization of lignin in aqueous 1-ethyl-3-methylimidazolium acetate $[C_2C_1Im][OAc]$ with H_2O_2 and found that $CoCl_2$ was the most active catalyst for the production of aromatic compounds from lignin. Whether heterogeneous or homogeneous catalysis, the conversion rate and yield of the catalyst in the depolymerization of lignin model compounds are much higher than that of real lignin. The real lignin has a complex structure with various functional groups and linkages, which cannot be fully simulated by using model compounds.

2.4.2.4 Catalysts from lignin

Lignin can be used as a carbon source to prepare carbon based catalysts through surface modification, loading or doping with other elements. The synthesis of lignin derived catalysts starts from the carbonization of lignin through hydrothermal carbonization or thermal pyrolysis. Due to the low surface area and limited functional groups of the hydrothermal char or pyrolysis char from lignin, post modification such as acid or base treatment is necessary. Elements such as N, P, S and metals doping can further enhance the catalytic activity for the target chemical reaction. Li et al. (2020) prepared a LAC-based solid acid by the activation with KOH and H_2SO_4 sulfonation; and used it for the dehydration of fructose to HMF, achieving a high product yield at 5.7%. In addition to non-metal doping catalyst, metal doped lignin-based catalysts are also used for thermal catalysis, electrocatalysis and photocatalysis. Pt-lignin-based carbon fiber electrocatalyst was prepared by electrospinning and thermochemical treatments and used for alcohol electro-oxidation (García-Mateos et al., 2017). Carbon-based Pd catalysts were prepared by loading Pd particles on the chemical activated kraft lignin with H_3PO_4. The catalyst showed high activity in toluene oxidation (Bedia et al., 2010). A magnetic catalyst with lignosulfonate supported Pd and Fe_3O_4 nanoparticles was developed and applied in aqueous Suzuki-Miyaura reaction, showing high activity for CS(sp^2)-C(sp^2) coupling in water (Nasrollahzadeh et al., 2019). However, the current preparation process of lignin-derived catalysts still faces harsh preparation conditions. For example, the preparation process may use a lot of acids, bases, and excessive metal salts, which may cause environmental pollution problems. Thus, in order to tackle this issue, the development of green preparation processes will be an important future trend.

2.5 Lignin-first pretreatment

Lignin-first pretreatment is a pretreatment method that considers the preservation of both lignin and polysaccharide as the first and foremost aspect in whole biomass valorization. This approach can actively reduce possible side and unwanted reactions that arise from the conventional biorefinery processes. The principle of the lignin-first pretreatment aims at fractionating lignin from the biomass while protecting its structure against condensation and repolymerization(Islam et al., 2020). The general lignin-first pretreatment processes are operated by staged, of which lignin is first extracted from woody biomass by various organosolv or acid-catalyzed pretreatment reactions in order to break the lignin-sugar linkages (Islam et al., 2021). The reactive intermediates are then stabilized by certain chemicals which prevent the formation of reactive functional groups that can lead to lignin condensation. The ether bond linkages of lignin and oligomers are then cleaved into monomers and stabilized through hydrogenolysis (Sun et al., 2018b).

Lignin-first technique in lignocellulosic biomass fractionalization has gained much attention and continued to contribute to the lignin biorefinery development and industry. Among the various techniques, the most common approach is RCF (Sun et al., 2020b). This approach involves the introduction of a transition metal catalyst into pretreatment spent liquor under reductive and inert atmosphere with the presence of hydrogen donors. Significant cleavage of β–O–4 bond can be observed with more than 50% mono-phenolic compounds. Stabilization of reactive intermediates formed during the depolymerization process is achieved by the metal catalyst. Solvent is also crucial for the delignification process and the selectivity of monomers (Renders et al., 2018). Polar solvents are excellent in delignification but may hydrolyze the polysaccharides, being reduced during the hydrogenation process or react with the monomers formed and solvents. Therefore, choosing suitable solvent is essential to attain the most optimal lignin yield and bond cleavage efficiency. The choice of solvents should depend on the targeted monomers and the proportions of cellulose, hemicellulose and lignin in a particular type of biomass. Stabilization of reactive intermediates and aldehyde groups can be achieved by the addition of diol as solvents. Ethylene glycol has been broadly used to trap C2 aldehyde, leading to the formation of acetals. Acetal terminated the aldehyde reactions to form benzylic cations, prevented the condensation and repolymerization reaction (Shuai et al., 2016). A lack of standard protocols in the process and product evaluations have been a great challenge for the performance evaluation that could advance the research field. The exact role of the transition metal catalyst has not been fully understood. Further research of the role and working mechanism of the related catalysts shall improve the reactor design and the related performances behind the reaction.

2.5.1 Reductive catalytic fractionation

Lignin depolymerization occurs to a certain extent in various lignocellulose fractionation methods. Although these methods do not specifically aim for extensive lignin depolymerization, a few fractionation methods are deliberately designed to yield substantially depolymerized lignin products. Among these techniques, RCF stands out as a method that links lignin isolation with effective depolymerization. RCF has been the focus of extensive investigation in recent years. In order to convert the lignin into biofuels using RCF, either the biomass can be directly put into the reactor or the lignin from biomass can be fractionated first and then put into the RCF reactor.

RCF allows for the total use of the biomass while particularly emphasizing the lignin part, which is sometimes overlooked by conventional methodologies (Parsell et al., 2015). This process of converting lignin to monomers consists of 3 stages: Lignin extraction/fractionation, depolymerization and stabilization. The first stage involves removing the lignin component from the biomass focusing on preserving lignin structure and the bonds specifically the β–O–4 linkages. In the second stage, the lignin is broken down into monolignols or the monomers under a reductive environment and finally, in the third stage, the monomers are stabilized in a catalytic environment (Jindal et al., 2023a). The three components that are absolutely necessary for an RCF type biorefinery to function are (a) lignocellulosic biomass, (b) an alcoholic solvent (cyclic type ether), and (Wang et al.) (c) a heterogeneous type redox-active catalyst. These are usually introduced to a highly pressurized reactor that is heated for around 2 to 6 hours at 180 to 250^{O}C. Heating triggers the lignin in the biomass to be extracted solvolytically, which is followed by limited fragmentation due to cleavage of ether bond. The reactive, unsaturated fragments produced by this first solvolysis process are prone to repolymerization. These unstable molecules are thus reductively stabilized by the redox active catalyst, which may also cause depolymerization (hydrogenolysis of remaining ether linkages) (Renders et al., 2019). The catalyst (redox-active) is not necessary for lignin extraction; this process is purely dependent on the solvolytic conditions. On the other hand, the heterogenous catalyst is the only factor that controls the reductive stabilization of the unsaturated fragments.

In the RCF, the depolymerization step, which follows two distinct pathways - solvolytic depolymerization (in which a hydrogen donor specie is used to provide hydrogen for reaction) and catalytic hydrogenolysis (high pressure hydrogen gas is used) is a bit complicated (Kumaniaev et al., 2017). It has been demonstrated that lignin depolymerization happens principally solvolytically under pretty harsh conditions (e.g., methanol, 250^{O}C), producing coniferyl type and sinapyl type alcohols as reactive intermediates (Van Den Bosch et al., 2017b). Coniferyl and sinapyl alcohols are thought to be formed through homolysis of β–O–4 links, according to such type of intermediates, which have similarly been seen in research using model compounds in solvolysis. The job of the catalyst material is restricted to the stabilization of the reactive species under mild RCF conditions (Anderson et al., 2017). In contrast, solvolytic bonds scission happens much more slowly under milder conditions (such as methanol at 190°C), and the catalyst also accomplishes hydrogenolysis of the various inter-units ether connections. It is crucial to understand whether solvolytic or catalytic cleavage of ether bonds occurs more frequently in order to structure the pathway (Kishimoto & Sano, 2002).

The success of lignin depolymerization in RCF is influenced by various factors, including the choice of solvent (Renders et al., 2016), additives (Huang et al., 2017), (Chesi et al., 2016), reaction temperature (Schutyser et al., 2015), and lignocellulose source. The yield of lignin products, degree of the delignification process, and carbohydrate preservation in the pulp are strongly dependent on these factors. Recent research findings indicate that lignin depolymerization predominantly occurs via solvolytic reactions, particularly utilizing methanol as a solvent. The catalyst's primary function is to stabilize the reactive intermediates reductively, effectively preventing repolymerization from taking place. Consequently, this activity yields depolymerized lignin oil that is abundant in the phenolic type monomers, dimers, as well as oligomers. Additionally, a solid pulp of carbohydrate is generated, which can be further utilized and transformed into valuable products (Anderson et al., 2016). Besides this, the focus of previous studies on lignin depolymerization primarily revolves around the production of various chemicals and the transformation of bio-oils using catalyst materials. Heterogeneous catalysts play a critical role in the catalytic hydrogenation of lignin, with several main types being employed, including noble-metal catalysts, non-metal catalysts, nickel-based catalysts, metal oxides, and some multi-metal composite catalysts. Scientists primarily concentrate on the liquefaction process and depolymerization of lignin, employing various catalyst materials to achieve higher rates of conversion and increase the yield of bio-oil or phenolic products. Noble-metal catalysts, such as Ru, Pt, Rh, and Pd, have demonstrated substantial catalytic activities in hydrogenolysis of the Carbon-Oxygen ether bonds (Bjelić et al., 2019) and hydrogenation of the aromatic rings found in the liquid product. Pepper et al. (1969) also investigated various catalysts (Pd/C, Raney Ni, Rh/C, Ru/C, Rh/Al_2O_3, Ru/Al_2O_3) for the hydrogenation process of lignin. Amongst the various catalyst materials, Rh/C demonstrated the highest yield of monomeric products, including 4-propylguaiacol and dihydroconiferyl alcohol (Pepper & Lee, 1969).

In addition to various parameters, different feedstocks have been investigated in RCF studies. A clear correlation has been observed between the lignin sulfur (S) content, which represents β–O–4 ether contents in lignin, and the monomeric yield (Mottiar et al., 2016). Higher amount of β–O–4 ether content in lignin leads to increased monomeric yields. This trend has been consistently observed in various woody substrates. Hardwoods generally exhibit monomer yields exceeding 30 wt%, with yields exceeding 50 wt% reported frequently, whereas softwoods typically yield below 30 wt%. Herbaceous crops typically fall within the range of 20 to 40 wt% yield, although some exceptions exist (Huang et al., 2016). These findings demonstrate the influence of feedstock type on reductive processing in RCF. The RCF for monolignol production has first been applied on the conversion of woody biomass. Van den Bosch et al. (2015) applied RCF on birch wood and produced about 50% yield of respective set of monomers over Ru/C and Pd/C catalyst (Van den Bosch et al., 2015a). Recently, RCF studies have begun to characterize and study unusual lignin rich biomass such as fruit and nutshell waste, with the focus to be used as sustainable feedstock for lignocellulosic biorefineries. The different studies are presented in **Table 2.2** and has shown promising results in monomer yield.

Table 2.2: RCF studies on different biomass with optimized parameters

Biomass	**Pretreatment**	**Type**	**Catalyst**	**Solvent**	**Time (hrs)**	**Temp (°C)**	**Pressure (bar)**	**Monomer yield (biomass)**	**Monomer Yield lignin basis(%)**	**Monomer Products**	
Vanilla seed	Flow through extraction	Extractive free biomass	Ni/C	Methanol	3 to 16	200- 250	30	-	6.13 - 7.90 (wt % extracted biomass)	Propyl Catechol, Propenyl Catechol	(Stone et al., 2018)
Hemp hurd	-	Extractive free biomass	Pd/C	Methanol/water	-	200	_	-	38.3	4-Ethyl guaiacol, 4-Propylguaiacol, 4-Propanolguaiacol, 4-Ethylsyringol, 4-propylsyringol, 4-Propanolsyringol	(Muangmeesri et al., 2021)
Plum	-	Extractive free biomass	Ru/C	THF	15	250	40	117.2	32	4-Ethylguaiacol, 4-Propylguaiacol, 4-Ethylsyringol, 4-propylsyringol	(Behaghel de Bueren et al., 2020)
Apricot	-	Extractive free biomass	Ru/C	THF	15	250	40	97.2	28	4-Ethylguaiacol, 4-Propylguaiacol, 4-Ethylsyringol, 4-propylsyringol	
Peach	-	Extractive free biomass	Ru/C	THF	15	250	40	72.1	20	4-Propylguaiacol, 4-Ethylguaiacol, 4-Propanolguaiacol, 4-propylsyringol, 4-Ethylsyringol, 4-Propanolsyringol	
Cherry	-	Extractive free biomass	Ru/C	THF	15	250	40	89.6	24	4-Ethylguaiacol, 4-Propylguaiacol, 4-Propanolguaiacol, 4-Ethylsyringol, 4-propylsyringol, 4-Propanolsyringol	
Hazelnut	-	Extractive free biomass	Ru/C	THF	15	250	40	44.4	11	4-Propylguaiacol, 4-Ethylguaiacol, 4-Propanolguaiacol, 4-propylsyringol, 4-Ethylsyringol	
Walnut	-	Extractive free biomass	Ru/C	THF	15	250	40	72.2	16	4-Ethylguaiacol, 4-Propylguaiacol, 4-Propanolguaiacol, 4-Ethylsyringol	

Almond	_-	Extractive free biomass	Ru/C	THF	15	250	40	65.3	21	4-Ethylguaiacol, 4-Propylguaiacol, 4-propylsyringol, 4-Propanolsyringol	
Castor seed coats	Enzymatic and mild acidolysis	C- Lignin	Ru/ZnO/C	Methanol	4	200	30	_-	18	Propenyl Catechol (major product), Propyl Catechol, Catechylpropanol, Pyrocatechol	(Wang et al., 2021b)
Castor seed coats	-	Extractive free biomass	Ru/C, Pd/C, Ni/C	DES	4	180-200	30	56.3	_-	Propyl Catechol (major product), Propenyl Catechol, Catechylpropanol	(Liu et al., 2021a)
Castor seed coats	-	Extractive free biomass	Ru/ZnO/C	Methanol	4	200	30	65	6.5 (wt % extracted biomass)	Propenyl Catechol (major product), Propyl Catechol	(Song et al., 2022)
Flax Shive	-	Raw biomass	Ru/C	Ethanol/Isopropanol	3	225	40	_-	10.2	4-Propylguaiacol,4-Ethylguaiacol, 4-Propanolguaiacol, 4-Ethylsyringol, 4-Propanolsyringol, 4-propylsyringol	(Kazachenko et al., 2020)
Wheat Straw	-	Extractive free biomass	Ru/C	Methanol	3	250	30	_-	25.2	Guaiacol, Syringol, 4-Methyl syringol, 4-Ethyl guaiacol, 4-Ethyl syringol, 4-Methyl guaiacol, 4-Propenyl guaiacol, 4-Propyl guaiacol, Propanol guaiacol, 4-Propanol syringol, 4-Propenyl syringol, 4-Proyl syringol	(Brienza et al., 2022)
Walnut	Enzymatic and mild extracted milled lignin	Lignin	Ru/C	Methanol	3	250	60	_-	25	4-Propylguaiacol, 4-Ethylguaiacol, 4-Propanolguaiacol, 4-propylsyringol, 4-Ethylsyringol, 4-Propanolsyringol	(Wang & Deuss, 2021)
Walnut	-	Extractive free biomass	β-zeolite	Ethanol/water	3	200	10	30	9.4	4-Ethylguaiacol, 4-Propylguaiacol, 4-Propanolguaiacol, 4-Ethylsyringol, 4-propylsyringol, 4-Propanolsyringol	(Kramarenko et al., 2021)
Candlenut	Organosolv	Lignin	Cu-PMO	Methanol	8 to 20	140-220	40	_-	63.7 % of catechols	Propyl Catechol, Propenyl Catechol, Catechylpropanol	(Barta et al., 2014)
Empty palm fruit bunch	Dilute nitric acid	Lignin	Cu/Al2O3	Methanol	1	180	70	_-	37	Benzoic acid, 4-methyl catechol, syringaldehyde, Vanillin, Sinapic acid, Acetovanillone, p-ydroxybenzaldehyde, others	(Chakraborty & Lali, 2021)
Vanilla seeds	Enzymatic and mild acidolysis	C- Lignin	Pt/C	Methanol	15	200	40	-	95 % on basis of caffyl alcohol	Catechylpropanol (major product), Propyl Catechol, Propenyl Catechol	(Li et al., 2018b)

2.5.1.1 Batch and Continuous Flow Reactors

The majority of previous studies on RCF have primarily focused on lab-scale batch reactors due to their ease of implementation and flexibility in varying process parameters. The RCF processes performed in the batch reactors can produce near maximum theoretical yield of lignin oil that is rich in lignin monomers (Khan et al., 2023). While batch systems have shown excellent performance, they possess inherent disadvantages. In batch reactors, multiple reaction steps occur simultaneously in a single chamber, thus making it challenging to study the different reaction steps and kinetics. The mixing of catalyst and biomass makes it difficult to recover the catalyst from the pulp thus complicating the in-depth details of solvolysis and catalysis (Cooreman et al., 2020). Additionally, the non-continuous cycle of operations, difficulties in separating the end products, catalysts, and the remaining biomass, mechanical disruption of biomass during stirring, and the slow heating profiles further limit their advantages compared to flow-through processes (Abu-Omar et al., 2021).

RCF in flow-through systems (FT) has been introduced with separated feedstock and catalyst beds during operation (Figure 2.6). In the FT reactors, the solvent is first passed at high temperature through the biomass bed, which partially extracts and depolymerizes the lignin polymer. The resulting mixture, that contains the reactive lignin intermediates, is then directed towards the catalyst bed to further depolymerize and stabilize the reactive lignin species. The decoupling of biomass and catalyst beds allows for straightforward separation and different conditions for each RCF step. The FT systems are particularly advantageous when targeting large-scale production (>10 ktons per year) as they offer cost-effectiveness and scalability. Furthermore, FT systems have been recognized by IUPAC as a key technology for enhancing sustainability in the chemical industry, with inherent safety advantages (Gerardy et al., 2020). Compared to batch reactors, the FT setup facilitates easier monitoring of solvolytic extraction and reduction over short time intervals, making it more suitable for kinetic investigations. However, it is important to consider the variation in composition and concentration of the liquid product stream to the catalyst bed over time as the lignin content of the biomass decreases. Despite this consideration, independent insights gained from kinetic analysis can still provide valuable support for RCF upscaling.

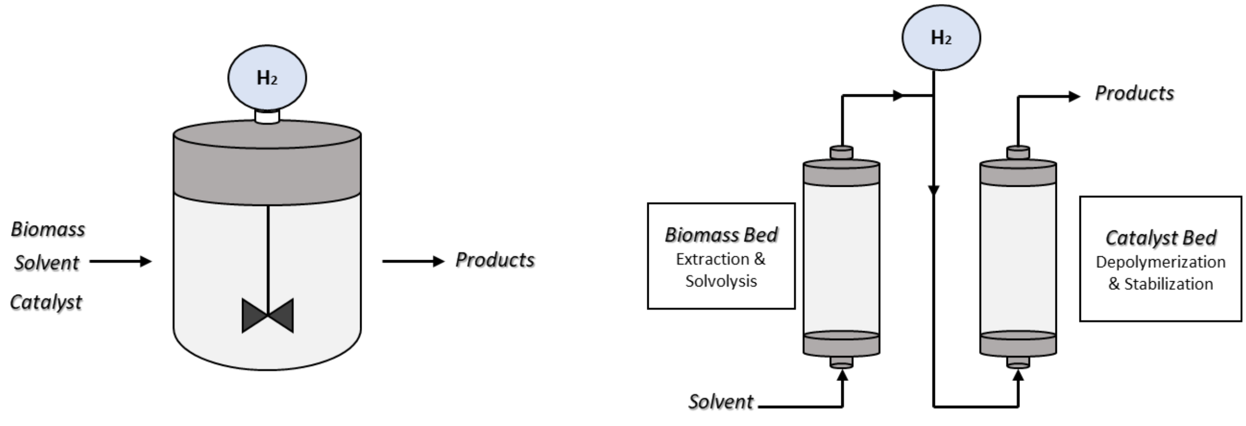

Batch Reductive Catalytic Fractionation **Flowthrough Reductive Catalytic Fractionation**

Figure 2.6: Representation of Batch and Flow through reductive catalytic fractionation process.

There is limited reports on RCF in flow-through systems. One of the studies combined a traditional batch solvolysis approach with catalytic flow hydrogenation of lignin, demonstrating improved product selectivity (>80%) in the FT-RCF system compared to the batch system (Li et al., 2019b). Kumaniaev et al. conducted a study on reductive lignocellulose fractionation in an FT reactor by separating the extraction and hydrogenolysis processes through the coupling of two systems, resulting in a maximum monomer yield of 31 wt% (Kumaniaev et al., 2017). In another study, Brandner et al. employed FT solvolytic extraction of lignin in combination with batch, in situ, and ex situ FT-RCF, showing that FT systems enable the production of lignin with native-like characteristics (Brandner et al., 2021). From the above studies it should be noted that the application of FT systems in lignin valorization is still in its early stages and to address certain challenges, it is crucial to develop an integrated reactor design that encompasses the advantages of both systems for future scale-up which should offer continuous operation, facilitate easy separation of biomass and catalyst, ensure efficient mass transfer, and provide prolonged catalyst and solvent lifetimes.

2.5.1.2 One-pot RCF

One-pot RCF enables the transformation of the whole lignocellulosic substrates in a single step. The processes do not involve the fractionation of lignin separately since both the lignin part and the carbohydrate part are transformed and solubilized. This streamlined approach simplifies the biorefinery deconstruction process but transfers the separation complexity to downstream processes, possibly limiting the adaptability of biorefineries due to the interdependence of the carbohydrate sugars and lignin segments. However, a few cases have documented that the productivity of the process majorly rely on the specific catalytic process which is being used and the system conditions employed. Li et al. proved that one-pot RCF process using a Ni-W2C catalyst supported by carbon in aqueous media, that resulted in the conversion of the lignin part into methoxyphenols substituted with propyl- and propanol, while the carbohydrate sugars were transformed into sugar alcohols (Li et al., 2012). Another study demonstrated one-pot transformation of sawdust into drenched alcohols using supercritical methanol. In this process, a Cu-doped spongy catalyst (PMO) facilitated the transformation of lignin and carbohydrates into replaced cyclo-hexanols and aliphatic alcohols with carbon ranging from 2 to 6, respectively

(Matson et al., 2011). Liu et al. productively converted numerous lignocellulosic feedstocks into wide range of alkanes (hexanes from cellulosic fraction and pentanes from hemicellulosic part) and some alkylated methoxyphenols as well (from lignin) using Ru/C and $LiTaMoO_6$ as catalysts in aqueous phase phosphoric acid (Liu et al., 2015). Furthermore, Xia et al. demonstrated that one-pot transformation of diverse lignocellulosic feedstocks to produce alkanes using a catalyst $Pt/NbOPO_4$ in cyclohexane as solvent. All three major components like Cellulose, hemicellulose, and lignin were transformed into hexanes, pentanes, and the alkyl cyclohexanes respectively (Xia et al., 2016). Notably, this process achieved high biomass conversion even at mild temperature condition (190 °C) and employed cyclohexane as solvent, which is typically acknowledged for its limited lignin solubility.

2.6 Chemicals from lignin

Comparing all the key types of renewable energy techniques that are researched till date, it has been observed that lignocellulose biomass is contemplated an essential source for creating renewable fuels for air, road, and marine transport (Patel et al., 2019). Recently, scientists from all around the world have been looking into the idea of biorefineries, which might turn lignocellulose biomass into competitively priced bio-based fuels and other potential valued products like biochemicals, organic acids, polyhydroxyalkanoates (Neeraj et al.), and bioplastics (Usmani et al., 2021). The three major classes of the valued products produced from the lignocellulose biomass are biofuels, biochemicals and bioproducts.

2.6.1.1 Biofuels

Biofuels, together with enhanced energy proficiency and the use of other fuels, are viewed as one solution for addressing rising energy costs. Many operational facilities generate power using biomass fuels like agriculture waste, wood waste from forestry, and other plant matter (Nunes Ferraz Junior et al., 2022). These biofuels include bioethanol, biodiesel, sustainable aviation fuel / jet fuel, biobutanol and biogas (Ashokkumar et al., 2022). (Ben et al., 2015) studied biofuel production from pine wood and pine bark. They reported weight average and number average molecular weight distribution of the bio-oils produced to be 447 g/mol and 170 g/mol for the pine bark and 293 g/mol and 119 g/mol for pinewood, respectively. It has also been reported that 20.2% light oil, 30.7% heavy oil and 14.5% biogas can be produced from pyrolysis of pine bark whereas, 21.9% light oil, 35.1% heavy oil and 16.3% biogas can be produced from pinewood pyrolysis at 600^{O}C.

Among the other biofuels, the low-carbon replacements for sustainable aviation fuel (SAF) that can be produced from lignocellulose biomass sources have recently obtained a lot of attention. Common organic chemical components of jet fuel include aromatics, paraffins, olefins, and naphthenes. SAF is produced from the depolymerization of lignin into its constituent monolignols and hence aromatics using RCF or hydrodeoxygenation. The oil hence produced contains fractions of the chemical components of jet fuel and are hence purified to be used as additives to conventional aviation fuels (Emmanouilidou et al., 2023).

2.6.1.2 Bioproducts

Lignin, as a component of biomass, is a renewable source of chemicals and other goods. This explains why lignin prices remain generally consistent throughout time and seasons. Although the prices for lignin can vary significantly based on factors such as geographical location, purity, and market conditions. In terms of purity, the price range for lignin ranges from low purity (50-280 USD/MT) to high purity (750 USD/MT). Lignosulphonates range in price from 180 USD/MT to 500 USD/MT, whereas lignin from the Kraft process has a market value of 260-500 USD/MT (Abbati de Assis et al., 2018). Soda lignin made from sulphur-free lignins is less expensive, costing between $200 and $300 per metric tonne. Organosolv lignin is priced somewhat more, starting at 280 USD/MT and reaching 520 USD/MT (Hodásová et al., 2015).

Table 2.3: Value-added bioproducts derived from lignocellulosic biomass

Lignin Biproducts	Structure/Formula	Properties	Relevant Applications	References
Carbon Nanotubes (CNTs)	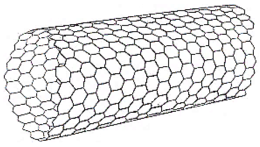	High tensile strength of 1.33 GPa and enhanced electrical conductivity of 1.19×10^5 S m^{-1}	Water / Wastewater Treatment	(Liu et al., 2022a; Rahzani et al., 2017)
Activated Carbon	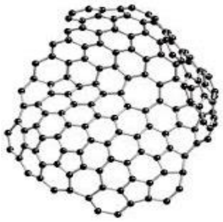	Increased Surface area and Pore volumes of 2000 m^2 g^{-1} and 1 cm^3 g^{-1}	Adsorption applications	(Demuner et al., 2019)
Graphene Quantum Dots	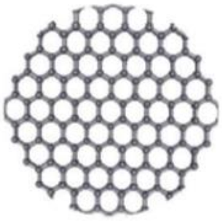	Excellent photoluminescent properties	Bioimaging, Anti-counterfeiting, Water Treatment, Energy devices	(Ghazali et al., 2023; Xu et al., 2016)
Biochar pellets	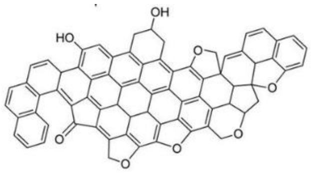	Higher adsorption capacities, High calorific value 31.49 MJ kg^{-1}	Water / Wastewater Treatment	(Wang et al., 2020a)

Nanocomposites	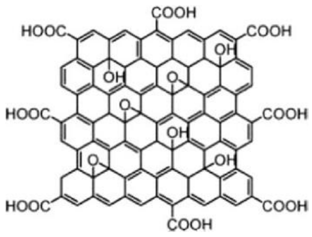	Non-toxic, High chemical stability, Resistance to degradation, Antioxidant potential	Photocatalysis, UV protection, Antimicrobial agents, Cosmetics, Super capacitors, Pharmaceuticals	(Kaur et al., 2021; Khan et al., 2024; Tse et al., 2022; Zhang et al., 2021c)
Dispersants and Adhesives	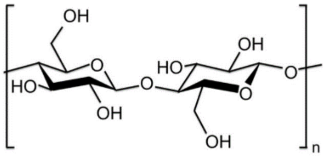	Uniform distribution, Better stability, High surface charge, Hydrophilic, Molecular weight from 8.1 to 14.8 kDa	Cosmetics, Construction and Plastic Industries, Pharmaceuticals	(Qin et al., 2015; Wang et al., 2023a)
Bioplastics	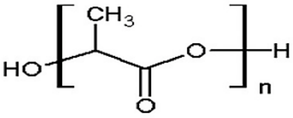	Increased grease resistance, Antibacterial, Antioxidant, High mechanical strength, UV stability, Fire resistant	Packaging applications	(Patria et al., 2024; Tedeschi et al., 2020)
Aerogels	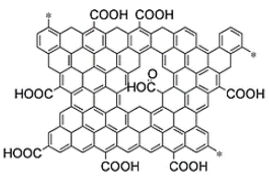	Specific capacitance of 504.7F g^{-1}, Power density of 16000 W kg^{-1}, High stability of 87.7% after 10,000 cycles, High specific surface area of 3742 m2 g^{-1}	Supercapacitors, Pulp and paper industry,	(Jõul et al., 2024; Wang et al., 2023b)

2.6.2 Current progress in valorization of lignin to high value materials

Recent research has functionalized lignin with various groups of chemicals which introduced new properties to lignin. The research roadmap and related product values toward future applications have been demonstrated in **Figure 2.8**. The most important lignin derived materials reported in recent years, including carbon fibers, resins, plastics, adsorbents, and energy storage devices, have been reviewed in the following section.

Figure 2.8: Roadmap of recent advanced of lignin valorization technologies. Key references for adhesives (Wei et al., 2019); adsorbent (Zhang et al., 2020); carbon fiber (Bengtsson et al., 2019); plastics/hydrogel (Dai et al., 2020); electrodes (Chaleawlert-

umpon & Liedel, 2017); colored lignin (Zhang et al., 2018a); and pharmaceuticals (Domínguez-Robles et al., 2020)

2.6.2.1 Carbon fibers

Carbon fibers (CFs) have attracted tremendous recent research interests due to their unique physical and chemical properties, while approximately 90% of the commercial CFs are manufactured from non-renewable polyacrylonitrile (PAN) (Patil et al., 2013). Lignin with its excellent physiochemical properties has served as a cost-effective and green precursor for CFs production. Production of lignin-based carbon fiber (LCFs) can be with high carbon efficiency and the carbonization is with no toxic emissions during the manufacturing process (Zhang et al., 2019b). Various technical lignins have been investigated as potential CF precursors, such as Kraft lignin (Otromke et al., 2019), organosolv lignin (Sun et al., 2016), and ionic liquid extracted lignin (Vincent et al., 2018). Sun et al. (2016) reported the synthesis of LCFs with novel microstructures, excellent mechanical properties, fiber diameter (30-80 μm) using chemical modification and/or physical blending. With the properties, Mandeep et al. (2020) stated the huge exploitation potential of LCFs for a wide variety of applications, such as supercapacitors, separation, electrodes, catalysis and dye-synthesized solar cells.

Despite all this progress of LCFs production, LCFs were struggling at lab-scale due to long stabilization time and low mechanical performance as compared to PAN-based CFs. The tensile strength of LCFs was less than 500MPa, and the highest reported value was ~1,200 MPa, much lower than that of PAN-based CFs in the range of 3-7 GPa. The lower mechanical strength was attributed to intrinsic heterogeneity of lignin structure, wide molecular weight distribution and low purity. By altering molecular orientation, structure modification, precursor pretreatment the mechanical performance of LCFs were further enhanced (Li et al., 2017a). The LCFs prepared by further optimizing the molecular weight of lignin had an average tensile strength and modulus of 1.39 GPa and 98 GPa, respectively. The study represented the LCFs with the highest mechanical properties ever obtained from low cost, chemically unmodified lignin (Jin et al., 2018), although the final properties of LCFs are not up to the mark due to its diversity, heterogeneity.

The high manufacture cost has also limited the wide production of LCFs, even though lignin itself is inexpensive. In order to address these challenges, the future trend of lignin chemical modification should focus on increasing molecular weight and polymer linearity by grafting lignin onto different polymers or via polymerization or copolymerization. More works are needed with the main focus on further investigating thermo-stabilization and carbonization of lignin fibers as currently both the mentioned processes are simply based on using PAN fibers as a reference. The other properties of LCFs such as electronic conductivity and thermal resistance should also be studied in order to excavate the other possible applications of LCFs. More efficient pretreatment methods should be adapted in order to extract and purify lignin with less impurities at low costs.

2.6.2.2 Plastics and resin

The production bio-based materials, specifically lignin or lignin-derived monomers has drawn an enormous interest among the scientific community. Lignin has been used for the polymer production such as polyurethanes, phenol-formaldehyde resins, polyesters, and phenolic and epoxy resins, typically by the various modifications in its chemical structure or as copolymers, blends, and composites (Rajesh Banu et al., 2019). Organosolv lignin has been successfully used as a 3D printing ink when mixed with nylon, revealing that lignin could improve the printability of the structure by reducing the melt viscosity and thus enhancing its stiffness and tensile strength (Nguyen et al., 2018).

From the structural perspective of lignin and the similarity between polyphenolic lignin and phenol, there has been extensive research on where lignin is used in the preparation of phenolic resins (Chen et al., 2020). The main focus of the recent related researches, in summary, is to synthesize purified, functionalized, and fractionated lignin with higher reactivity for application in phenolic resin systems. However, the substitution rate of classic phenols using lignin-based resins is still limited, partially due to incomplete depolymerization and high diversities of monolignols in the reaction products. A more comprehensive pretreatment and depolymerization process is needed by the integration of various techniques. In addition to polyphenolic resins, epoxy is also of immense importance. The use of lignin in the composition of epoxy resins is a natural fit as such renewable precursors are responsible for the strength and rigidity of the molecular architectures. Therefore, the production of epoxy precursors based on lignin, has been widely reported and reviewed accordingly (Banu et al., 2019). Generally, lignin with low molecular weight, low glass-transition temperatures (Panovic et al.), and high polydispersity with high phenolic-hydroxyl group content, would be more preferred for resin production. However, the synthesis of epoxies from lignin is complicated by the varied reactivity resulting from epoxy groups created from the crosslinked structure of lignin. Applying lignin with lower molecular weights for epoxy resins may create critical impacts to the properties of the epoxy resins products (Diaz-Baca & Fatehi, 2021).

To sum up, a large variety of promising methods and approaches have been developed with high scientific interests in lignin based adhesives; but how to obtain lignin-rich phenolic compounds with higher reactivity at low cost and in an environmentally friendly manner still remain challenging. For 3D printing, the lignin-based feedstock needs to be benchmarked against established feedstock to assess feature resolution and shape-forming flexibility. A holistic approach towards the specific goal and application is most recommended. While the science and engineering of lignin 3D printing is valuable new knowledge as itself, it will be in as valuable as it paves the way to commercial utilization of lignin.

2.6.2.3 Adsorption materials

Lignin have been known as a suitable precursor in the synthesis of activated carbons (LAC) for the adsorption of dyes, organics, gases, and metals (Lee et al., 2018). Derived from acid hydrotropic lignin, alkali lignin, and lignosulfonate the surface area of LAC achieved more than 2,000 $m^2 \cdot g^{-1}$ by phosphoric acid at moderate temperature (450°C) (Yang et al., 2020). The application of lignin and its derivatives for adsorption covers a wide range of chemicals such as air pollutants, dyes, and metals (Supanchaiyamat et al., 2019). In addition to LACs, lignin-based hydrogels have also been synthesized for water purification (Thakur et al., 2017) and tissue engineering (Figueiredo et al., 2018). Overall, LACs and lignin-based hydrogels are with comparably high surface areas and pore volumes similarly to the commercial activated carbon. More studies are expected with special emphasize on cross-linking, grafting, copolymerizing, and hybridizing to develop more advanced lignin adsorbents.

Despite of the outstanding properties and performances, lignin derived adsorbents however still face significant challenges toward full-scale commercialization. Even though lignin from pulp industry is a low cost feedstock, activated carbon is also with variable or even marginal market values. There are many other low-cost and sustainable carbon materials to be applied as the precursor of adsorbents. The sources of current activated carbon are generally agricultural waste (*e.g.*, coconut shell biomass), which is also a non-fossil based carbon as lignin. The technique is green and established. Even with carbohydrates, similar practices applied on lignin may also be used on raw biomass. Lignin based adsorbent need to provide extraordinarily outstanding or biomass-specific functions in comparing with other carbon materials, such as selectivity, costs, and recyclability. Its applicability may otherwise be limited in certain applications or industries. More studies would be critical on the sustainability and economic aspects of the lignin based adsorbents in the future.

2.6.2.4 Energy storage applications

In order to meet the fast growing demands of the energy storage market, lignin has been utilized as electrochemical electrodes in batteries and supercapacitors, *e.g.*, the expander of lead-acid batteries and organic cathodes in lithium batteries (Luo et al., 2018).

Supercapacitors are more favorable than batteries because of their high-power density and long lifespan. Along with the other unique properties of lignin, the high abundance of oxygen-containing functional groups on the surface of processed lignin could offer extra pseudo capacitance in such materials (Yun et al., 2019). The research related to the uses of various types of lignin for energy storage devices development has increased enormously, but it is still very challenging for applying it in commercialized rechargeable batteries and fuel cells. With the expectation of boosting demand of energy storage and usage, more detailed techno-economic analysis of new lignin-derived materials is required to identify the bottlenecks of the process for further study.

2.7 Downstream processing of lignin products

The various valued products produced from lignin have already been discussed in the previous section. However, these products are not in their pure form to be used as substitutes. Hence, downstream processing and purification is an important step that has gained quite serious interest of the scientific community. Lignin is a hetero-polymer which consists of more than one repeating units with different linkages, resulting in lengthened retention time and high energy consumption for separation. Different methods have been developed in order to ease the separation methods and reduce the energy used during the separation methods. Gomes and Rodrigues (2019) adopted resins and ultrafiltration methods to separate vanillin, vanillic acid, and acetovanillone from the reaction mixture due to the differences in polarity. The authors have also utilized low toxicity solvent extraction methods aiding with crystallization under mild pH conditions (Gomes & Rodrigues, 2020). Anion exchange chromatography was also adopted to separate vanillin from the monolignol mixture with amination and pH workup (Liu et al., 2020).

Separation of lignin monomers are usually performed by gas chromatography and liquid chromatography techniques, which utilize inert gas and mixed solvent systems for product separations. However, a small volume of reaction mixture can only be inserted for chromatographic separations. The separation methods of monomers derived from lignin depolymerization are scarce to the best of our knowledge. Non-ignorable and undesirable proportions of dimers having small molecular weight and high molecular weight compounds, including oligomers and unaltered hemicellulose, are additionally found in the phenolic products containing monomer-rich lignin oils after depolymerization and further increases the difficulties in separating products from reaction mixture. Therefore, it is crucial to develop novel techniques for the isolation of lignin monomers, and potentially of the other elements as well, to enhance downstream processing effectiveness (Sun et al., 2020a).

2.7.1 Liquid-liquid extraction

One of the very popular techniques for the preparation of lignin based oils is liquid-liquid extraction. For example, ethyl acetate along with water can be effectively employed to isolate lignin species having lower molecular weight (Van den Bosch et al., 2015b). It was showed that hexane is an efficient extraction solvent, particularly for the cleansing of nonpolar 4-alkylphenolics (Wang et al., 2018a). To avoid this downstream liquid-liquid separation, n-Butanol and water were used as solvents during the treatment of raw lignocellulose in the existence of a hydrogen environment and a Ru on C catalyst. Both lignin and hemicellulose were concurrently extracted and depolymerized using this ingenious co-solvent mixture, and after cooling down, the organic (n-butanol) phase and aqueous phase spontaneously segregated. This technique presents a superficial and efficient approach for fast segregation of lignin-derived phenolic compounds in the n-butanol phase which is an organic phase from the aqueous phase containing hemicellulose-derived polyols (Renders et al., 2018).

2.7.2 Membrane filtration

Industrial lignin have been fractionated and purified using membrane technology. Applying Raney-Ni catalyst and isopropanol as a hydrogen donor system, membrane separation technique for the fractionation of lignin produced by a unique process Catalytic Upstream Biorefining (CUB) was investigated. The lignin stream was separated and concentrated using a two-stage cascade method, which produced lignin-rich fraction, a high molecular weight as retentate and a filtrate containing low molecular weight monophenol-rich fraction (Sultan et al., 2019b).

2.7.3 Distillation

Distillation being one of the oldest and very significant isolation practices in labs and industry, thus incorporating it for the lignin first biorefineries is crucial. A distillation strategy for rapidly purifying complicated recovered lignin oils containing monomer-enriched hexane was developed (Koelewijn et al., 2018). The system consisted of two stages, n-hexane was eliminated in the initial atmospheric distillation column, and 4-propylguaiacol and 4-propylsyringol were subsequently segregated after traversing a second stage of vacuum column. The study publicized a 94.5% by weight retrieval yield of 4-propylsyringol having purity of 98.4% while about 100% recovery yield of the monomer 4- propylguaiacol with purity of 67.3%.

2.7.4 Column chromatography

Another approach to successfully extract certain monomers of analytical purity from lignin oil is column chromatography. Barta and co-scientists extracted the principal product 4-propanolguaiacol 6.9% by weight from depolymerized pine wood utilizing flash column chromatography employing the solvent pentane integrated with ethyl acetate acting as eluent. A second sample acquired from maple wood depolymerization contained two principal constituents 4-propanolguaiacol and 4-propanolsyringol, which were yielded 4.2% and 6% by weight, respectively (Sun et al., 2018a). Bruggen and Sels reported 98% pure 4-propylguaiacol with isolation yield of 34% from birch wood chips depolymerization (Koelewijn et al., 2018).

2.8 Summary

This chapter provides a summary of recent studies and industrial advancements in the field of lignin valorization. It highlights the potential of lignin-based aromatics as a viable alternative to, or substitute for, petroleum-based aromatics and explores the ongoing research on lignin structures, reaction routes, important linkages, fractionation and depolymerization technologies, and downstream processes, all aimed at harnessing the potential of lignin products in novel applications. Furthermore, the importance of lignin isolation methods such as RCF is highlighted in order to achieve high yields of lignin while preserving its reactivity. The chapter underscores the significance of further research and innovation in the field of lignin valorization to unlock its full biorefinery potential and promote its integration into a more sustainable industrial landscape.

Chapter 3. Influence of Process Design and Control of Biomass Pretreatment and RCF on the Quality and Yield of Lignin

3.1 Introduction

In conventional biorefinery processes, lignin is considered a major hindrance of cellulase, xylanase, and other enzymes in accessing cellulose and hemicellulose for producing fermentable sugars. Consequently, many pretreatment strategies were developed to mitigate, modify, or degrade the lignin through biomass fractionation (Liu et al., 2016). However, those processes showed little to no concern for the fate of the lignin as a valuable substrate (Mosier et al., 2005). Over the years, there is an increased emphasis on obtaining reactive lignin and converting it into biofuels and biochemicals. Extensive research has been dedicated to efficiently isolate lignin with minimal structural degradation, aiming to maximize the efficiency of biomass valorization and to improve the economic viability and sustainability of biorefineries (Khan et al., 2022).

Among the various pretreatment methods, the organosolv lignin extraction has emerged as a promising, environmentally-friendly, and non-destructive delignification technique (Van den Bosch et al., 2015b; Zhang et al., 2016; Zijlstra et al., 2020). This non-destructive nature is particularly advantageous as it helps preserve the crucial β–O–4 linkages in lignin, which are essential for downstream lignin utilization (Van den Bosch et al., 2015b). Another notable approach is the application of biphasic pretreatment systems, which physically separate lignin, cellulose, and hemicellulose from inhibitors during the pretreatment process. In addition to these strategies, the concept RCF has gained momentum, which focuses on obtaining reactive lignin. Unlike the conventional approaches that passively obtained lignin and required multiple steps to enhance its reactivity, RCF involves direct utilization of biorefinery processes for extracting lignin (Liu et al., 2021b; Xu et al., 2022). Consequently, researchers have explored the conversion of lignin into aromatic monomers (Deuss et al., 2015; Rinaldi et al., 2016a) through RCF of the original biomass, which offers milder conditions compared to lignin upgrading (Huang et al., 2017). However, gaining a comprehensive understanding of the relationship between the different pretreatment and RCF process conditions and their impacts on the main biomass constituents is crucial for steering and modifying biorefineries towards desired outcomes. In Chapter 3, fruit and nutshell wastes have shown their potentials in lignin biorefinery, and mango seeds have showed highest monomer yield (37%) among those fruit and nutshell biomass. This unique biomass was further justified by the substantial global consumption of mangoes and the generation of significant waste volumes during industrial processing (Henrique et al., 2013). Also, for the purpose of comparative evaluations of different pretreatment technologies and to gain insights into the pretreatment mechanisms by eliminating substrate variability, we specifically chose mango seed as the sole biomass for further analysis in this chapter.

This study explored the depolymerization of mango seed biomass using various pretreatment methods, including organosolv, biphasic, and staged organosolv. The objective was to investigate the accessibility and reactivity of lignin and compare it with the one-pot RCF process. We employed organosolv pretreatment with 1,4-butanediol (BDO) in a single step and staged pretreatment processes, and the biphasic pretreatment using 1-pentanol with optimized parameters to obtain high-quality lignin while preserving the crucial β–O–4 bonds. Subsequently, the pretreated lignin was then subjected to a one-pot reaction for depolymerization into lignin monomers. Moreover, the same catalytic conditions were directly applied to raw mango for comparative analysis.

3.2 Experimental section

3.2.1 Materials and chemicals

The mangoes were purchased from the local grocery stores in Hong Kong. To prepare the seeds for further experimentation, they were thoroughly washed, dried, and grounded into a coarse powder with particle size smaller than 3-5 mm. All the reagents and chemicals used in this study were of analytical grade (J&K Acros Organics, Beijing, China).

3.2.2 Biomass chemical composition analysis

The compositional analyses of raw and pretreated mango samples were performed according to the NREL Laboratory Analytical Protocol (Sluiter et al., 2008) as discussed in detail in section 3.2.2.

3.2.3 RCF of biomass

The RCF experiments were performed using a 50-mL batch reactor (Parr Instruments & Co.). For each test, approximately 500 mg of biomass was placed in the reactor with various combination of temperature, pressure, catalyst, and time. For comparison and optimization, one variable was varied, and all the other parameters were kept same. The reactor was sealed and pressurized with H_2. After the RCF, the reactor was opened and depressurized, then the mixture was passed through filter to separate the solid residual and the solvent. The solvent residues were washed and dried at room temperature, which were later used for carbohydrate analysis. The lignin oil containing monomers and some sugars was kept at 4°C for further analysis.

3.2.4 Pretreatment design and conditions

The experimental procedure involved feeding approximately 30g of mango seeds into the reactor with a liquid-to-solid ratio of 8. To ensure thorough mixing, a set of eight reactors were positioned within a large rotating digester made of stainless steel. This digester was tightly sealed to create an airtight environment and mounted on a rotating shaft, enabling continuous mixing at a constant speed. The entire system was heated to a controlled temperature of 160°C. Subsequently, the reactor underwent cooling to reach room temperature, and the treated biomass was filtered and subjected to air-drying for subsequent analysis of its chemical composition. The filtrate containing dissolved lignin was later used for RCF. The dissolved lignin was precipitated by adding deionized (DI) water and then stored at a temperature of -20°C for a duration of 12 hours. The lignin was subsequently freeze-dried, which was used for the RCF experiments.

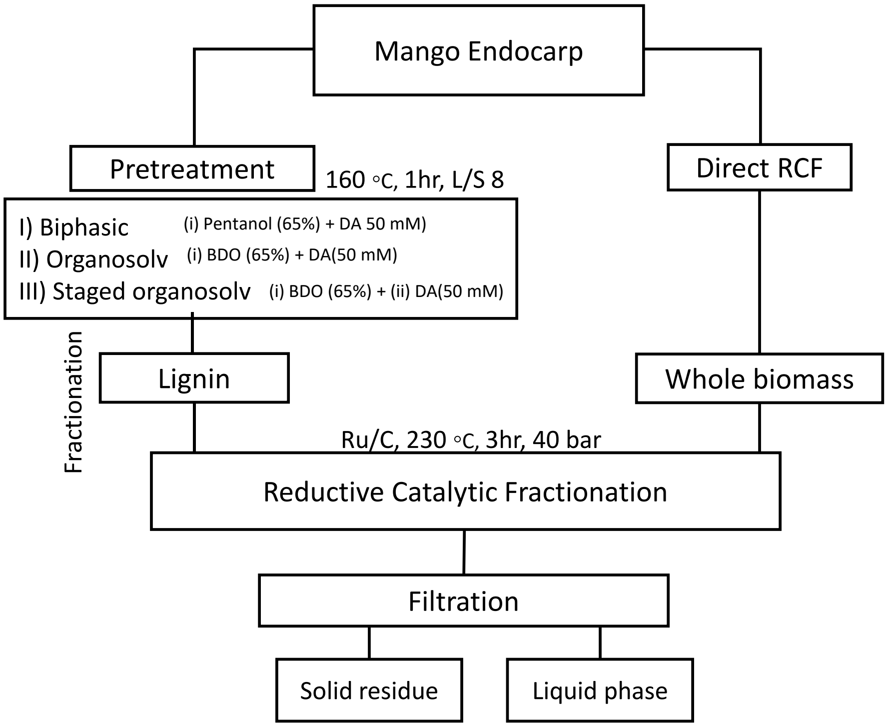

Figure 3.1: Experimental plan and methodology for this study

The experimental plan and methodology are illustrated in **Figure 3.1**. Three pretreatment methods, namely biphasic, organosolv, and staged organosolv, were employed. In the biphasic system, pentanol was mixed with dilute acid (DA) to evaluate the extraction capability of lignin in a separate phase. The organosolv pretreatment involved a single-step process using an organic solvent and DA. Additionally, a staged process was implemented, where the biomass was first treated with an organic solvent and then with dilute acid. This staged process aimed to assess the quality of the obtained lignin, as it is believed that most of the lignin should be extracted during the initial cooking step using the organic solvent. Optimized pretreatment conditions were applied to extract lignin from the mango seed biomass.

3.2.5 Characterization Tools

The monomer identification was performed by a gas chromatography (GC, Agilent Technologies 7890B) equipped with flame ionization detector (FID) detector. The injection temperature was 300°C. The column temperature program was 40°C (3 min), 30°C/min to 100°C, 40°C/min to 300°C and 300°C (5 min), and the detection temperature was 300°C. Sensitivity factors of the products were obtained by using estimates based on the effective carbon number (ECN) due to lack of commercial standards. Briefly, 1 mL of the solvent was filtered into the vial with 100 uL of the internal standard before the quantitative determination of monomers. The GC peaks were determined by the retention time and each peak was integrated with pre-calibrated data. Identification of monomer peaks in the GC-FID chromatograms was performed initially by a GC with Agilent 5977A mass spectroscopy detector and a HP5-MS capillary column. The peaks in the GC-MS chromatogram appear in the same order as those in GC-FID chromatogram due to the use of a similar capillary column. The operating conditions for the GC/MS test were the same as the GC-FID.

The structure and interunit linkages of the lignin were determined by two-dimensional heteronuclear single quantum coherence nuclear magnetic resonance (2D-HSQC NMR) analysis, using a JEOL ECZR 500 MHz NMR spectrometer with a 5 mm ROYAL probe. For the NMR experiment, 100 mg of lignin sample was dissolved in 0.6 mL of dimethyl sulfoxide (DMSO-d6) and injected into the NMR equipment for peak identification and quantification. The HSQC correlation peaks were determined by comparison with the peak values in the literature (Schneider et al., 2020). The software JEOL's Delta 5.2.1 was used to record the volume integrals of HSQC correlation peaks. A Gel-Permeation Chromatography (GPC) was used to measure the molecular weight of the dissolved lignin samples (Meng et al., 2019). The enzyme lignin was dissolved in THF and was sonicated for 10 mins. The sample was then passed through 0.2 µm poly(tetrafluoroethylene) (PTFE) filters and stored in 1.5 mL vials before tested in a Shimadzu HPLC for the GPC analysis.

3.3 Results and Discussion

3.3.1 Chemical Composition analysis

The results of the compositional analysis conducted on raw and pretreated mango seed biomass is presented in **Figure 3.2**. The biphasic pretreatment method achieved a removal of 73% lignin and approximately 75% hemicellulose from the substrate, showing comparable levels of removal for both components. In the case of organosolv pretreatment, the solid yield was reduced due to the removal of easily hydrolysable hemicellulose. Specifically, the organosolv pretreatment removed 91% hemicellulose and 65% lignin from the mango seed biomass. While hemicellulose removal was relatively higher, the removal of lignin was comparatively lower. NMR data revealed a decrease in β–O–4 bond linkages, potentially indicating lignin condensation. Therefore, the combined organosolv and DA pretreatment may not be a promising option for obtaining reactive lignin, as the primary objective of this study focused on lignin extraction rather than hydrolysis. On the other hand, the staged approach yielded similar results to the biphasic pretreatment, with a hemicellulose removal rate of 73% and a lignin removal rate of 65% from the raw mango seed biomass. Additionally, approximately 90% of the original cellulose content was recovered from the solid residue, suggesting that both the biphasic and staged organosolv pretreatments were not excessively harsh in terms of cellulose hydrolysis. These findings align with our previous pretreatment studies (Islam et al., 2021).

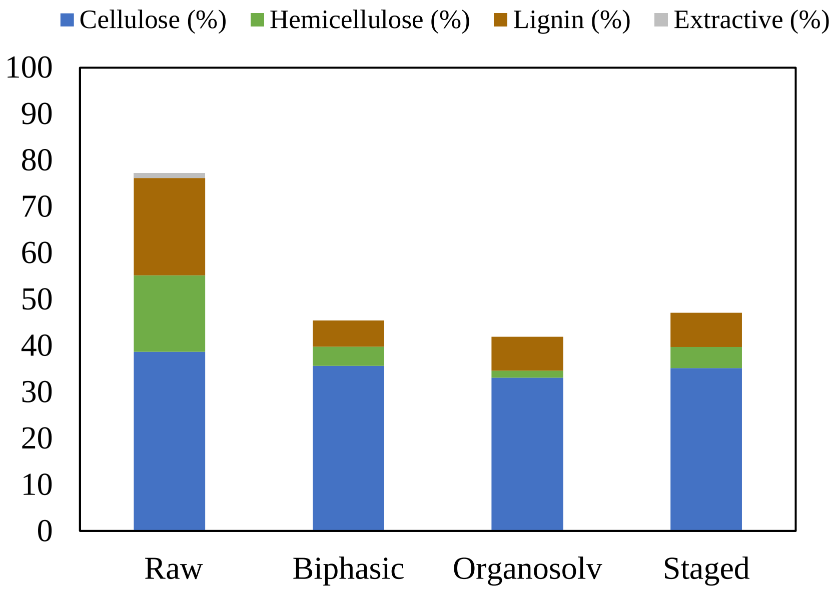

Figure 3.2: Chemical Composition analysis of raw and pretreated mango seed

The results demonstrated that during the first stage of the 1,4-butanediol (BDO) followed by DA process, condensation effects were not observed. This could be attributed to a reduced occurrence of lignin acidolysis and the stabilization of lignin carbocation by the organosolv process (Islam et al., 2021). The extracted lignin was characterized as reactive lignin, as more β–O–4 linkages were preserved, as analyzed through 2DHSQC NMR spectra (discussed in section 4.2.4). Based on these results, both the staged-organosolv and biphasic pretreatment methods can be considered favorable options for obtaining reactive lignin.

3.3.2 Optimization of RCF

When comparing the yields of monomers, it becomes evident that the reaction temperature and time plays a crucial role in achieving a high monomer yield. The results show the influence of these parameters indicating that depolymerization occurs rapidly, primarily within the first two to three hours and by increasing the temperature from 200 to 230°C. To assess the effects of treatment time, experiments were conducted for durations of 1, 3, 5, and 7 hours.

The results showed an increase in monomer yield as the RCF duration increased from 1 to 3 hours and no further increase in the monomer yield beyond 3 hours. Consequently, all subsequent RCF experiments were conducted keeping the time at 3 hours. Additionally, the influence of H_2 pressure (ranging from 20 to 40 bars at room temperature) was evaluated in the Ru/C-catalyzed RCF of mango seeds. The results revealed that increasing the H_2 pressure leads to an increase in the total phenolic monomer yield. For instance, at 20 bar H_2 pressure, the total phenolic monomer yields were around 40 mg/g biomass, while at 40 bar H_2 pressure, they nearly doubled to 77 mg/g biomass. Furthermore, the impact of catalyst loading (Ru/C) on the RCF of mango seeds was assessed. Reactions were performed with catalyst loadings ranging from 10 to 30 wt% relative to the biomass. Typical RCF conditions (230 °C, 3 hours, 40 bar H_2 at room temperature) were employed. It is evident that, within this range, the Ru/C catalyst loading strongly affects the phenolic monomer yield and selectivity. As shown in **Figure 3.3**, an increase in catalyst loading results in a higher total phenolic monomer yield. This can be attributed to the fact that a higher catalyst loading reduces repolymerization, leading to a higher phenolic monomer yield. These results demonstrate that the extent of lignin conversion is primarily governed by the "process severity," which is a combination of temperature and time. On the other hand, parameters that govern catalyst activity (such as catalyst loading and H_2 pressure) primarily influence the chemical stabilization of lignin fragments, thereby determining the monomer yield and selectivity.

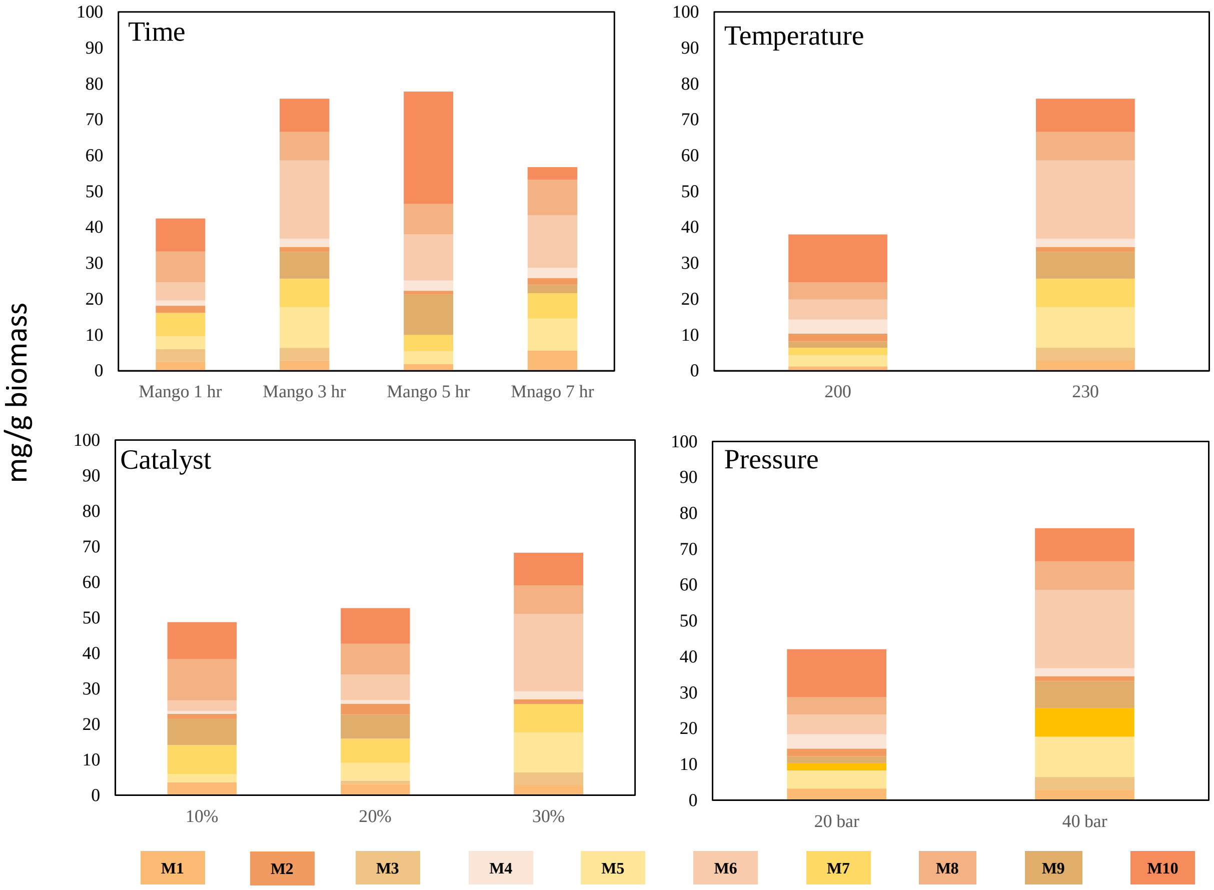

Figure 3.3: Optimized parameters for maximum monomer yield by RCF

3.3.3 Characterization of lignin

After harvesting at the optimized pretreatment conditions, the fractionated lignin was subjected to analysis using 2D-HSQC NMR, and the results were compared with ball-milled enzyme lignin. The NMR spectra provided detailed information about the cross signals of methoxy groups and interunit linkages. The potential of fractionated lignin to yield value-added chemicals depends on their structural properties, which are largely affected by the pretreatment conditions of lignocellulose. Harsh pretreatment, characterized by high acidity, can lead to the formation of detrimental C–C linkages (condensed lignin), thereby reducing the presence of beneficial β–O–4 linkages in the fractionated lignin, as shown in **Figure 3.4**. Therefore, in a lignin-first biorefinery, the main concern is the fractionation of lignocellulose components while preserving the maximum amount of beneficial β–O–4 linkages in lignin.

The results showed that biphasic pretreatment preserved the original β–O–4 linkages to a greater extent in the fractionated lignin compared to organosolv pretreatment. Additionally, G-lignin contains more reactive sites and can readily react with other groups to form condensed structures. The degree of this conversion depends on the pretreatment conditions and the solvent used for fractionation. The organosolv-pretreated lignin exhibited the lowest amount of G-lignin compared to S-lignin, indicating severe condensation during pretreatment (Yoo et al., 2018). Conversely, biphasic and staged pretreated lignin showed the highest amount of G-lignin, which supported lignin stabilization and protection.

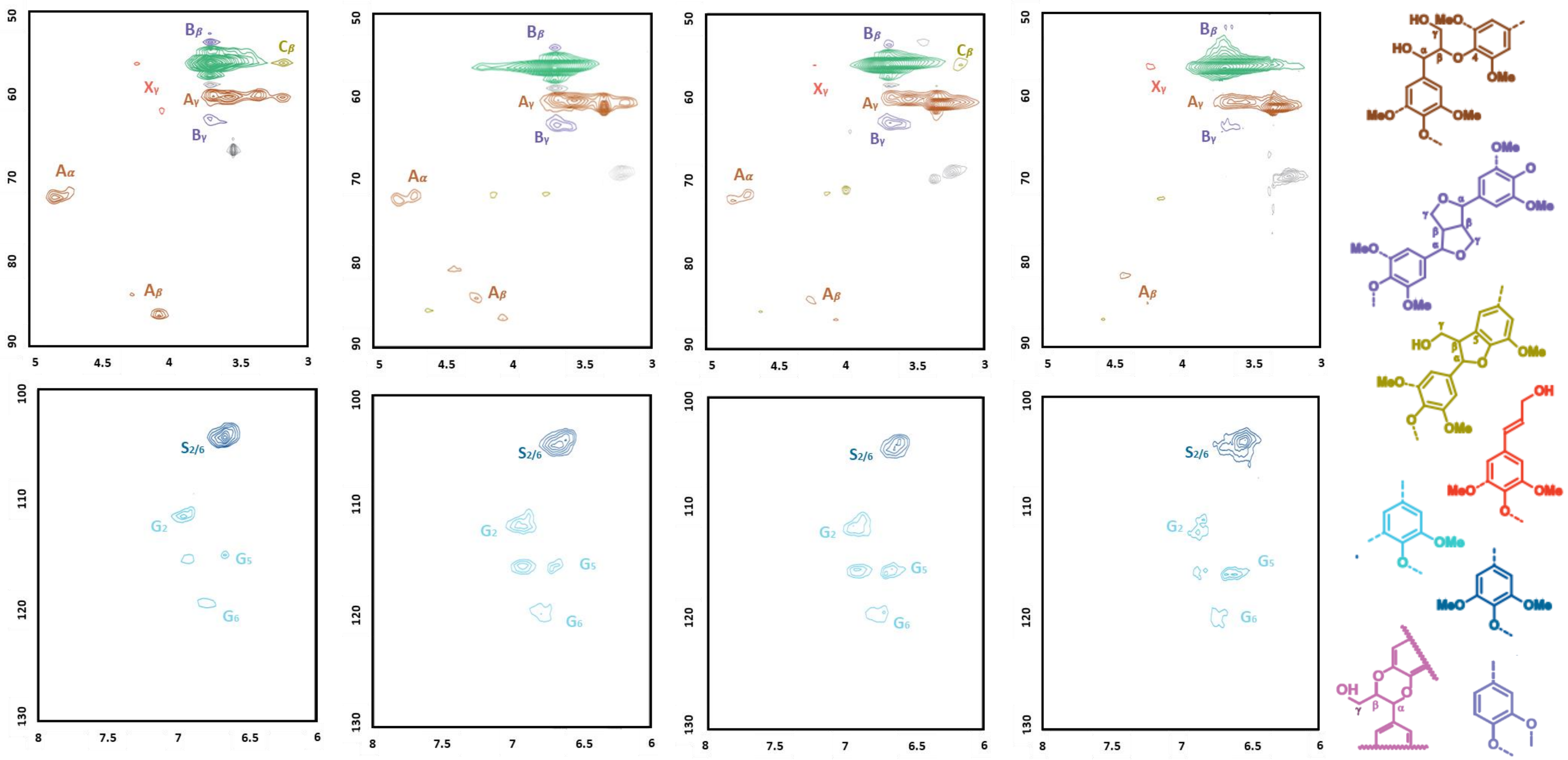

Figure 3.4: 2D 1H-13C HSQC NMR spectra of enzyme lignin and pretreated lignin.

3.3.4 Pretreatment and direct RCF effect on lignin monomer yield

To achieve comprehensive biomass utilization, it is important to selectively depolymerize isolated lignin and obtain a specific range of monomeric products. In this study, we conducted experiments using both pretreated lignin and raw biomass in a Parr reactor, employing optimized RCF parameters, to compare their respective monomer yields. **Figure 3.5** illustrates the results obtained. The findings revealed significant differences in the abundance of G- and S-units, as well as variations in the monomer yields. Direct RCF of mango seed exhibited the highest monomer yield, accounting for 38% based on lignin (>70 mg/g-dry biomass). On the other hand, the monomer yield from the pretreated lignin was less than 15%. The lower monomer yield observed in the pretreated lignin indicates that direct RCF, without subjecting the lignin to the severe conditions of pretreatment, is more advantageous. This suggests that the lignin depolymerization through direct RCF provides better outcomes as it avoids the rigorous conditions imposed during the pretreatment process as evident from the structural analysis presented in **Figure 3.4**.

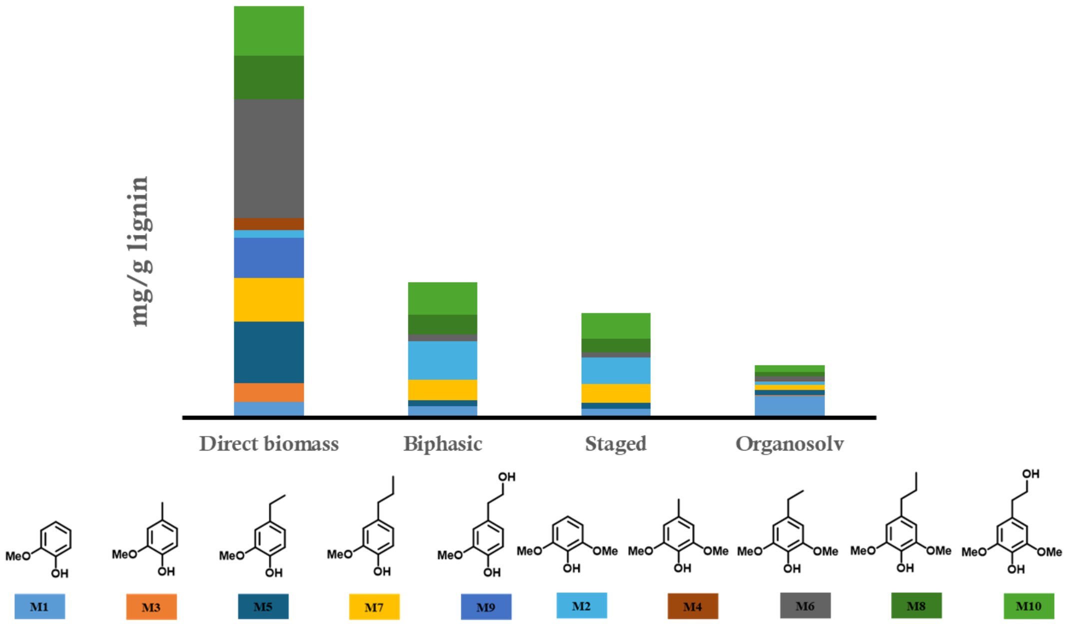

Figure 3.5: Monomer yield of pretreated lignin and direct biomass after RCF

3.4 Summary

This study focused on investigating the impact of pretreatment and direct RCF of biomass on the quality and yield of lignin. Different pretreatment methods, including organosolv, biphasic, and staged pretreatment, were employed using mango seed as the biomass feedstock. The objective was to assess the accessibility and reactivity of lignin and compare it with a one-pot RCF process. The study found that direct RCF resulted in a higher yield of lignin monomers compared to pretreatment methods. However, among the pretreatment methods, biphasic and staged pretreatments showed better performance in obtaining reactive lignin. These pretreatment approaches preserved the crucial β–O–4 linkages in lignin, which are important for downstream utilization. The findings highlight the potential of biphasic and staged pretreatments in producing high-quality lignin with enhanced reactivity for further conversion into valuable chemicals.

Chapter 4. Monolignol Potential and Insights into Direct Depolymerization of Fruit and Nutshell Remains for High Value Sustainable Aromatics

4.1 Introduction

As the world faces the challenge of climate change, the pursuit of carbon neutrality has emerged as a critical objective toward our sustainability, such as the continuous development and implementation of innovative techniques to replace fossil fuel feedstock. Effective utilization of lignin has become a critical subject to enhance the cost-effectiveness and economic viability of the lignocellulose biorefinery (Islam et al., 2020). The three major phenylpropanoid units, i.e. H, G, S, and C lignin have been shown in **Figure 4.1a**. These units are linked together to form a highly interconnected structure, which enhances the rigidity and strength of lignin molecules, making them highly recalcitrant to conversion in biorefinery processes. In addition, lignin condensation is a side-reaction occurring with the removal of benzylic alcohol from the lignin backbone, resulting in the formation of a benzylic carbocation which decrease the monomer yield (Questell-Santiago et al., 2020). To address this challenge, RCF processes were developed to obtain lignin monomers directly from lignocellulosic biomass (Renders et al., 2017). As RCF requires the least operational steps in the conversion process and the lignin is still in its original form in the biomass, some researchers have implied the production of monomer in RCF with near-theoretical yield (Renders et al., 2017).

Fruit and nutshell wastes have high potential to contribute to the lignin biorefinery. The overall production of those biomass is approximately 24-31 million tons annually worldwide (Mendu et al., 2012). This type of waste can be classified into the food remains and food processing waste based on the sources of production (Guan et al., 2022). The fruit and nutshell wastes, with its high lignin content (50 wt%), makes it an attractive source of monomer production in the biorefinery (Li et al., 2018a). The fruit and nut-processing industry has a well-established infrastructure, stable and logistically efficient feedstock procurement, and is ready for the purpose of lignin valorization practices (Rodriguez et al., 2008). Despite its importance, the studies regarding the importance and utilization of fruit and nutshell waste for chemicals are limited (**Table 2.2**). In addition, many important factors of the food-lignin biorefinery have never been explored, including (i) the monolignol potential of the important food residues in the magnoliid, monocots, and malvids families; (ii) the detailed analyses on the different types and origins of lignin; and the possible variation and correlation among the selected waste biomass. The information of the specific lignin structures of the mentioned biomass, such as the G/S ratios, have not been investigated and compared.

To clarify those points, ten phylogenetically diverse fruit and nutshell species were selected to analyze their potential of monomer production by RCF. A total of twelve monomers (M1 to M12) were identified (**Figure 4.1b**). Lignin structures and interunit linkages were determined and quantified using state-of-the-art analytical tools and associated with monolignol properties. The data matrix was analyzed using Mantel’s and Pearson correlation statistics to clarify the relationship between lignin characteristics and the monolignol products.

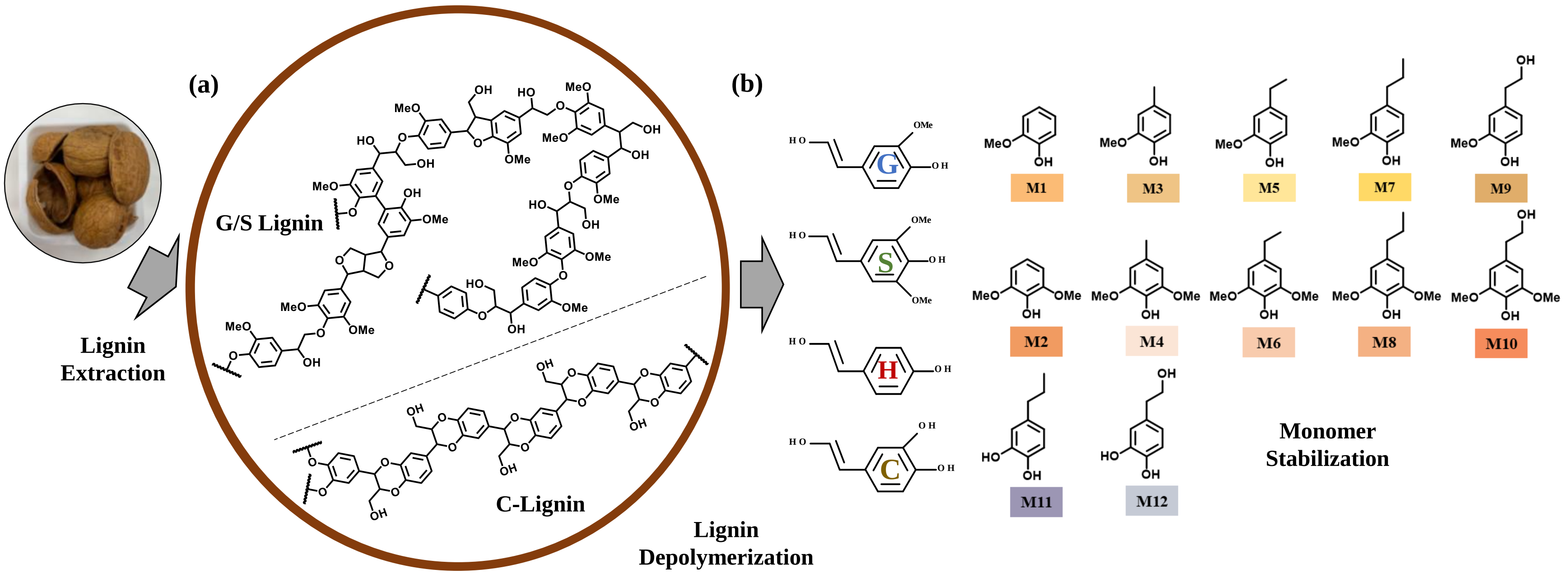

Figure 4.1: Schematic representation of lignin structures, three monolignols, and forms of lignin products (M1 to M12) after the RCF process.

4.2 Experimental Section

4.2.1 Biomass feedstock and chemicals

The fruits and food nuts (i.e. Peach, Mango, Cherry, Avocado, Date, Pistachio, Peanut, Macadamia, Walnut) were purchased from the local grocery shops in Hong Kong. The Candlenut fruits were collected at a local park at 22.34378, 114.18216. The food nuts were oven dried and removed from the shells (**Figure 4.2**). The shell biomass was washed, air dried, and grounded into course powder with particle diameter smaller than 3-5 mm, using a shaker mill. The biomass samples were kept in airtight containers before the RCF experiments. All the reagents and chemicals used in this study were of analytical grade (J&K Acros Organics, Beijing, China).

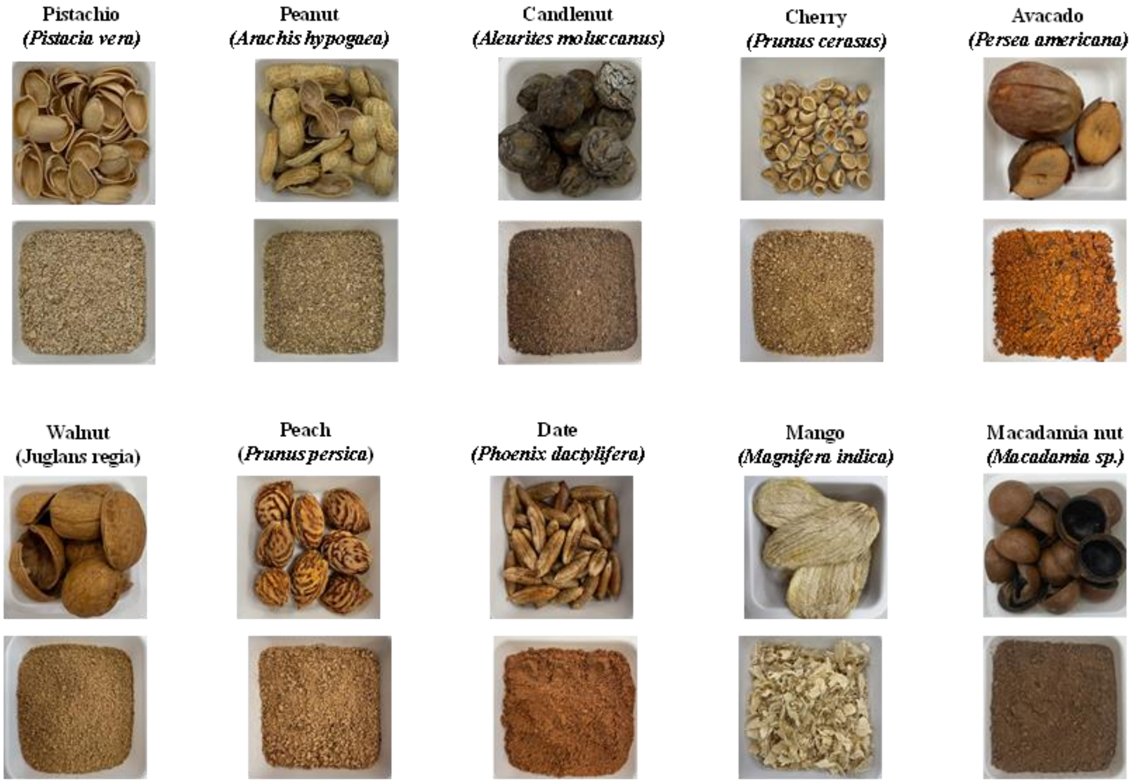

Figure 4.2: Washed and grinded sample of fruit and nutshell biomass

4.2.2 Compositional analysis of the biomass

The biomass samples were extracted by ethanol and toluene for polar extractives and non-polar extractives, respectively. For each test, 10 g of biomass sample was placed in the thimble and then fitted in the Soxhlet apparatus. The ethanol extraction was conducted for 6-8 cycles and then the ethanol was replaced by toluene for another 4-6 cycles, or until the solvent becomes clear. The thimble was removed and oven-dried at 50°C overnight, the extractive-free samples were then used in the compositional analysis. The ethanol and toluene solvents were evaporated to harvest the polar and non-polar extractives, and then 1 mL of the sample was mixed with 9 mL methanol and filtered by 0.2 µm filter paper. The extractives in the filtered liquids were analyzed by a LC-MS Quadrupole-ToF (Agilent 6540, CA, USA). All the experiments were conducted in duplicates and the results were presented with averages and standard deviations.

The compositional analyses of the biomass samples were performed according to the NREL Laboratory Analytical Protocol (Sluiter et al., 2008). The extractive free biomass samples (150 mg) were placed in 50 mL falcon tubes and treated with 1.5 mL of 72% sulfuric acid in the water bath at 30°C. The suspension was stirred every 10 min for 1 hour, followed by the addition of 42 mL distilled water and autoclavation at 121°C for 1 hour. The solutions were kept at room temperature to cool down and then 5-7 mL of the supernatant was transferred to 15 mL tubes. The liquids were neutralized with barium carbonate before determining the sugar composition of the samples by a high-performance liquid chromatography (HPLC, Shimadzu) equipped with CHO-782 column (Supelcosil™). The remaining solutions were filtered with pre-weighed glass crucibles. The filtrate was washed by distilled water and oven-dried to determine the lignin content. Ash content was determined by placing the crucibles in the furnace at 575°C for 6-8 hours.

4.2.3 Reductive Catalytic Fractionation

The RCF experiments were performed using a 50-mL batch reactor (Parr Instruments & Co.) and based on the optimized conditions provided in another study (Van den Bosch et al., 2017a). For each test, approximately 500 mg of biomass was placed with catalyst Ru/C (150 mg) and 20 mL THF into the reactor. THF was chosen due to its excellent solvating properties which could effectively dissolve the lignin for further processing. The reactor was then sealed and pressurized with H2 (40 bar). The reaction mixture was stirred and heated to 230°C for 30 mins. When the reaction temperature reached 230°C, it was kept constant for 5 hours. After the RCF, the reactor was opened and depressurized, then the mixture was passed through filter to separate the solid residual and the solvent. The solvent residues were washed and dried at room temperature, which were later used for carbohydrate analysis. The lignin oil containing monomers, and some sugars was kept at 4°C for further analysis.

4.2.4 Enzyme lignin preparation

The enzyme lignin was prepared to obtain the structural information of the original lignin in the biomass based on the standardized method (Wang et al., 2017). Extractive-free samples were used for the analysis. A total of 20-50 g biomass samples were planetary ball milled at 450 rpm with 10 min rest time between cycles; and then the cycle was reversed after every 10 mins. The treated sample (~20 g) was taken in 250 mL flasks and treated with 20 mL of 15 FPU cellulase (CTec2, Novozyme Corp., Denmark) at 10% solid loading; and 10 mL of sodium acetate buffer was placed in the shaking incubator at 35°C and 250 rpm for 48 hours. The solids were pelleted by centrifugation and the liquid was decanted. The solids were washed 3-4 times with distilled water and then freeze dried. The dry sample was then dioxane extracted to yield the enzyme lignin. 10-15 g of the sample was taken in the glass bottle and 50 mL of dioxane was added and left on the magnetic heater at 30 rpm and 50°C for 8 hours. The solution was membrane filtrated, and the remaining solids on the membrane were washed and then freeze-dried for 24 hours. Finally, the sample was scrubbed off from the membrane and kept in the vial for further analysis.

4.2.5 Lignin and monomer characterization

The procedures and characterization equipment employed for monomer identification, quantification, and the study of lignin sample structure and linkages were consistent with those described in Chapter 3, Section 3.2.5.

4.2.6 Statistical analysis

Pearson's correlations and Mantel's test were visualized using linkET and ggplot2 packages on R (Huang, 2021; Wickham, 2016). Pearson's correlations were performed to evaluate the correlations among different lignin characteristics and potential of monomer productivities by RCF. Mantel's test was applied to validate whether there is a significant correlation between lignin/monomer characteristics over plant species and sample's sources (i.e. botanical classification on order level and position of biomass).

4.3 Results and Discussion

4.3.1 Classification of tested fruit and food nutshell biomass

To better understand the lignin of the tested biomass samples, we first classified the fruit and food nutshell based on the phylogenetic tree and the harvested portions of the biomass in the fruits (**Figure 4.3**). The heavily lignified seed coats found in many fruit and nut seeds suggest that lignin plays a crucial role in seed protection. During evolution, the composition of the fruits structure and cell wall compositions in these seed plants change over stages with the mitigation of environment factors, among the different cell types, and between different species (Buchanan et al., 2015). This heterogeneity poses a great challenge in achieving consistent material composition that can be delivered to the biorefinery. To maximize the recovery of biomass carbon into the desired biofuels and co-products, it is important to produce cell-wall architectures capable of being easily and completely deconstructed for the conversion processes (McCann & Carpita, 2015).

The fossil evidence suggests that the earliest land plants emerged during the Late Ordovician period about 440 million years ago (Figure 2a) (Stewart & Rothwell, 1993). Plants started developing the phenylpropanoid metabolism for monolignol biosynthesis, but they remained small since the lack of true lignin (Bateman et al., 1998). The true lignin was developed in Tracheophytes, which soon dominated the land ecosystem. The forms of lignin were diversified for many functions. Euphyllophytes or the seed plants (gymnosperms and angiosperms) occurred approximately 370 million years ago with varied phenylpropanoid units (Boerjan et al., 2003). The gymnosperm lignin is primarily composed of G-units with a small fraction of H-units, while the angiosperm lignin is composed of G/S copolymers that also can contain some H-units. Angiosperms are the only vascular plants that produce flowers, fruits, and seeds in the ovary. In angiosperms, S-lignin is as a more evolved trait in fiber cells, while the tracheary elements are often enriched with G-lignin (Nakashima et al., 2008). This observation emphasizes that G-lignin's ancestral function associated with reinforcing the cell wall of water-conducting tracheary element

(TE)s, whereas S-lignin may serve other functions such as support and defense (Barros et al., 2015; Weng et al., 2010).

In addition to the phylogenetic classification, the tested fruit and nutshell waste were classified into four categories based on the non-eatable biomass portion in the fruits (Figure 2b). For example, avocado and date belong to Category I, where the whole seed was used for the analysis. Categories II and III are both where the outer covering of the seeds were used while the edible part is the mesocarp (INC) in Category II (i.e. peach, cherry, and mango) and seeds in Category III (i.e. macadamia nut, walnut, candlenut, and pistachio), respectively. Category IV (peanut) is different from the rest of the eudicot species where the whole outer covering is used for monolignol production.

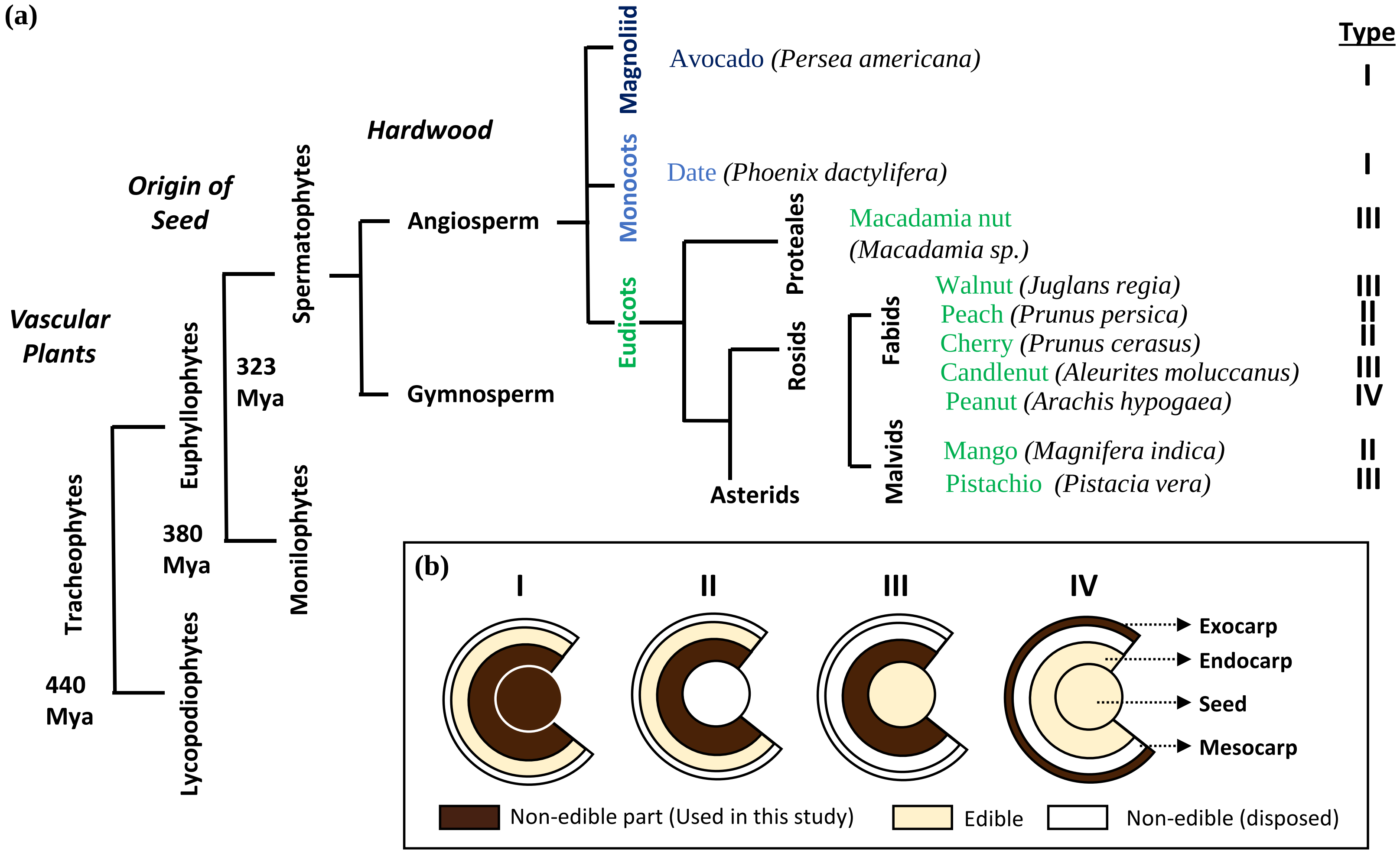

Figure 4.3: Basic phylogeny of selected biomass highlighting the relationships between different (a) plant species and (b) positions of biomass in fruit

4.3.2 Chemical compositional analysis and monomer yield of the selected biomass

The results of compositional analysis and monolignol yields of tested fruit and nutshell biomass (with corresponding images) are shown in **Figure 4.4**. High lignin contents were recorded in most of the samples. The nutshells of macadamia and candlenut from the family Proteales and Fabids show >40% lignin contents followed by peach with 38% lignin on the dry mass basis. Walnut, cherry, and peanut from Fabids family have lignin contents in the range 30-40 % while the remaining samples were near or below 20%. The high lignin contents in these samples prove them to be ideal biomass for lignin valorization, while the lignin here does not limit to those observed in woody biomass which have been discussed in NMR spectra as detailed in later chapter of this article. Along with lignin, the cellulose and hemicellulose contents were also determined. Avocado and date are both rich in carbohydrates. They belong to monocots and have more cellulose (40-60%) than hemicellulose (<5%). Interestingly, the date sample was rich in mannose, which was the only found in all the tested biomass samples. The remaining nutshell sample from the other eudicots have cellulose and hemicellulose in the range 15-40%. Those carbohydrate-rich samples could be more useful in biological conversion rather than RCF.

The monomer yields of tested biomass samples are also shown in the bar charts of **Figure 4.4**. The results showed difference in the abundance of the G- and S- units along with variation in the monomer yields. Mango seed and walnut shell have the highest monomer yield (>70 mg/g-dry biomass) and the monomer yield of peach, candlenut, cherry, and pistachio biomass were all higher than 50 mg/g-dry biomass. The monomer yields of peanut, macadamia, and date were in the range of 20-30 mg/g-dry biomass, with avocado biomass being the lowest at only 11 mg/g-dry biomass.

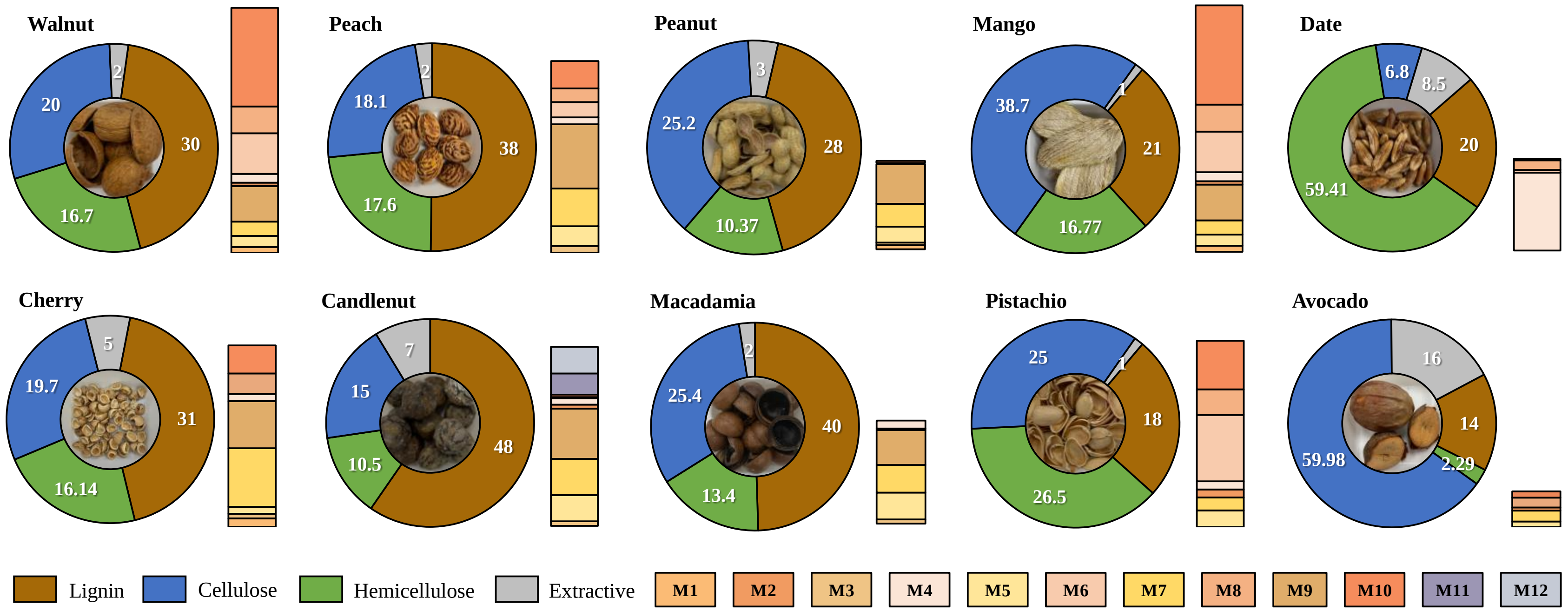

Figure 4.4: Chemical compositions (pie charts) of tested biomass and monolignol yields after RCF processes (Ru/C, THF, 230°C, 40 bar)

Meanwhile, significant variation in the abundance of S- and G- monomers was observed in all the species. Mango seed and walnut shell belong to different clades of eudicots, while both are rich in S- monomers along with pistachio; and macadamia, peach, candlenut, cherry, and peanut shell biomass were rich in G-type monomer. Date biomass only yielded in S-type monomer, and the candlenut shell biomass produced G-, S-, and C- types monomers. The abundance of different types of monomers enhances the selectivity of the monomers among these species.

4.3.3 Lignin structural analysis

The composition and basic structure of lignin was studied by analyzing the enzyme lignin of the tested biomass by 2D-HSQC NMR. The NMR spectra of four representative samples are shown in **Figure 4.5**: mango, walnut and peanut have been selected due to the obvious variation in S- and G- units; candlenut has been selected due to presence of C-lignin along with the conventional lignin monomers. The NMR spectra give detailed information of the cross signals of methoxy groups and interunit linkages, such as β−O−4, β−5, and β–β between the monomeric units in the side chain region (upper figures, δC/δH: 50−90 ppm/3−5ppm); and different components of polymeric chains such as S-, G-, C- units in the aromatic region (lower figures, δC/δH: 100-130 ppm/6-8 ppm). In summary, walnut, mango, and pistachio biomass had the highest levels of S-units at 76, 75, and 84%, respectively, while peanut showed the highest level of G-units, i.e. approximately 94% and very low S-units.

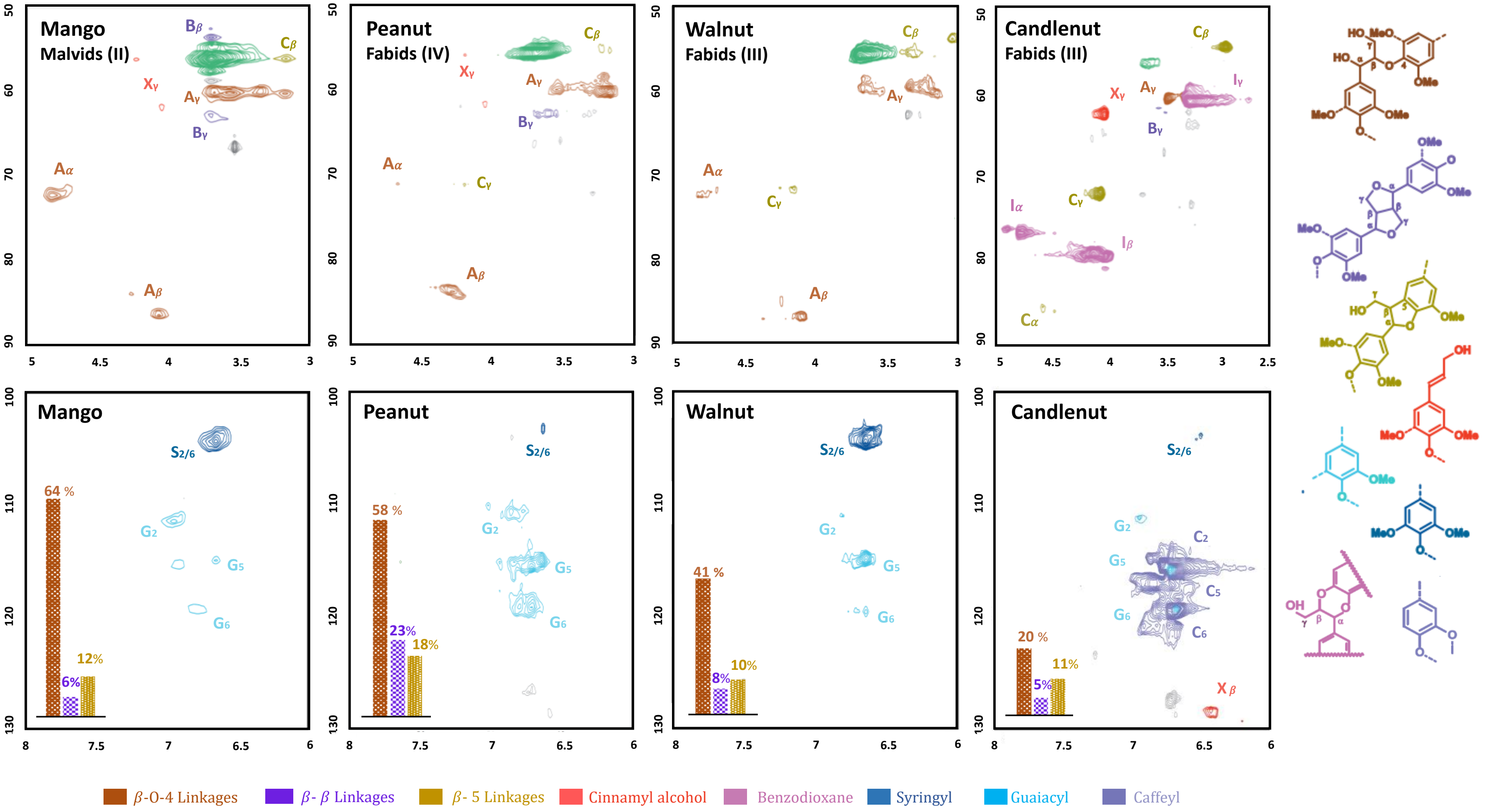

Figure 4.5: 2D 1H-13C HSQC NMR spectra of enzyme lignin of selected fruit and nutshell feedstock.

In addition, the incest bar charts in the NMR spectra show the integrated peak volume of interunit linkages including β–aryl ether (β−O−4, left bars), phenylcoumaran (β−5, middle bars), and resinol (β−β, Right bars). The mango lignin contained the highest number of β−O−4 linkages, peanut shell had a higher number of G-units and more β−5 linkages, while walnut shell were rich in S-unit and less β−5 units. C-lignin (C2 δC/δH = 116 × 7.02 ppm, C5 δC/δH = 117.5 × 7.02 ppm, C6 δC/δH = 120.6 × 6.92 ppm) was observed in candlenut sample, with detection of G/S lignin, cross signals of benzodioxane moieties, β–O–4 units, the resinol structures as well as the cinnamyl alcohol end-units. This scenario was in line with the observation from GC-FID analysis. In addition, less abundant but non-negligible signals from resinol units were present in the candlenut samples. Given the very low level of G/S lignin, it was supposed that some resinol units were biosynthesized from the polymerization of caffeyl alcohol monolignol,(Chen et al., 2012) rather than coniferyl or sinapyl alcohols (Tobimatsu et al., 2013).

4.3.4 Extractive analysis

Extractives of the fruit and nutshell waste were analyzed by LC-MS, and all the ten biomasses were rich in polar and non-polar extractives, such as flavonoids, lignan, sugars, sugar acids, and fatty acids (**Table 4.2**). The contents of polar extracts were higher than the non-polar ones in all the samples; and most of those were of commercial relevance. The extractives showed very little effects on the monomer yield when the raw biomass and the extractive-free biomass were subjected to RCF.

Table 4.2. Extractive analysis of fruit and nutshell lignin sample by LC-MS.

Formula	Compounds	*m/z*	Retention time
FLAVONOIDS			
$C_{15}H_{12}O_7$	Taxifolin	303.0512	2.38
$C_{21}H_{20}O_{11}$	Quercitrin	447.093	2.47
$C_{11}H_{10}O_5$	Tomentin	221.0457	2.51
$C_{18}H_{18}O_5$	Flavokawain A	313.1083	2.76
$C_{18}H_{18}O_6$	4-Hydroxy-2,3,9-trimethoxypterocarpan	329.1031	2.95
$C_{15}H_{12}O_5$	Naringenin	271.0613	3.93
$C_{16}H_{12}O_4$	isoformononetin	267.0664	4.15
$C_{18}H_{16}O_6$	4'-Hydroxy-5,6,7-trimethoxyflavone	327.0876	4.22
$C_{17}H_{14}O_5$	Sayanedine	297.077	4.77
$C_{18}H_{14}O_4$	Glyzarin	293.0822	5.02
PHENOL			
$C_7H_6O_5$	Gallic acid	169.0144	1.09
$C_7H_6O_3$	Protocatechuic aldehyde	137.0244	1.49
$C_{14}H_6O_8$	Ellagic acid	300.9991	1.78
$C_9H_8O_3$	p-coumaric acid	163.0401	1.99
$C_9H_{10}O_5$	Syringic acid	197.0461	2.21
$C_9H_8O_2$	3-Phenyl-2-oxiranecarbaldehyde	147.0452	2.85
$C_{20}H_{22}O_7$	Wikstromol	373.1291	2.85
$C_{10}H_8O_4$	Scopoletin	191.0351	3.13
$C_{16}H_{14}O_6$	divanillin	301.072	4.59
$C_{20}H_{18}O_5$	curcumin II	337.1083	5.04
$C_{22}H_{34}O_3$	Ginkgoic acid	345.2438	17.92
$C_{24}H_{38}O_3$	MFCD09752804	373.2745	20.11
FATTY ACIDS			
$C_{14}H_{10}O_4$	Moracin M	241.0508	3.30
$C_{14}H_{26}O_5$	3-Hydroxytetradecanedioic acid	273.1711	3.31
$C_{18}H_{34}O_5$	(-)-pinellic acid	329.2336	7.07
$C_{18}H_{34}O_4$	Octadecanedioic acid	313.2384	11.62
$C_{18}H_{32}O_3$	13S-hydroxyoctadecadienoic acid	295.228	13.62
$C_{22}H_{44}O_3$	MFCD00083370	355.3219	16.88
$C_{22}H_{40}O_4$	1-Octadecyl (2Z)-2-butenedioate	367.2853	17.26
$C_{24}H_{48}O_3$	2-hydroxy Lignoceric Acid	383.3531	18.56
$C_{23}H_{46}O_4$	1,3-Dihydroxy-2-propanyl icosanoate	385.3322	20.21
$C_{21}H_{42}O_3$	(2S)-3-[(1Z)-1-Octadecen-1-yloxy]-1,2-propanediol	341.3062	20.38
$C_{24}H_{48}O_4$	1,3-Dihydroxy-2-propanyl 19-methylicosanoate	399.3479	21.81
$C_{24}H_{40}O_3$	Lithocholic acid	375.2905	23.72
SUGAR DERIVATIVES			
$C_5H_{11}AsO_8$	1-O-Arsonopentofuranose	272.9589	0.75
$C_6H_{12}O_6$	D-Fructose	179.0562	0.82
$C_5H_{10}O_6$	L-Xylonic acid	165.0405	0.90
$C_7H_5NO_3S$	Saccharin	181.9919	1.24

4.3.5 Molecular weight distribution and monomer yield

The GC-FID spectra of all the fruit and nutshell samples with typical monomer distribution are presented in **Figure 4.6a** and **Table 4.3**, showing the S- and G- type (ethyl-, methyl, propyl, propanol-) monomer along with C-lignin in the candlenut sample. The GPC spectra of the lignin RCF oil is presented in **Figure 4.6b**. The GPC results showed a highly depolymerized lignin oil from the mango, pistachio, and walnut samples with large signal for monomers, relatively smaller signal for dimers, and very small signal for the oligomers.

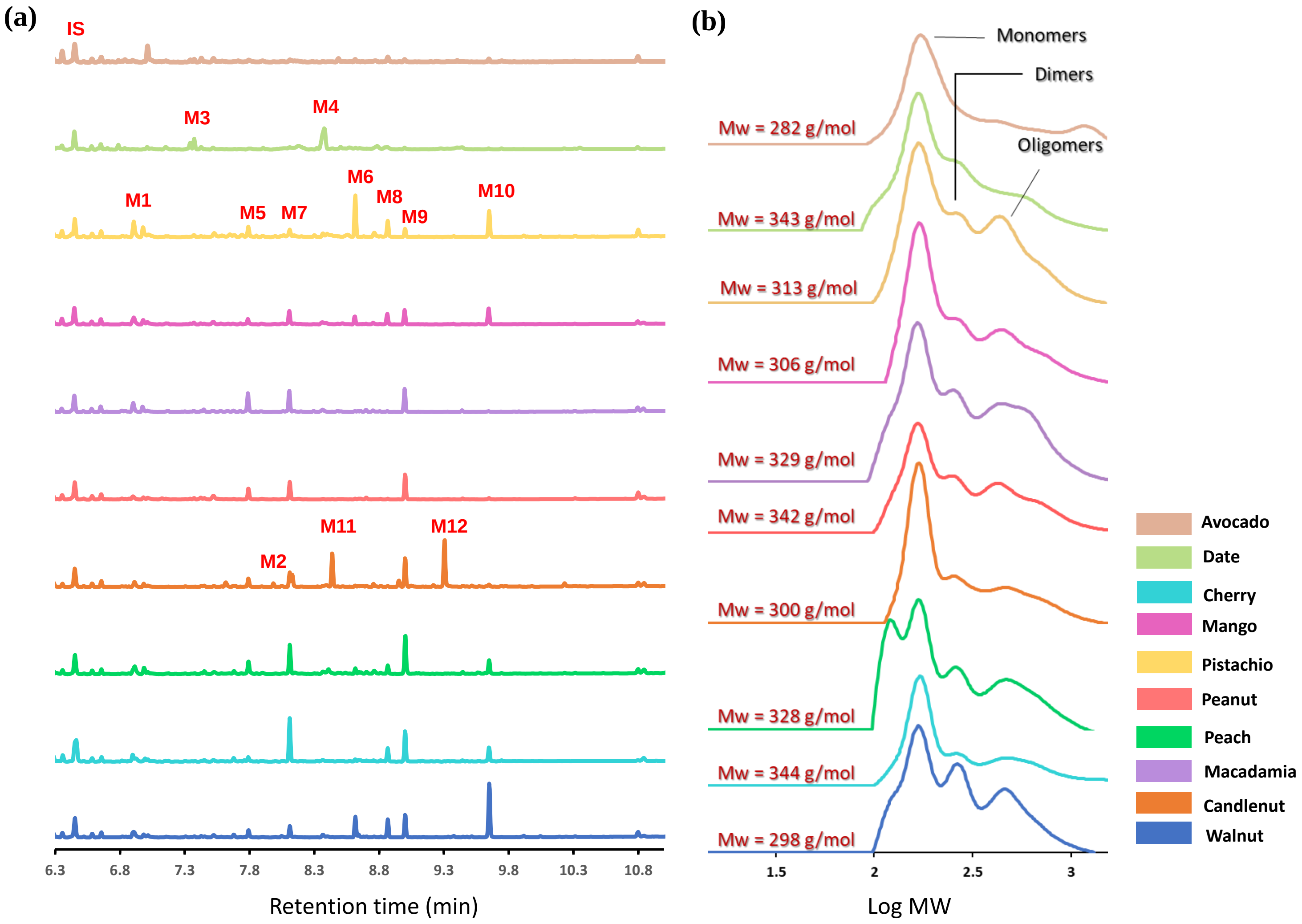

Figure 4.6 (a) GC/FID spectra of monolignol production and (b) GPC spectra for RCF oil from fruit and nutshell biomass.

Table 4.3. Monomer name with retention time used for the yield calculations from GC areas obtained using THF as solvent.

Monomer	Name	Retention Time
M1	Guaiacol	6.99
M2	Syringol	8.05
M3	4-Methylguaiacol	7.456
M4	4-Methylsyringol	8.37
M5	4-Ethylguaiacol	7.793
M6	4-Ethylsyringol	8.626
M7	4-Propylguaiacol	8.12
M8	4-Propylsyringol	8.87
M9	4-Propanolguaiacol	9.013
M10	4-Propanolsyringol	9.65
M11	4-Propylcatechol	8.438
M12	4-(3-Hydroxypropyl) catechol	9.302

4.3.6 Correlation between lignin properties and monomer yield

Pearson correlation and Mantel's test were performed to examine the polymeric structure and monolignol production of the studied lignin in **Figure 4.7**. In the results of Pearson correlation, the bigger color-coded boxes represent the more significant correlation between the discussed parameters (blue = positively and red = negatively correlated). A positive correlation between S/G ratios and β–O–4 linkages was observed, which indicated that the sample having high amount of S-lignin can result in the formation of more cleavable β–O–4 linkages. A strong correlation was observed between the β–5 linkage and the G-lignin, indicating that during the lignin biosynthesis the G-type could result in the formation of β–5 linkages. In Mantel's test, the thickness of linkage lines showed the strengths of dependencies between the controlled categories, i.e. plant species (green) and recovered parts (orange), and the monolignol production factors. Clear trends were observed among the various parameters such as linkages, S- and G-unit, depolymerization yields, and molecular weights of lignin. Among all the parameters related to monolignol production, β–O–4, Mn, and S-type (M4 and M10) monomers were the most sensitive ones influenced by the plant species. While the fruit and nutshell composition were most associated with β-5 followed by molecular weight and M4 monomers.

The S/G ratios of the enzyme lignin are heavily correlated with the contents of β–O–4 linkages. High S/G ratios or more β–O–4 linkages represents extra methoxy groups in the S-monomers which prevent C–C linkages during biosynthesis (Boerjan et al., 2003). The selected biomass species that were rich in G-type monomers resulted in less monomer yield as compared to those rich in S-type monomers. The high level of S-unit in the biomass was crucial for the depolymerization process as the units located at the 3rd and 5th positions of the ring do not contribute to the formation of extra C–C bonds (Li et al., 2018b). This result agrees with the fact that the high content of G-units expose the C5 positions on the aromatic ring, which is prone to form into β−5 linkages via coupling C–C bonds during lignin biosynthesis. When both C3 and C5 positions are occupied by methoxy groups in the S-unit, the formation of interunit C–C linkages is unfavorable.

Preserving the β−O−4 linkages during the biorefinery process is a widely applied approach to increase the monomer yield. However, when the preserved β−O−4 bonds are cleaved, it does not guarantee to release monomers. The β−O−4 linked moieties can be connected to other moieties by the C–C interunit bonds, such as the abundant β−β and β−5 linkages observed in peanut and macadamia, reducing the monomer yields of these samples. Low contents of β−5 linkages were observed in mango and walnut lignin which were rich in S-units and with significantly higher monomer yields than other biomass samples.

The GPC results for molecular weight distribution demonstrated positive correlations among the β–O–4 linkages, monomer yields, and S/G ratios. Highly depolymerized lignin oils (with more monomer signals and less oligomer) were obtained from the mango, pistachio, and walnut biomass. They were with the highest β−O−4 content that resulted in higher monomer yield than all the other samples. While the lignin oils of the remaining eudicots and monocot species contained a relatively higher number of oligomers that are likely to be linked by strong C–C bonds thus resulting in lower monomer yields than the three biomass. The samples with lower S/G ratio could result in more condensed structure with less amount of cleavable ether bonds (Vangeel et al., 2019).

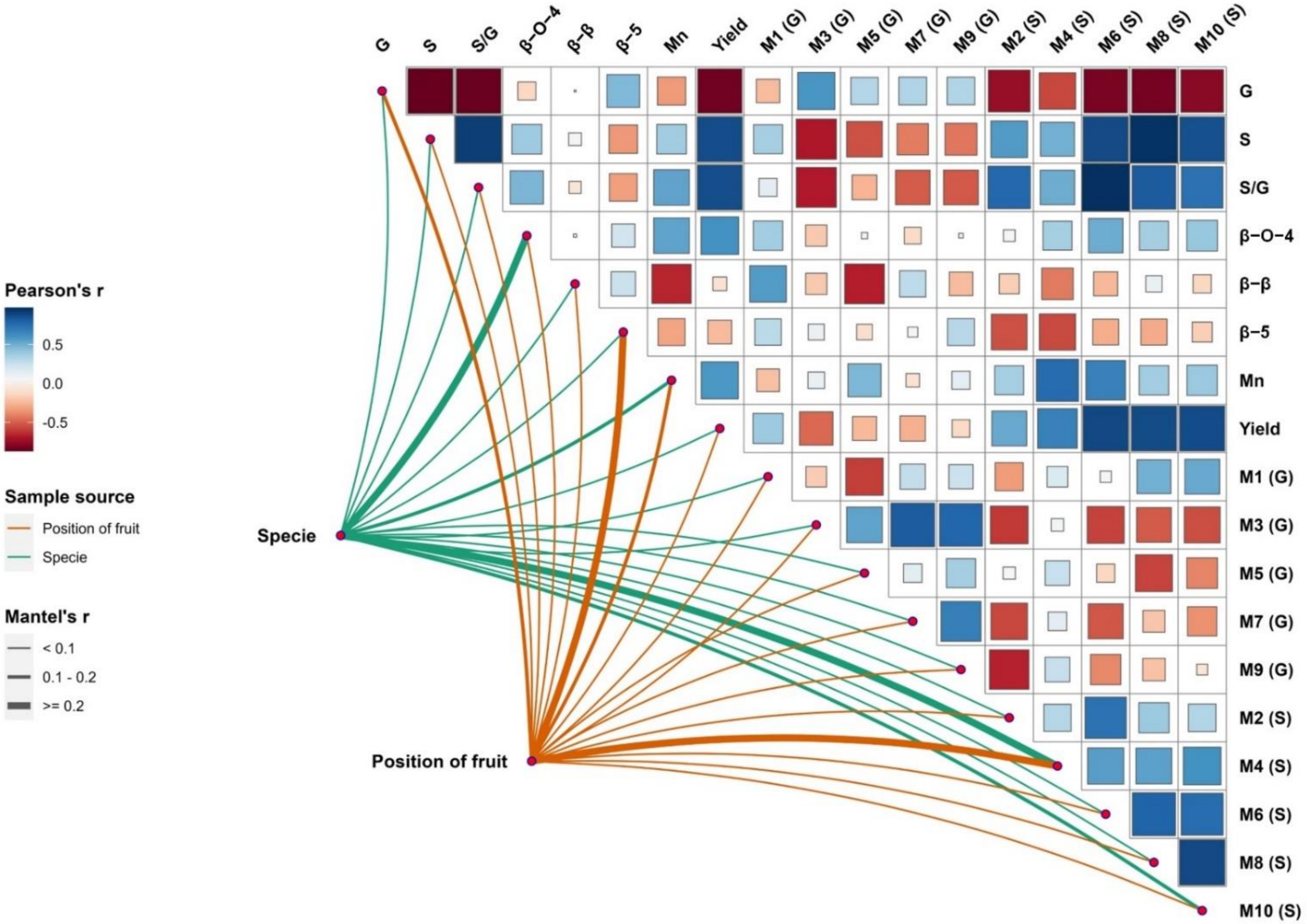

Figure 4.7: Correlations between lignin properties and monomer yields of the selected phylogenetically diverse fruit and nutshell wastes. The width of orange and grey lines indicates the r-value of the Mantel test. Comparisons among the lignin properties are also shown with a color gradient denoting Pearson's correlation coefficient.

4.4 Summary

The theoretical monolignol yields of ten fruit and nutshell wastes were investigated through RCF processes. Mango seed demonstrated the highest potential of monolignol yield at 37.1% per dry biomass, followed by walnut, pistachio peach, and cherry biomass. Candlenut shell was with the highest lignin content (~48%) and provided reasonable monolignol production including the special C-type lignin. Macadamia seed shell showed surprisingly low monolignol yield in RCF disputing with its high (~40%) lignin content. Peanut, date, and avocado remains are not suitable for monolignol production. On the crucial lignin properties, β−O−4 was the most critical factor impacting the monomer yield (Wang et al., 2020b). Other lignin properties such as molecular weight, the β–5 bonds and G/S ratios also showed correlations to monomer production. Overall, endocarp of eudicots seems to provide the most valuable lignin for monolignol production, while seeds and exocarp can be removed before the depolymerization process.

Chapter 5. Wood Waste Derived Nano Lignin-Enabled Membrane with High Structural Stability for Efficient Wastewater Treatment

5.1 Introduction

Lignin has recently unveiled great potential for its variety of applications (Tse et al., 2022) and has become an outstanding target of valuable building block chemicals in the new generation biorefinery (Khan et al., 2022) With high abundance and low cost, ease of functionality due to abundant reactive functional groups within the molecule, remarkable adsorption capacity, and other exciting properties such as antioxidant, antifungal and antimicrobial nature, lignin has gradually made its way in environmental remediation, i.e., wastewater treatment and membrane fabrication (Beck et al., 2017; Colburn et al., 2019; Ge and Li, 2018; Oribayo et al., 2017).

Dyeing wastewater has become one of the most significant contributors to aquatic pollution due to the unprecedented use of synthetic chemical dyes in textile, printing, tannery, cosmetic, and food processing industries. Approximately 10-25 % of textile dyes are lost during the dyeing process, and nearly 2-20 % are directly discharged into the receiving waters (Carmen and Daniel, 2012). These reactive and persistent chemicals have posed severe health risks to human and aquatic ecosystems, even at concentrations as low as one ppm (Hassaan and Nemr, 2017). Various technologies, including adsorption, chemical oxidation, photocatalytic or electrochemical degradation, ion exchange, and biological treatment, have been developed and used to remove these chemical species from industrial wastewater effluents (Donkadokula et al., 2020; Khan et al., 2018). The techniques achieved viable results, but most of them cannot completely remove the dyes; and, more importantly, could carry other environmental, economic, and operational concerns to hinder their large commercial-scale applications (Gosavi and Sharma, 2014; Zaharia et al., 2012). More reliable techniques are to be developed for dyeing wastewater. Various technologies including biological treatment processes, chemical oxidation, photocatalytic or electrochemical degradation, ion exchange, and adsorption have been developed and used over the years to remove these chemical species from industrial wastewater effluents (Donkadokula et al., 2020; Hynes et al., 2020). Apparently, the conventional techniques achieved viable results in treating dyeing wastewaters, however most of these methods remain insufficient to completely remove the dye from the water and most importantly can cause other environmental, economic, and operational concerns, which hinders their large commercial scale applications (Gosavi and Sharma, 2014; Zaharia et al., 2012). For instance, traditional biological treatment processes are not capable of completely mineralizing the target dyes, particularly when present in low concentration. Besides the large area, complex management, longer treatment time, and non-biodegradability of certain chemical dyes further limits their applications (Donkadokula et al., 2020). Similarly, the physicochemical methods such as coagulation, adsorption, oxidation, photocatalytic degradation also have multiple limitations including high operation and maintenance cost, process complexity (requiring highly skilled operators), generation of highly toxic breakdown byproducts (in case of oxidation and photocatalytic degradation), adsorbent saturation, regeneration and separation from the treated water, and production of large amounts of sludge that requires secondary disposal and so forth (Hynes et al., 2020; Yaseen and Scholz, 2019).

Relative to conventional treatment methods, ultrafiltration membrane separation techniques demonstrate its significant benefits of inherent operational simplicity, no phase change requirements, and high selectivity for complex wastewaters (Chen et al., 2015; George et al., 2022; Nawaz et al., 2021). To ensure the longevity and superior performance of the UF process for wastewater treatment, an ideal UF membrane is expected to have high permeation flux and solute rejection, superior structural integrity and chemical stability, and high antifouling properties (Chu et al., 2016; Yong et al., 2019). The most recent trend in the research of new generation membranes for the UF process is the composite membranes, where micro/nano-sized organic or inorganic materials are used in membrane fabrication to improve its performance for selective separation and complex wastewater treatment (Zahid et al., 2018a; Zhang et al., 2017). To date, various micro/nano-sized organic and inorganic materials have been incorporated into the polymer matrix to improve the intrinsic properties and performance of the UF membranes (Ali et al., 2019; Isawi, 2019; Farid et al., 2017; Zahid et al., 2018b). It is well-established in the literature that the physicochemical characteristics (i.e., size, morphology, solubility, charge properties, and the nature of functional groups) of the composite material determines the functionality, structure, morphology, and thus the performance of the prepared UF composite membrane in wastewater treatment applications. Several studies recently reported high adsorption capacity of lignin materials for various organic contaminants from the aqueous environment (Colburn et al., 2019; Supanchaiyamat et al., 2019). However, most of the previous studies utilized lignin and its derivative materials in static adsorption-based wastewater treatment, while there are only limited reports on the application of lignin as a composite material for the UF process.

The present study aims to synthesize nano-sized lignin particles (LNPs) fractionated using organosolv pretreatment method (the details of organosolv pretreated lignin have been provided in the supporting information) and employ them as a low-cost, efficient, and environmentally friendly biopolymeric additive for UF nanocomposite membrane fabrication. The effects of LNPs incorporation in the polymer matrix and their influences on the physiochemical and surface properties of the nanocomposite membrane were first studied and analyzed with advanced technologies. The LNP membranes were tested for treating synthetic dyeing wastewater containing methylene blue (MB; basic/cationic) and methylene orange (MO; acidic/anionic dyes) as model contaminants in a crossflow filtration setup.

5.2 Experimental Section

5.2.1 Materials and chemicals

Polyethersulfone (PES, MW = 58,000) was purchased from Sigma Aldrich USA to fabricate the membranes. Polyvinylpyrrolidone (PVP, MW = ~ 40,000) was obtained from Aladdin Shanghai, China, and used as a pore-forming agent. Acacia confusa wood chips were harvested from slope maintenance works and kindly provided by a local supplier in Hong Kong (RecycleGreen Project Ltd.). Methylene blue and methylene orange dyes were obtained from Shanghai Zhanyun Chemicals, China. The chemical properties and structure of the two tested dyes are presented in **Table 5.1**. All the other solvents and chemicals used for the organosolv pretreatment and lignin nanoparticle synthesis were purchased from Aladdin Shanghai and J&K Acros Organics Beijing, China. All materials and chemicals were used without any modification unless specified.

Table 5.1: Characteristics of dyes used in the study.

Dyes	Molecular Formula	Chemical Structure	Charge	Wavelength (λmax)
Methylene Blue	$C_{16}H_{18}N_3SCl$	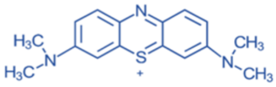	Cationic	665
Methylene Orange	$C_{14}H_{14}N_3NaO_3S$	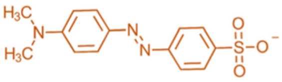	Anionic	465

5.2.2 Lignin fractionation using organosolv pretreatment

A series of steps were followed to prepare Acacia confusa chips for experimentation. Firstly, the chips were manually stripped of their bark and subsequently subjected to Wiley milling. The resulting material was sieved using a mesh size smaller than 2 mm. Next, a Soxhlet extraction was performed using a mixture of ethanol and toluene (in a 1:2 ratio, v/v) for 24 hours to remove extractives. After removing extractives, the sawdust was treated with a water-based organosolv process, employing sulfuric acid as a catalyst. This process was carried out using a custom-built rotating digester consisting of eight vessels, each with a capacity of 500 ml. The digester was manufactured by Xian Yang Tong Da Light Industry Equipment Co. Ltd., located in (Shanxi, China) (Islam et al., 2021) .In brief, 50 g portion of wood powder that had been dried in an oven was mixed with a sulfuric acid catalyst and organosolv reagents (65% v/v) at a liquid-to-solid ratio of 7:1. The digester was gradually heated to 170 ± 3 °C at a rate of 3 °C per minute and maintained at this temperature for 60 minutes (**Figure 5.1**). The substrate was separated from the liquor by using nylon cloth. The substrate underwent three rounds of washing with warm aqueous organosolv (75 mL each at 60 °C) at the same concentration as the spent liquor. The spent liquor and the organosolv washes were merged and blended with three parts of water (anti-solvent) to aid in the precipitation of dissolved lignin. The resulting residue, known as organosolv pretreated lignin (OL), was washed multiple times with tap water and subsequently freeze-dried before further experimentation.

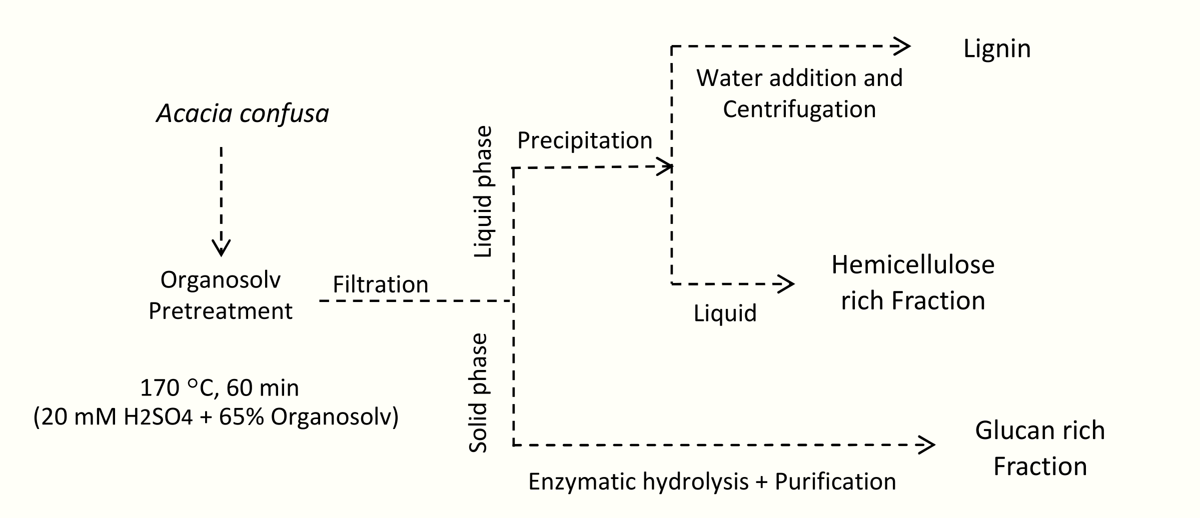

Figure 5.1: Schematic representation of steps in organosolv pretreatment of Acacia confusa feedstock with optimized pretreatment conditions: 20mM H_2SO_4, 65% Organosolv,170 ^{o}C, and 1 hr.

5.2.3 Synthesis of lignin nanoparticles

The lignin nanoparticles (LNPs) were synthesized following the anti-solvent precipitation method. For that purpose, 10 mg/mL of OSL was dissolved in the acetone/water (9:1 v/v). The suspension was then filtered using a 0.2 μm Millipore membrane to remove suspended particles. The filtrate was rapidly added (<1 min) to deionized water at a stirring speed of 500 rpm with a volume proportion of 1:2. The acetone was removed after continuous stirring for 30 min at 20 °C under vacuum by rotary evaporation. The suspension was then centrifuged at 20 °C and 5000 rpm for 15 min to free the suspension from aggregates. In the end, the LNPs were recovered from the supernatant after centrifugation for 40 min at 5 °C at a stirring speed of 16,500 rpm.

5.2.4 Characteristics of organosolv lignin and its nano-sized particles

The molecular weight of OL and LNPs was measured using Gel-permeation chromatography (GPC). Quantification of hydroxyl groups in the OL and LNP samples was performed using pulsed nuclear magnetic resonance (pNMR). Morphology, size, and size distribution analysis of LNPs were conducted using both transmission electron microscope (TEM) and scanning electron microscope (FE-SEM Hitachi SU5000). The SEM and TEM images were utilized to assess the size and distribution of LNPs, with ImageJ software employed to analyze the data. Mean values were calculated based on measurements from at least 100 NPs and presented as the average. The chemical composition of OL and the changes in its chemical makeup after its transformation from macro to nano size were analyzed using the Fourier transform infrared (FTIR) spectroscopy (Shimadzu IRAffinity-1). Additionally, a quantitative ^{31}P NMR spectra of LNPs were obtained using an inverse-gated decoupling pulse sequence on a JEOL ECZR 500 MHz spectrometer, following established protocols (Dong et al., 2019). The determination of hydroxyl groups through quantitative calculation relied on the quantity of the internal standard. The surface charge properties of OL and LNPs were studied from the zeta potential value of the particles. The zeta potential of both OL and LNPs was measured by a Zetasizer (Nano ZS90, Malvern, UK).

5.2.5 Fabrication of PES-LNP composite ultrafiltration membrane

PES-LNP ultrafiltration membranes were fabricated using the wet phase inversion method. The schematic of the membrane fabrication process is illustrated in **Figure 5.2.** First, a casting dope solution was prepared by mixing PES, LNPs, and PVP in a 1-methyl-2-pyrrolidone (NMP) solvent. A specific quantity of LNPs was dissolved in NMP while stirring for 30 minutes at 90 °C to achieve complete dissolution. Subsequently, the corresponding amount of PES polymer was introduced into the lignin-NMP solution, resulting in a final concentration of 13% and 2% for PES and LNPs, respectively. After 2 hours, PVP was added as a pore-forming agent, and the mixture was stirred for an additional 12 hours to ensure thorough blending. This process yielded a homogeneous casting solution with a brown hue, which was then left undisturbed for 24 hours to allow for the complete release of any trapped air bubbles. The next day, the casting solution was carefully poured onto a dense glass plate and cast using an automatic membrane/film coater with a thickness of 200 µm. After 15-20 s, the glass plate with cast solution was immersed in a coagulation bath containing room-temperature deionized (DI) water. After solvent–non–solvent exchange, the solid membrane detached from the casting glass and was soaked into the new tank of DI water to remove any residual solvent. Subsequently, the membranes prepared in the previous steps were immersed in DI water for seven days to facilitate comprehensive exchange of the solvent and non-solvent components.

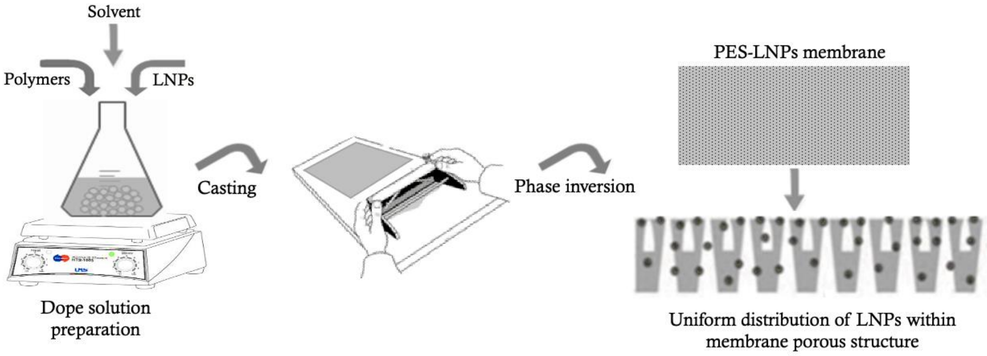

Figure 5.2: Schematic of PES-LNP membrane fabrication using wet immersion phase inversion

The PES membranes with OL or without any additive were also fabricated for comparison following the same procedure. The fabricated membranes were named PES, PES-OL, and PES-LNP membranes based on the presence of the additive material. Detailed membrane fabrication conditions are provided in **Table. 5.2**.

Table 5.2: Membrane fabrication conditions method.

Membranes	Concentrations			
	PES	PVP	OL	LNPs
PES membrane	13 %	2 %	-	-
PES-OL membrane	13 %	2 %	2 %	-
PES-LNPs membrane	13 %	2 %	-	2 %

'-' represents that material was not added

5.2.6 Characteristics of prepared membranes

The fabricated membrane samples' surface and sub-surface morphology and structure were evaluated using FE-SEM. Before the analysis, the membrane samples were sputter-coated gold-coated for 80 sec. To prepare cross-section samples for analysis, the membranes were immersed in liquid nitrogen for 15 seconds to achieve rapid freezing, followed by immediate fracturing. Before the examination, the fractured samples were coated with a layer of gold. Energy-dispersive X-ray (EDX) spectroscopy was used to perform the elemental analysis of the membranes. FTIR was used to attain information about the functional groups present on the membrane surface. The water contact angle (WCA) was measured by the Kris GmbH contact angle analyzer to assess the surface hydrophilicity of the membranes. The mean pore size of the membranes was measured using a porometer (PoroLuxTM, Germany) and confirmed by the pore size estimation from the top view SEM images using Image J. The thickness of the membranes was determined utilizing a precision micrometer. To assess the porosity of the membranes, their dry-wet weight was measured, and the following equation was employed to calculate the porosity:

$$Porosity\ (\%) = \frac{m_{wet} - m_{dry}}{\rho\ V_s} \qquad (1)$$

where ρ represents the density of the wetting liquid, V represents the membrane volume (obtained by multiplying the membrane area by its thickness), and mwet and mdry represent the mass of the wetted and dry membrane samples.

5.2.7 Membrane performance test

The performance of the fabricated membranes was assessed based on two performance indicators: water permeation flux and dye rejection rate. A crossflow filtration setup, equipped with a membrane module with an effective area of 0.00225 m^2 (as shown in **Figure 5.3**), was used to evaluate the membrane performance. To prevent the impact of membrane compaction, the membranes underwent hydraulic compaction with deionized water at 1 bar for 30 minutes before each filtration test. During the filtration tests, a synthetic dyeing wastewater with a concentration of 10 ppm, containing either MB or MO, was continuously circulated through the membrane at a constant operating pressure of 1 bar for 6 hours. Hourly samples of the permeate were collected to measure the dye concentration. The permeate flux during the filtration process was determined by monitoring the change in weight of the permeate over time and dividing it by the active area of the membrane.

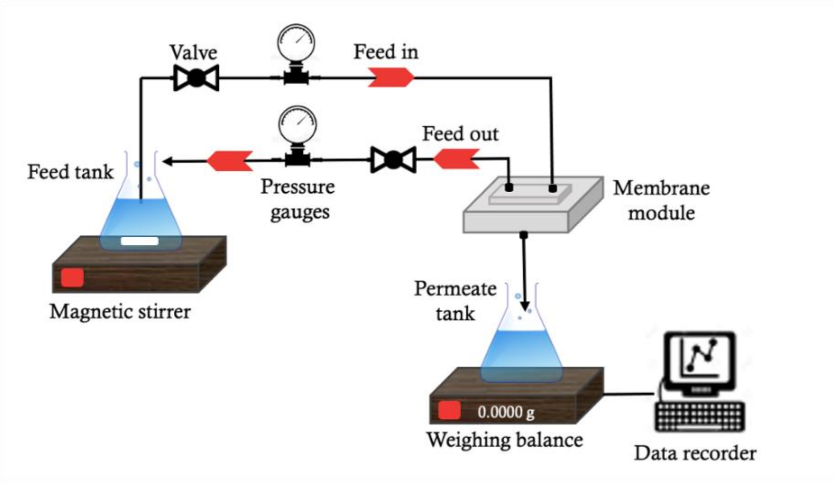

Figure 5.3: Schematic representation of crossflow ultrafiltration setup used in the study.

In the filtration test, the concentration of MB and MO in the permeate was measured using an ultraviolet-visible spectrophotometer (Shimadzu, Japan). The instrument utilized in this study is capable of detecting light absorption at a specific wavelength for both MB and MO (as detailed in Table S1). This information enables the calculation of the dye concentration in the permeate. The following equation determined the dye rejection efficiency R (%):

$$R\,(\%) = \left(1 - \frac{Cp}{Cf}\right) \times 100 \qquad (2)$$

In the equation, Cf (mg/L) represents the initial dye concentration in the feed, while Cp (mg/L) represents the final dye concentration in the permeate. To ensure the reproducibility of the results, each test for permeation flux and dye rejection was repeated at least twice.

5.2.8 Membrane stability test

The structural integrity and stability of the PES-LNP membrane were tested using both hydraulic flushing and ultrasonic agitation. Briefly, the possibility of LNPs leaching from the membrane (PES matrix) was measured by analyzing the total organic carbon (TOC) content in DI water after the hydraulic flushing operation and ultrasonication. For hydraulic flushing, the PES-LNP membrane was continuously flushed using DI water with a known TOC value at 3 bar pressure for 6 h, and the permeate was continually collected at one-hour intervals for subsequent TOC analysis. For the ultrasonication test, a 250 mL glass beaker containing DI water and a PES-LNP membrane coupon (4 x 4 cm) was placed in an ultrasonicator and operated at a power output of 80 W for 6 h. The water was sampled from the beaker at hourly intervals for TOC analysis. Any increase in the TOC concentration of the permeate or in beaker water as a function of time reflects the LNPs leaching from the PES matrix.

5.3 Results and discussion

5.3.1 Characteristics of OL and LNPs

Due to their high surface area, uniform size, and homogenous morphology, nano-sized materials are often preferred over larger materials of the same chemical composition for various applications (Boriskina et al., 2019; Zhao et al., 2018). Since lignin's chemical structure and properties determine its reactivity and, thus, the characteristics of LNPs, unveiling the physicochemical properties of the OL and LNPs is essential for their application in membrane fabrication. The molecular weight analysis of the lignin samples reflects the variations in depolymerization reactions occurring during the organosolv pretreatment. The molecular weight and the number-average molecular weights of the OL sample characterized using GPC were recorded as 9,945 and 5,790 g mol^{-1}, respectively. A polydispersity index (PDI) value calculated as 1.71 indicates a moderate Mw distribution of the lignin fractionated by the organosolv pretreatment, which improves its processability and facilitates the formation of LNPs.

The size and morphology of OL and LNPs were characterized using FESEM and TEM. As illustrated in **Figure 5.4a**, the OL particles exhibit agglomerated globular clusters composed of spherical lignin particles with no definite size and morphology. A possible explanation for such aggregated morphology of OL is its intrinsic amphiphilicity and self-assembly behavior that strongly favor the aggregation phenomena (Sipponen et al., 2018; Zhao et al., 2017). On the other hand, **Figure 5.4b** presents the successful transformation of raw OL into nano-sized lignin particles with uniform size and morphological characteristics, which are desired for membrane fabrication. As shown in **Figure 5.4c**, the synthesized LNPs exhibit uniform colloidal spherical morphology and moderate size distribution in the range of 60-240 nm, with an average particle size of ~150 nm (inset of **Figure 5.4c**). The dispersity index value of LNPs was calculated as 0.08, which further confirms that the LNPs prepared from the lignin fractionated by organosolv pretreatment exhibited uniform distributions with more than 81% of the LNPs possess a diameter between 120-180 nm.

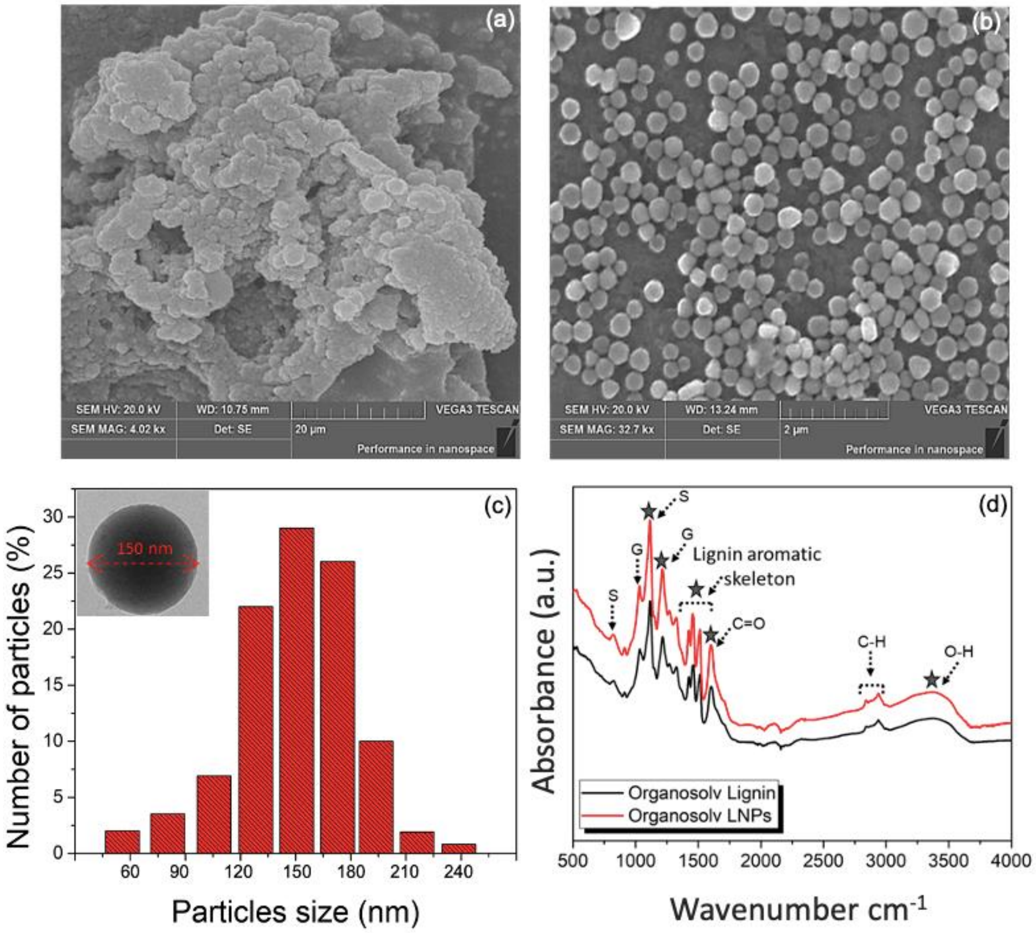

Figure 5.4: Characteristics of OL and LNPs; (a) SEM monograph of OL, (b) SEM monograph of LNPs, (c) Size distribution chart of LNPs (inset in c shows TEM image of a single LNP), (d) FTIR spectra of (a) OL and LNPs (Star represents changes/shifts in peaks for the LNPs samples in comparison to the raw OL)

Generally, the size and morphology of the LNPs synthesized via antisolvent precipitation technique are highly dependent on the initial lignin concentration, type and concentration of solvent used, solvent-to-water ratio, and the rate of antisolvent (water) dilution (Iravani and Varma, 2020; Tang et al., 2020; B. Wang et al., 2019). It is worthwhile to mention that herein, we investigated multiple

LNPs synthesis conditions; however, we have reported the representative optimal conditions that yielded uniform and stable LNPs with a relatively smaller diameter, uniform shape, and lower dispersity, which may suggest superior performance for their applications. Zeta potentials of OL and LNPs were measured to quantify the net surface charge and predict the colloidal stability of NPs dispersion, where a high positive or negative zeta potential value indicates adequate electrical double layer repulsion between suspended nanoparticles, preventing their aggregation (Figueiredo et al., 2018; Huang et al., 2017). The results of zeta potential values demonstrate the effects of acetone content during the solvent exchange process. Both OL and LNPs possess negative zeta potential values for −27.3 ± 1.8 mV and −39.9 ± 0.9 mV, respectively. The negative zeta potential values for both OL and LNPs were ascribed to the negative charge of the phenolic groups in lignin and due to the adsorption of OH^- ions on the lignin surface (Lee et al., 2020). The higher zeta potential value for LNPs shall be attributed to the increase in total phenolic moieties on the lignin surface. The zeta potential values for OL and LNPs align with their representative SEM images in **Figure 5.4**. LNPs with a high negative zeta potential value are electronically stabilized, and their aggregation is prevented due to enhanced electrostatic repulsion induced by the high surface charge of individual LNPs. In contrast, OL with a relatively lower negative zeta potential value is more likely to create amorphous aggregates due to weaker electrostatic repulsive forces.

The amounts and distribution of various hydroxyl groups were thereafter quantified in LNPs using quantitative ^{31}P NMR according to previously reported procedures (Dong et al., 2019). The hydroxyls within the LNPs are key functional groups responsible for influencing the overall properties of the nanocomposites. The ^{31}P-NMR spectra of LNPs are illustrated in **Figure 5.5**, while the functional group identification and content analysis are presented in **Table 5.3.**

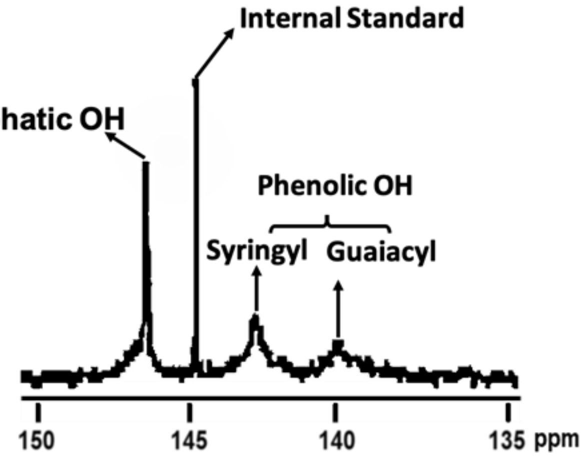

Figure 5.5: ^{31}P-NMR spectra of LNPs.

Table 5.3. Quantitative ^{31}P-NMR analysis of Lignin nanoparticles (LNPs).

Chemical Shift (ppm)	Assignment	Content (mmol g^{-1})
148.5 - 145.5	Aliphatic hydroxyl	1.60
143.5 - 141.5	Syringyl phenol hydroxyl (S)	0.90
140.2 - 138.2	Guaiacyl phenol hydroxyl (G)	0.46
—	Total phenolic hydroxyl	1.36
	Total hydroxyl	2.96

The results reveal that aliphatic hydroxyl groups were the dominant hydroxyl type in synthesized LNPs fractioned from organosolv pretreatment (1.60 mmol g^{-1}), followed by total phenolic hydroxyl groups (1.36 mmol g^{-1}). This is mainly because organosolv pretreatment employs aggressive extraction solvents (e.g., EtOH and 1,4-BDO) with sulphuric acid as the catalyst tended to extensively cleavage the β–O–4 linkages in the biomass lignin and thus, forms a large amount of free phenolic hydroxyl groups (Dong et al., 2019). A previous study reported that the high content of both aliphatic and phenolic OH groups in lignin could facilitate the synthesis of highly stable LNPs with a uniform size. Due to the enhanced electrical double layers, the LNPs are likely more desired as an adsorbent material.

To further verify the formation mechanism of LNPs during the solvent shifting, the FTIR spectra of OL and LNPs were measured, and the result is illustrated in **Figure 5.4d**. As observed, a prominent peak around 3,410 cm^{-1}, which originated from the hydroxyl (O-H) stretching vibration of aromatic and aliphatic structures, was present in both OL and LNPs. Peaks at 2,934 and 2,844 cm^{-1} were attributed to the C-H skeletal vibration in the CH_2 and CH_3 groups, respectively. Additionally, peaks at 1,593, 1,506, and 1,424 cm^{-1} corresponded to the lignin aromatic skeleton, while the presence of a peak at 1,456 cm−1 indicated C-H deformation associated with aromatic ring vibration, indicating the preservation of the primary structure of lignin during LNP synthesis. The peak at 1,327 cm^{-1} is assigned to the condensed syringyl and guaiacyl ring. Moreover, the peaks at 1,123 and 1,032 cm^{-1} resulting from the aromatic in-plane C-H bending deformation for syringyl and guaiacyl type lignin units were found in both OL and LNPs. In sum, the FTIR spectra of OL and LNPs samples exhibit similar characteristics of raw OL, apart from some slight shifts or increases in the intensity of individual peaks (marked in **Figure 3d** by star shape), suggesting no significant impacts on the lignin structure following the anti-solvent precipitation process.

5.3.2 Characteristics of fabricated membrane

To determine the chemical structure and the interactions between LNPs and host PES, the FTIR spectra of PES and PES-LNP membranes were obtained and compared (**Figure 5.6a**). Due to the relatively lower concentration of LNPs, and the overlapping of most of the peaks with PES, the characteristic peaks of LNPs could not be explicitly distinguished in the FTIR spectra of the PES-

LNP composite membrane. The characteristic peaks of PES present in the FTIR spectra of both membranes included benzene ring, aromatic skeletal, ether, and sulfone bond. The bands at 1,249 and 1,134 cm^{-1} are attributed to the stretching vibrations of S=O asymmetric and S=O symmetric, respectively, whereas peaks at 1,480 and 1,570 cm^{-1} represented bending vibration of PES aromatic rings (1,400–1,600 cm^{-1}). The appearance of carbonyl groups (1,650 cm^{-1}) and aliphatic C–N stretching (1,250–1,020 cm^{-1}) is attributed to PVP contained in membranes. The strong, broad band between 3,700 and 3,100 cm^{-1}, centering at around 3,430 cm^{-1}, is assigned to the O-H stretching vibration of aromatic and aliphatic structures attributable to LNPs and PES. However, the most prominent change observed in the PES-LNP membrane spectra was that the characteristic O-H band became more intense and broader after the incorporation of LNPs in the structure of the modified membrane. This change can be explained by the abundant hydroxyl groups in LNPs, which is in line with the ^{31}P NMR analysis of the LNPs. Apart from this, two new peaks that appeared at 2,934 and 2,844 cm^{-1} were observed in the spectra of PES-LNP membranes, which corresponds to the C-H skeletal vibration in the CH_2 and CH_3 groups in the LNPs, respectively. The higher intensity and the broadening of existing peaks, along with the newly appeared peaks in the FTIR spectra of the LNP membrane, confirm the effective incorporation of LNPs into the PES matrix. This PES-LNP incorporation can be ascribed to two possible interactions, i.e., the π– π interaction between benzene rings and hydrogen bonding between the OH- groups in LNPs and oxygen atoms of sulfone groups in PES (**Figure 5.6a** inset). A previous study reported similar behavior of interactions between a PES polymer and lignin materials (Esmaeili et al., 2018).

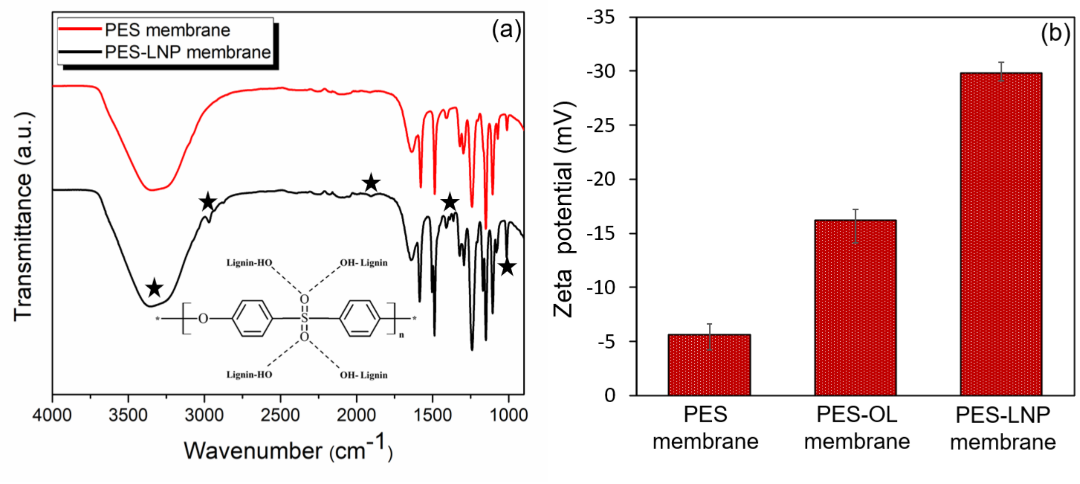

Figure 5.6: (a) FTIR spectra of PES and PES-LNP membranes (inset illustrates the bonds between LNPs and PES) (b) Zeta potential of PES, PES-OL, and PES-LNP membrane membranes

Next, the zeta potential measurements at neutral pH value were recorded to analyze the surface charge on the prepared membranes. The results revealed negative zeta potential values for all three membranes (PES, PES-OL, and PES-LNP), indicating that the prepared membranes carry negatively charged surfaces. The zeta potential value for the PES membrane was recorded at around -5.6 mV, which was closer to electric neutrality. Previous studies reported similar zeta potential values for the pure PES membranes (Salinas-Rodriguez et al., 2015). For PES-OL and PES-LNP, the zeta potential values were recorded as -16.2 mV and -29.8 mV, respectively (**Figure 5.6b**). These values correlate well with the zeta potential values recorded for OL and LNPs (with LNPs being more negatively charged than OL) and with the complete and uniform incorporation of LNPs in the polymer matrix.

The pore density, size, uniformity, and distribution of the UF membranes determine its final performance for wastewater treatment applications. Thus, the surface morphology and pore parameters of the prepared membranes were examined. Fig 5a-c presents the SEM monographs of the top surface view of pure PES and the two composite membranes prepared with OL and LNPs as an additive. The porous structure of all three prepared membranes can be observed with no noticeable difference in **Figure 5.7a-c**. This confirms that the technique (phase inversion method) and the optimized conditions (PES, PVP, lignin, solvent concentrations) used here were effective in fabricating the UF membranes. The composition and polymer-to-solvent ratio in the casting solution significantly impacted the phase inversion operation mechanism that needs to be optimized for a high-performing UF membrane fabrication. Regardless of the surface morphology, the pore size, density, and size distribution differed for the three membranes. Apparently, the pure PES and PES-OL membranes exhibit low pore density with non-uniform pore distribution. In contrast, the PES-LNP membrane presents relatively higher pore density and a more uniform pore size distribution. The inset of **Figure 5.7a-c** shows the real images of the prepared membranes. As expected, the pure PES membrane is white; however, the addition of 2 % OL and LNPs changes the membrane color from white to light and dark brown, respectively. Different colors of the two composite membranes with the same lignin (OL and LNPs) concentration indicate that OL with low aqueous stability and highly aggregated morphology (**Figure 5.7b**) was not completely incorporated with the host polymer and leached out during the phase inversion process, thus the prepared membrane exhibits light brown color. In contrast, the LNPs with superior aqueous stability, uniform size, and morphology were fully incorporated with the PES and thus, no leaching of LNPs was witnessed during the fabrication process all the LNPs were incorporated within the PES matrix. This hypothesis was further verified by the elemental examination of the membranes using energy dispersive X-ray (EDX), where the change in the concentration of two major elements (carbon and oxygen) in membranes served as an indicator to determine the final incorporation of additive material in the PES structure.

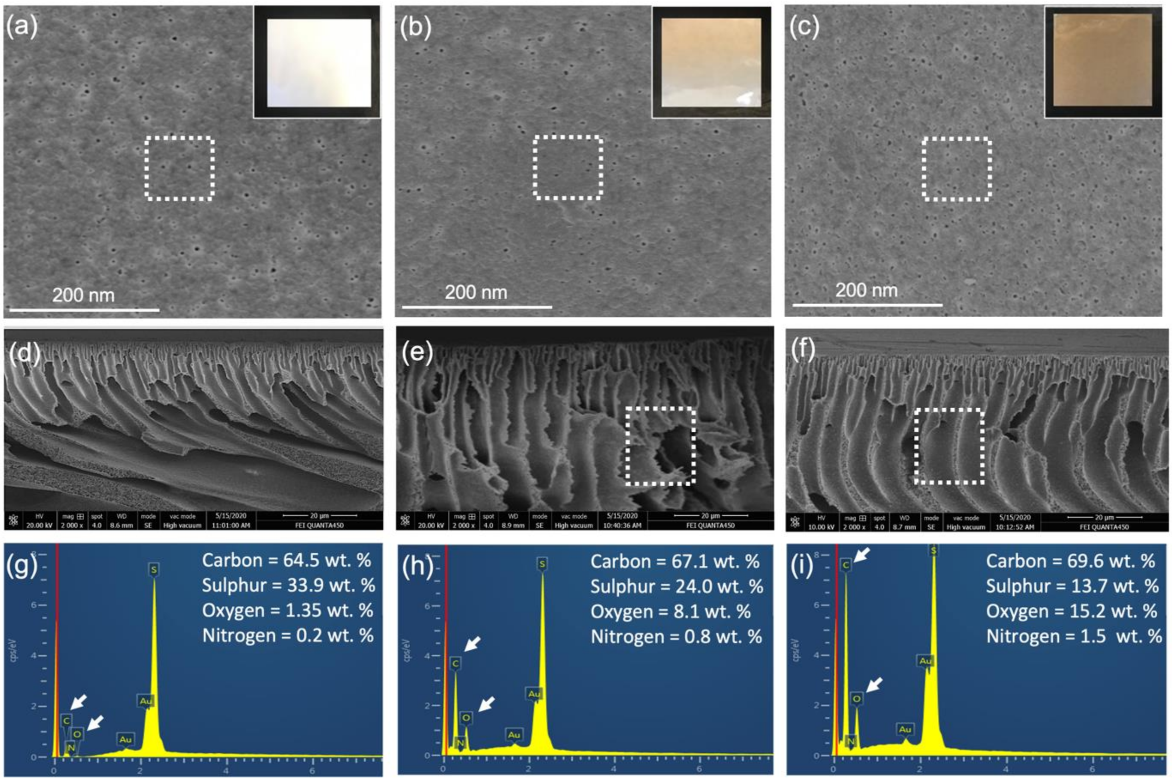

Figure 5.7: Top view SEM images and corresponding EDX spectra of prepared membranes: (a,g) SEM image and EDX spectra of pure PES membrane; (b,h) SEM image and EDX spectra of PES-OL membrane; (c, i) SEM image and EDX spectra of PES-LNP membrane; (inset of in a-c present the representative real images of the prepared membranes); Cross-sectional SEM images of (d) pure PES membrane; (e) OL-PES membrane; (f) LNP-PES membrane.

EDX spectra of pure PES membrane shows that the weight percentage of C and O was 64.5 % and 1.35 %, respectively, with negligible % of nitrogen (N) traces found (0.2%) (**Figure 5.7g**). The percentage of C and O increased from 64.5 – 67.1 % and from 1.36 – 8.1 %, respectively when 2 % OL was added in the membrane structure. The small traces of N in the chemical composition of the OL membrane were also observed (0.8 %) (**Figure 5.7h**). However, when the same concentration (2 %) of LNPs were added to the membrane, the percentage of C, O, and N increased up to 69.6 %, 15.2 % and 1.55 %, respectively (**Figure 5.7i**). These changes in the elemental composition confirms that complete incorporation of LNPs in the PES matrix.

The cross-sectional morphology of as-prepared ultrafiltration membranes was also examined to determine the porous architecture of the membranes. As illustrated in **Figure 5.7d-f**, all three membranes (PES, PES-OL, and PES-LNP) presented a typical asymmetric structure of the UF membrane, consisting of a dense surface layer and a finger-like macroporous sub-layer structures(Wan and Jiang, 2021). In the process of phase inversion, the presence of PVP resulted in the formation of elongated finger-like pores throughout the membrane's thickness. This phenomenon occurred because PVP is soluble in water and removed from the polymer matrix during membrane formation using a DI water coagulation bath. However, despite the basic structural similarity, PES-OL and PES-LNP membranes showed different macro-void microstructure from the pure PES membrane. For the PES-OL membrane, the finger-like structures of the composite membrane were partially damaged (messy and irregular voids appeared all over the entire cross-section) due to the change in chemical compositions, where the presence of hydrophobic OL with low dispersity and aggregated morphology interrupted the phase separation process (**Figure 5.7e**). In contrast, the PES-LNP membrane exhibits a more open structure with wider internal macrovoids (**Figure 5.7f**), higher sub-layer porosity, and a relatively thinner surface layer (**Figure 5.7f**). The thinner surface layer and wider and well-connected macrovoids are the two important factors that enhance the separation and permeation performance of the UF membranes respectively, whereas the higher sublayer porosity increases the overall surface area of the internal structure, which is highly desirable for adsorptive filtration applications. Adding LNPs with a high concentration of hydrophilic OH groups improves the mass transfer during the phase inversion and increases the thermodynamic instability in the casting solution, promoting the formation and expansion of macro-voids (Wan and Jiang, 2021). Moreover, LNPs accelerate the diffusion rate of water into the sub-layer during the phase inversion process, which increases sublayer porosity in the PES-LNP membrane.

Next, the wettability characteristics of the prepared membranes were studied by measuring the water contact angle (WCA) on the membrane surface. **Figure 5.8 a-c** inset shows the WCA of pure PES, PES-OL, and PES-LNP membranes. The WCA of pure PES membrane was measured at 52.9 ± 0.9 o, which increased to 64.4 ± 3.2 o when OL was added to the PES. Since OL is intrinsically hydrophobic in nature (Harris et al., 2017; Hrůzová et al., 2020), its presence in the membrane decreased the hydrophilicity. For the PES-LNP membrane, the hydrophilicity of the membrane (WCA = 55.8 ± 0.5 o) also decreased upon the addition of LNP s, however, the decline was not as significant as it was observed for the PES-OL membrane.

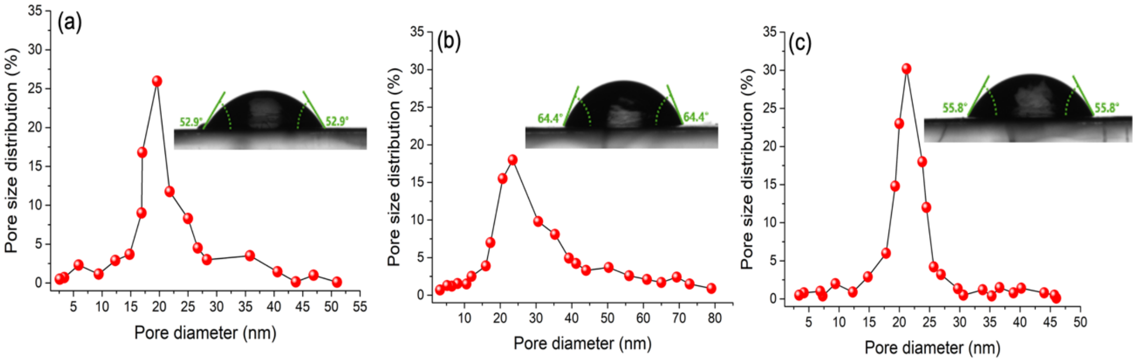

Figure 5.8: Pore size distribution (PSD) of (a) pure PES membrane (b) PES-OL membrane; (c) PES-LNPs membrane; (inset of in a-c present the representative water contact angle (WCA) of the prepared membranes)

This could be attributed to multiple factors, i.e., (a) the increase in total hydroxyl groups in LNPs upon antisolvent precipitation (polar functional groups can interact with water by hydrogen bonding); (b) the high surface area of LNPs can lead to higher adsorption of water molecules that balances the hydrophilicity on membrane surface; and (c) higher surface porosity. The analysis indicates that adding LNPs in the membrane did not significantly affect membrane hydrophilicity, which is an important factor in the UF membrane's performance for wastewater treatment applications.

The disparities in the pore size, pore size distribution (PSD), and pore density in the prepared membranes, as observed in the SEM images, were further verified by calculating the total porosity and PSD of the membranes. The PSD and porosity of prepared membranes are presented in **Figure 5.8 a-c**, respectively. The pure PES membrane with PVP as a pore-forming agent offers an average pore size of 18.2 nm, with nearly 50% of the pores falling within the range of 15 – 40 nm (**Figure 5.8a**). The total porosity of the pure PES membrane was calculated as 72.5 ± 0.9 %. All the pore parameters were significantly affected upon the addition of OL in the PES matrix. **Figure 5.8b** shows that the average pore size of the PES-OL membrane increased to 23.7 nm with relatively large PSD, where the pore size ranged from 2 - 81 nm. As expected, the total porosity of the PES-OL membrane also significantly declined to 63.6 ± 1.4 %. The significant shift in the average pore size, porosity, and PSD of the PES-OL membrane could be explained by the low dispersity and aggregation of OL in the casting solution. Since OL was not incorporated completely and uniformly within the PES matrix (more in some regions and less in others), so it significantly affected solvent-non-solvent mixing, the basic principle of pore formation during the phase inversion process. Similarly, the non-uniform morphology and size of OL affected the solvent-non-solvent reaction, thus resulting in broad PSD and low total porosity. The composite PES membrane with LNPs, in contrast exhibited an average pore size of 21.1 nm with narrow pore size distribution having around 85 % pores between 16 - 26 nm (**Figure 5.8c**). The PES-LNP membrane also exhibits the highest total porosity of 83.2 ± 0.9 %. This superior shift in membrane pore parameters is attributed to the high dispersity and stability of LNPs. As indicated by the zeta potential value, LNPs possess a strong negative charge on their surface, making them electronically stabilized and thus prevents their aggregation due to enhanced electrostatic repulsion induced by the high surface charge of individual LNPs. Moreover, the complete incorporation of consistently shaped and sized nanostructured lignin in the PES matrix further facilitates the solvent non-solvent mixing, thus resulting in uniform mean pore size in a narrow range. There is also a hypothesis suggesting that nanoparticles with consistent size and morphology can serve as pore-forming agents by creating hindrance effects within the polymer-solvent interphase during the membrane formation process (Guillen et al., 2011), which verifies the high total porosity of PES-LNP membrane.

The mechanical properties of composite membranes are also crucial in filtration operations as they determine the ability to withstand physical stress. Tensile strength testing was conducted to evaluate the mechanical properties of prepared membranes. The results indicated a reduction in mechanical strength for composite membranes when both OL and LNPs were added to the casting solutions compared to the pristine PES membrane. However, the degree of reduction varied between OL and LNPs. The pristine PES membrane exhibited a tensile strength of 5.92 ± 0.46 MPa, significantly decreasing to 4.7 ± 0.81 MPa for the OL PES membrane but remained nearly unchanged when LNPs were incorporated (5.71 ± 0.63 MPa). The superior mechanical strength of the pristine PES membrane can be attributed to its inherent properties, such as high strength, rigidity, creep resistance, and dimensional stability. The uniform dispersion of nano additives is crucial in composite membranes, as it strongly influences the mechanical strength during the phase inversion process. The SEM image confirmed that OL had aggregated structures, non-uniform size, and morphology, leading to non-uniform dispersion within the PES matrix. This resulted in decreased interfacial strength, reduced cross-link density, increased micro-structural inhomogeneity, and weakened links, ultimately lowering the tensile strength. Complementary evidence from EDX analysis, pore size distribution, and membrane color further supported the non-uniform dispersion of OL in the PES matrix. In contrast, adding LNPs to the PES matrix mitigated the decrease in tensile strength, preserving the mechanical properties of the pristine PES membrane. This can be attributed to the abundant OH groups in LNPs, which facilitated strong interfacial adhesion with the PES matrix. The OH groups formed hydrogen bonds with the polymer chains, enhancing compatibility and bonding, thereby improving stress transfer and overall strength. Furthermore, the uniform size and morphology of LNPs ensured a more homogeneous distribution within the composite membrane, minimizing weak points and stress concentration regions. Additionally, better alignment and packing of the polymer chains during the phase inversion process resulted in a more ordered and structurally stable membrane with improved tensile strength.

5.3.3 Permeability of the prepared membranes

In wastewater treatment applications, permeate flux and solute retention are considered the two most important indicators to evaluate the performance efficacy of a UF membrane. Therefore, the pure water (distilled water; DI) permeation flux was investigated through the PES, PES-OL, and PES-LNP membranes under the same operating conditions. For each test, the DI water was continuously passed through the membrane at 1 bar constant operating pressure for 1 h. The permeate flux during filtration was measured by recording permeate weight change over time and dividing it by the membrane active area. As expected, no flux decline was observed for all the tested membranes since the DI water has no suspended/dissolved solids or chemicals that can cause the blockage of the membrane porous structure (fouling of membrane). However, the three tested membranes (pure PES, PES-OL, and PES-LNP membranes) noted a significant difference in the initial permeation flux. **Figure 5.9** shows that the *pure water permeation flux* through each tested membrane was directly related to its wettability, structure, and morphology (hydrophilicity, number of pores and their size in the membrane surface layer, and morphology and structure of macrovoids in the sub-layer). The initial permeate flux for the PES, PES-OL, and PES-LNP membranes was recorded as 61.6 L $m^{-2} \cdot h^{-}$

^{1}, 41.8 L m^{-2}·h^{-1}, and 92.3 L m^{-2}·h^{-1}.

The lowest and highest initial permeate flux recorded for the PES-OL and PES-LNP membranes, respectively, can be attributed to their wettability, structural, and morphological characteristics. PES-LNP membrane possesses a thinner surface layer that induces low resistance to water flow, high pore density with large and uniformly distributed pores, wider and well-connected internal macrovoids with higher sub-layer porosity, and a low water contact angle. All these superior properties collectively contribute to the improved water permeation through the PES-LNP membrane. The PES-OL membrane exhibited a higher water contact angle (low hydrophilicity), low porosity, and partially damaged sub-layer structure, which explains the lowest initial flux recorded for the OL membrane.

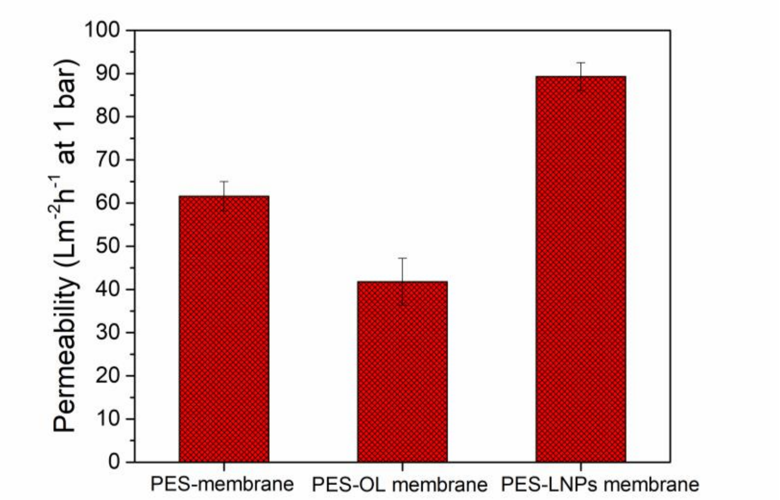

Figure 5.9: Water permeability of the prepared membranes

Since we confirmed that raw OL is not a suitable membrane additive for fabricating a high-performance UF composite membrane, the OL-prepared membranes are not further tested in this study.

5.3.4 Performance efficacy of PES-LNP membrane for dyeing wastewater treatment

The potential applications of the PES-LNP membrane for treating synthetic dyeing wastewater were investigated in a crossflow filtration setup. Two chemical dyes (basic/cationic MB and acidic/anionic MO) were used as model contaminants to simulate dyeing wastewater for the test. The filtration experiments were performed at 0.1 mPa pressure for 6 h with an initial dye concentration of 10 ppm, and the wastewater permeation flux and dye rejection rate were recorded (details are provided in section 2.7). The experimental results illustrated in **Figure 5.10** reveal an evident difference in the water flux recorded through the PES and PES-LNP membranes.

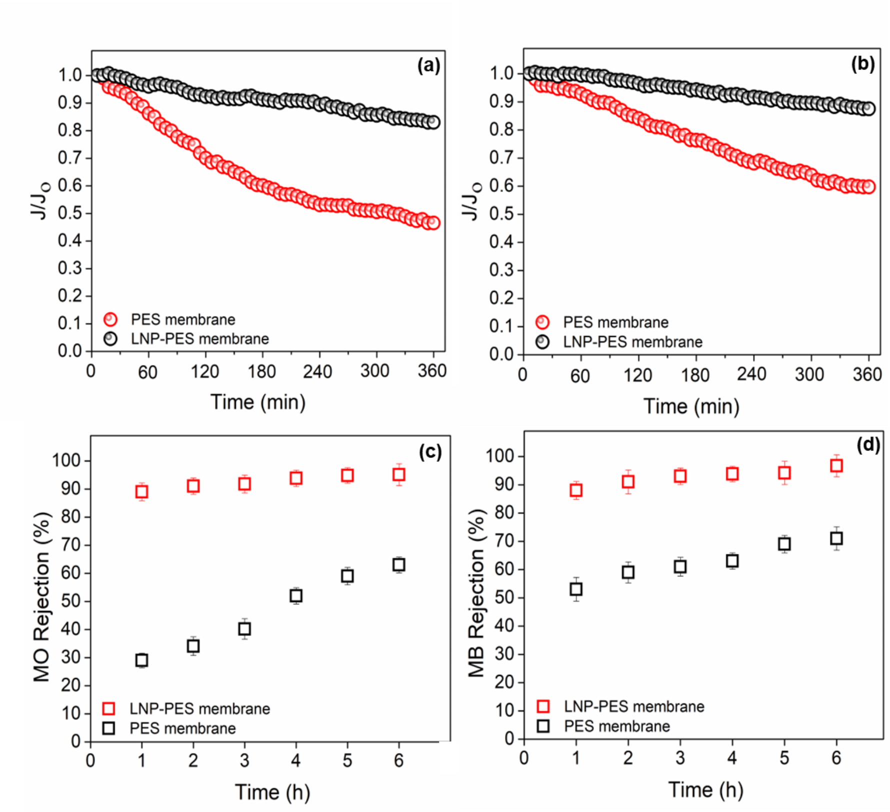

Figure 5.10: Performance parameters of pure PES and PES-LNP membranes: (a) MO normalized permeation flux through both membranes, (b) MB normalized permeation flux through both

membranes, (c) MO percentage rejection by both membranes, (d) MB percentage rejection by both membranes. Operating conditions: Operating pressure = 0.1 MPa, Initial MO and MB concentration = 10 ppm, Feed solution pH = neutral.

A higher initial MO flux value was recorded for the PES-LNP membrane as compared to the PES membrane, which is in line with our previous observation using DI water (**Figure 5.10a**). The flux value for MO-containing water through the PES-LNP membrane was almost stable throughout the filtration operation. In contrast, the permeation flux through PES membrane started to decline after the 3 h of filtration but eventually becomes stable at the lower value. For the MO removal efficiency, the PES membrane initially exhibited low MO retention (49 %) for 4 h of filtration but after that the removal rate started to increase with filtration time (61 % at 6 h) (**Figure 5.10c**). In contrast, the PES-LNP membrane exhibited significantly higher initial MO removal efficiency (89 %) that further improved with the operation time (95 % at 6 h) (**Figure 5.10c**). Since the average pore size of both PES and PES-LNP membranes is bigger than the molecular weight of MO, its rejection, herein cannot be solely explained by pure sieving mechanism (retention of molecules based on size). Instead, the MO rejection mechanism of the prepared membranes is governed by combined size exclusion and surface charge effects that work together to create a highly selective membrane. The anticipation can be confirmed by the lower MO removal efficacy of the PES membrane compared to the PES-LNP membrane. As aforementioned, at neutral pH both membranes exhibit negatively charged surface, but depicted by the zeta potential values, the PES-LNP membrane present a much higher negative zeta potential value (-29.8 mV; due to the negative charge of the phenolic groups on LNPs and also due to the adsorption of OH^- ions on the lignin surface), thus a stronger negative charge than the pure PES membrane (-5.6 mV closer to the electric neutrality). In this regard, we attributed the lower MO removal with PES membrane to the inferior electrostatic repulsive forces between the membrane surface and MO molecules, and thus apart from electrostatic interactions, other mechanisms, like surface complex formation via hydrogen and/or ionic bonding, and hydrophobic interactions may have also contributed to the removal of MO with PES membrane. The adsorption of negatively charged MO on the surface or within the porous structure of the PES membrane creates resistance to water flow and enhances the negative surface charge on the PES membrane, thus promoting the electrostatic repulsion between the membrane and the dye. This, in fact explains the observed flux decline and increased rejection through the PES membrane after a 3-4 h operation. For the PES-LNP membrane, since it exhibited a highly negatively charged surface, strong electrostatic repulsion between the membrane surface and MO molecule hindered the surface complex formations, thus, stable permeation flux and rejection of MO was achieved throughout the operation.

For the cationic MB dye, the permeation flux and rejection rate as a function of filtration time are illustrated in **Figure 5.10 b,d**. The results show that the initial permeation flux of MB spiked water through both membranes exhibited similar trends (higher for PES-LNP and lower for PES) (**Figure 5.10b**). In this case, however, the flux decline for the PES membrane after 2 h of filtration was much more significant than it was recorded for MO. For PES-LNP, the flux remained nearly stable for the initial 5 hours but tended to decline in the last hour. As for the rejection, the PES membrane exhibited low MB removal for the initial hours (51 % at 1 h), and thereafter the removal rate slightly increased with the operation time (69 % at six h) (**Figure 5.10d**). Since the charge on PES membrane at neutral pH is close to the electric neutrality, adsorption of positively charged MB on the PES membrane via electrostatic attraction would be negligible. Therefore, low MB removal was observed for the initial hours, which could be ascribed to the adsorption of MB molecules on the membrane surface via surface complexation mechanisms. It is well-reported in the literature that the PES membrane contains limited adsorption sites, which verifies the low removal of MB in this test (Huang and Cheng, 2020). This also explains the slight increase in the MB removal at the later hours, once all the sites are consumed, the membrane might become positively charged, and thus the electrostatic repulsion forces are again prevalent. The PES-LNP membrane, on the other hand, showed high removal of MB throughout the test owing to strong electrostatic attraction forces between the negatively charged PES-LNP membrane and positively charged MB molecules that facilitated the adsorption of MB molecules on the membrane surface. In brief, the adsorption process relies on several factors, such as the nature of the surface, active sites, and interaction behavior of both dye molecules and membranes. Adsorption can occur through various mechanisms, including electrostatic interactions, chemical bonding, ion exchange, hydrogen bond, hydrophobic attraction, and van der Waals force. Herein, we highlight the synergistic effect of supramolecular interactions, such as electrostatic attraction, cation-π interaction, and π-π interaction, which govern the adsorption of MB on the PES-LNPs membrane. Ionic bonds form between positively-charged functional groups of MB and negatively-charged groups of the LNP membrane. Dipole-dipole and Yoshida hydrogen bonding can occur between hydrogen and nitrogen atoms, and carboxyl groups and aromatic rings, respectively. Aromatic rings can act as electron donors or acceptors, forming cation-π, CH-π, anion-π, or n-π interactions. The oxygen-containing groups can achieve ion-dipole interactions. The presence of these supramolecular interactions amplifies the adsorption capacity (qe), while the diffusion within the boundary layer and inside the particles also plays a role in the adsorption of MB. The mechanistic illustration of both MO and MB rejection by the PES-LNP membrane is presented in **Figure 5.11c**. The superior adsorption of MB on the PES-LNP membrane could be further attributed to two significant factors. The higher surface and sub-surface porous structure of the PES-LNP membrane increase the overall surface area of the membrane and thus offers numerous adsorption sites for MB molecules to adsorb on the membrane surface or within the membrane pores; the nano-sized lignin particles with high surface area and superior adsorption capacity for MB dye further improved the adsorption performance of the membrane. The flux decline and the slight decrease in the rejection with the PES-LNP membrane in the later hours can be directly linked to the high adsorption capacity of the membrane. More MB adsorbed on or within the membrane structure may have created a resistance to the flow and shifted the charge of the membrane towards the point of electric neutrality, which ultimately weakened the electrostatic attractive forces.

5.3.5 Effect of solution chemistry on the performance of PES-LNP membrane for dyeing wastewater treatment

In order to verify the predominant role of electrostatic interaction (repulsion/attraction) and adsorption mechanism in the removal of both anionic and cationic dyes, we have studied the effects of changing pH on the performance of PES-LNP membrane for dyeing wastewater treatment. The LNP membranes were tested at three different pH values (acidic=3, neutral=7, and basic=9). The MO and MB wastewater flux and rejection as a function of pH through the PES-LNP membrane is presented in **Figure 5.11**. The results revealed that the rejection of both anionic MO and cationic MB dyes was highly pH dependent. For MO, the percentage removal increased from 59.7 % to 97.4% as we increased the feed solution pH from 3 to 9, respectively (**Figure 5.11a**). For MB, a relatively lower rejection (45.9 %) was recorded at pH 3 but at higher pH values the rejection increased up to 96.4% at pH 9 (**Figure 5.11b**). On the other hand, the permeation flux for MO was lower at pH 3, which increased as the solution pH was increased from 3 – 9 (**Figure 5.11a**). The opposite trend was observed for MB, where highest permeation flux was recorded at pH 3, which decreased with increase in solution pH (**Figure 5.11b**). The variations in the recorded rejection and permeation flux at different pH values can be explained by the change in membrane surface charge under acidic and basic conditions. The PES-LNP membrane exhibits a high negative zeta potential value at neutral pH due to highly negatively charged LNPs in its structure. However, at low pH (pH = 3), the zeta potential value of the PES-LNP membrane shifted towards the positive side, thus presenting a net positive charge on the surface.

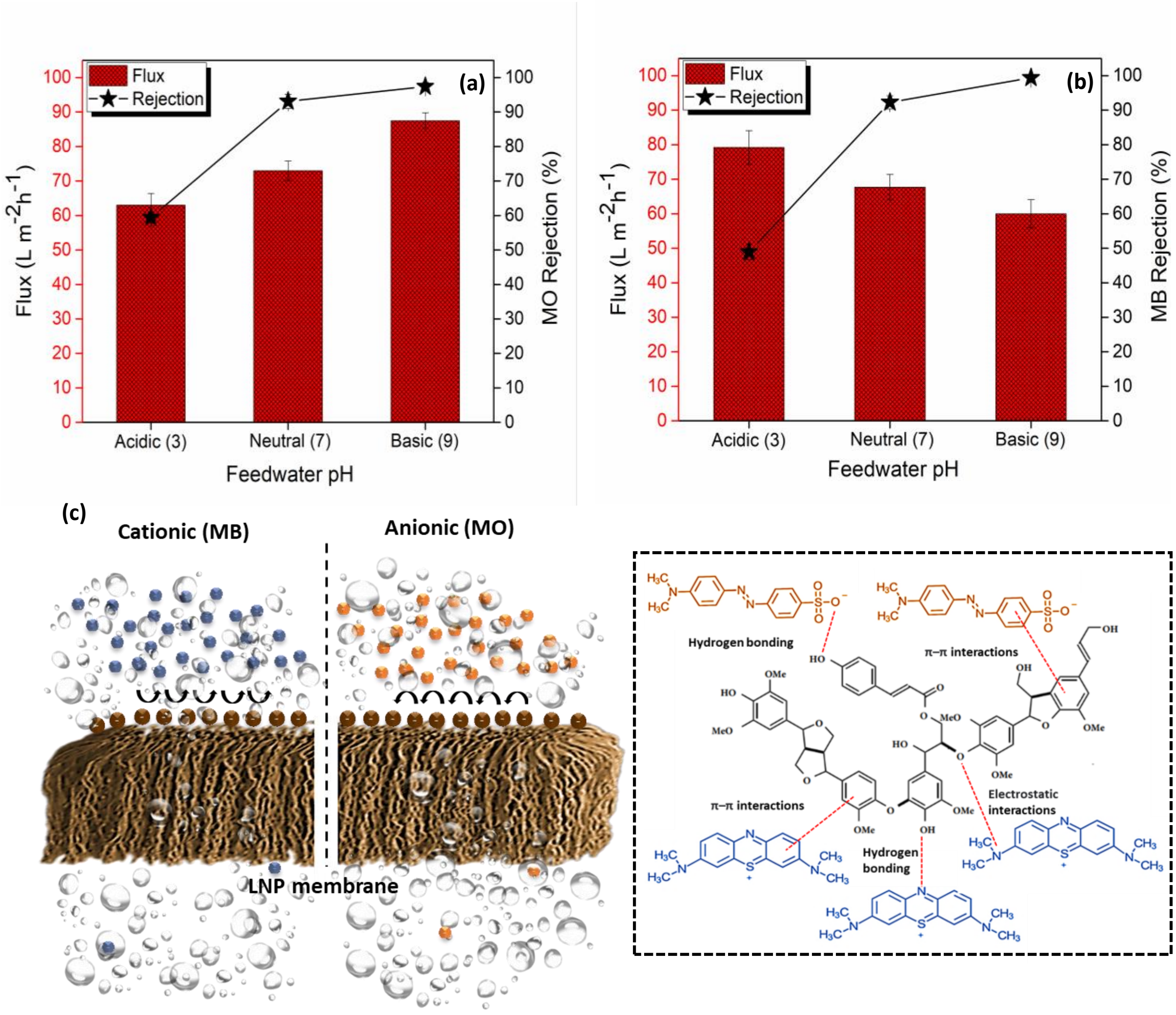

Figure 5.11: Performance parameters of PES-LNP membranes as a function of feed solution pH; (a) MO permeation flux and rejection through PES-LNP membrane as a function of pH, (b) MB permeation flux and rejection through PES-LNP membrane as a function of pH; Operating conditions: Operating pressure = 0.1 MPa, Initial MO and MB concentration = 10 ppm, Feed solution pH = acidic (3), neutral (7), basic (9), (c) Mechanistic illustration of cationic MB and anionic MO dye rejection by PES-LNP membrane

In contrast, at a higher pH (pH = 9), the zeta potential value of the membrane becomes more negative, thus presenting a much stronger negative charge on the membrane surface. This shift in the zeta potential value (surface charge) of the PES-LNP membrane is primarily attributed to the protonation and deprotonation of surface functional groups (high phenolic and aliphatic hydroxyl contents) on LNPs incorporated in the PES matrix under acidic and basic condition, respectively (Lievonen et al., 2016). It is well-reported that both anionic MO and cationic MB retain their net negative and positive charge in a wide pH range. Therefore, at pH 3, the electrostatic attraction between the charged membrane surface (4.7 mV at pH 3; slightly positive) and the negatively charged MO molecules results in dye rejection. However, once all the possible adsorption sites on the PES-LNP membrane are used up, the rest of the molecules may pass through the pores, leading to a low overall MO rejection at low pH. This also explains the low average flux recorded for MO at this pH. In contrast, at a high pH value, the electrostatic repulsion between the highly negatively charged membrane surface (-41.7 mV at pH 9) and MO molecules resulted in the highest rejection of the dye. Certainly, for MB , the explanation of this behavior should be the opposite in the case of anionic dye. Electrostatic repulsion between the membrane and MB molecules is the mainstream mechanism at low pH values, whereas electrostatic attraction is the primary interaction at higher pH. The relatively lower flux and high MB rejection at pH 9 further verify the role of electrostatic exclusion of MB dye. Table S3 summarizes the polymeric UF membranes of the previously reported works for removing different dye species wastewater.

5.3.6 Structural stability of PES-LNP membrane

A critical factor for the real-world applications of nanocomposite membranes is their structural integrity. Generally, in nanocomposite membrane-based wastewater treatment applications, there is a possibility of nanoparticles leaching from their respective incorporated membrane during filtration, leading to an ultimate decline in the membrane performance as well as some environmental concerns.

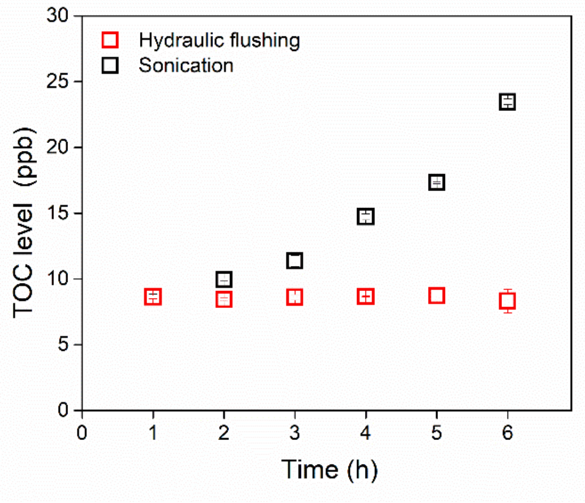

Figure 5.12: Structural stability of PES-LNP membrane upon hydraulic flushing and ultrasonication

Although LNPs have no known toxicity, their leaching from the membrane structure can significantly affect the performance and longevity of the membrane. Thus, herein, the stability and durability of the PES-LNP membrane was evaluated by quantitatively analyzing the possibility of LNPs leaching from the membrane (PES matrix). Briefly, the prepared PES-LNP membranes were exposed to two different physical testing conditions (ultrasonication and hydraulic flushing), and the total organic carbon (TOC) content in the water was measured. In the case of hydraulic flushing, DI water with known TOC concentration was continuously filtered through the PES-LNP membrane at 1 bar for 6 h, and the permeate was continually collected as consecutive fractions (1 h interval) for the TOC analysis. Any increase in the permeate TOC concentration as a function of pure water flushing time will determine LNPs leaching from the fabricated membrane. The results illustrated in Fig. 10 reveal no increase in the TOC concentration of the permeate water throughout 6 h filtration, verifying that the LNPs were completely incorporated (immobilized) within the PES matrix and did not leach out or dissolve during the test. To further evaluate its mechanical stability, the PES-LNP membrane was subjected to 3 h mild ultrasonication in DI water, and the TOC level in the water was measured after the test. A small increase in the TOC level after ultrasonication can be attributed to harsh high-power ultrasonication conditions, which are barely experienced in real-world applications.

Summary

This study introduces the synthesis and application of organosolv LNPs derived from wood waste as a cost-effective and environmentally friendly biopolymeric additive for ultrafiltration composite membranes. The process involved lignin fractionation through organosolv pretreatment, followed by LNPs synthesis using an anti-solvent precipitation method. Incorporating the as-synthesized LNPs into a polyethersulfone matrix led to significant improvements in the physicochemical and surface properties of the resulting nanocomposite ultrafiltration membranes. When applied to the treatment of synthetic dyeing wastewater, the PES-LNPs membrane demonstrated higher permeation flux stability and remarkable removal efficiencies (>95%) for both tested dye species, namely cationic methylene blue (MB) and anionic methylene orange (MO), across a wide range of environmentally relevant pH conditions. Furthermore, the structural and mechanical stability analysis of the lignin nanocomposite membrane confirmed the complete immobilization of LNPs within the PES matrix. This finding underscores the potential of reactive LNPs as a cost-effective and environmentally friendly additive for water purification membrane fabrication, highlighting their suitability for practical applications in the field of membrane technology.

Chapter 6. Techno-economic Evaluation of Biorefinery Utilizing RCF

6.1 Introduction

6.1.1 Economic trajectory and mass balance

Lignin plays a vital role in sustainable biorefineries and circular bioeconomy, but the lack of its economic feasibility has become the real bottleneck in lignin commercialization. To assess the economic viability and competitiveness of lignin-based processes, the techno-economic analysis (TEA) plays a crucial role. TEA evaluates the overall cost of production, including raw materials, energy consumption, equipment, and operational expenses, to determine the minimum selling price (MSP) of the target product. By conducting TEA, researchers can identify the critical cost-determining steps in the process and focus their efforts on optimizing those areas to improve economic feasibility. In addition to economic potential, understanding the technological maturity of lignin-based processes is vital for selecting the most promising pathways for commercialization. Assessing the maturity level helps researchers gauge the readiness of a technology for industrial-scale implementation and identify the gaps that need to be addressed to bridge the transition from lab-scale to commercial production. This information is valuable for making strategic decisions regarding research and development investments and prioritizing efforts to accelerate the deployment of lignin-based technologies.

Comprehensive TEA studies have started to emerge in the field of lignin valorization, shedding light on the economic and technical aspects of various processes. It is worth noting that TEA is not the sole factor in determining the commercial viability of lignin-based processes. Other factors, such as environmental sustainability, regulatory considerations, market demand, and scalability, also play crucial roles in the decision-making process. The situation of effective lignin valorization is further aggravated by its heterogeneity and wide molecular mass distribution from different feedstock. One of the challenges is the ineffectiveness of downstream processes used to produce the value-added chemicals from lignin, which lacks technological feasibility and economic viability. In-depth knowledge on the market demand, economic potential, and maturity of technology is crucial. The economic potential is important concept that can be used as a benchmark to identify whether the process is profitable or not in the long run. To clarify the technical, economic, and energy related factors affecting the economic feasibility of biorefinery technologies, Huang et al. (2020) performed TEA on γ-valerolactone-based process and obtained a minimum ethanol selling price (MESP) of US$3.44/ gasoline gallon equivalent from the optimized system (not including lignin). Martinez - Hernandez et al. (2019) performed TEA and greenhouse gas (GHG) analyses on IL pretreated lignocellulosic biomass for lignin derived phenol and cellulosic ethanol, suggesting a MESP of US$2.02/GGE. The market analysis (as MESP) would not only set the choice of product to be manufactured, but will also enables the researcher to predict on the future market trends. In this way, one may clearly identify the research efforts that can lower the barrier of the "cost-determining" step. Similarly, a comprehensive understanding of the maturity of a technology is important in selecting the most promising process that is viable at the current stage of technological development, which will also help highlighting the distance away from commercialization.

Recent advances in lignin depolymerization via many creative methods produces identified products in high yields, at the same time, raises the question: lignin-first biorefinery is reaching the commercial market or not (Sun et al., 2018b). Few TEA study on lignocellulosic biorefinery has been reported recently, however, only self-generated data was used, and there is a lack of comparison with other lignin depolymerization processes (Yadav et al., 2021). A comprehensive TEA that evaluates recent lignin works is needed to reveal the gap between technology development and real application, which further provide feedback to the researcher of where the improvement is required from an economic perspective. Recently, Khwanjaisakun et al. (2020) demonstrated the TEA of vanillin produced from Kraft lignin (synthesized via the oxidation process) and compared with the vanillin produced from petroleum-based feed. The study simulated three different separation cases, i.e., solvent extraction followed by distillation (Case I), solvent extraction (Case II), and vacuum distillation (Case III) and were then compared to identify the most suitable separation process. The results revealed that the highest vanillin yield of 9.25% was attained using 30 g/L feed concentration of Kraft lignin. Case I appeared to be the most suitable method of separation since it consumes the lowest amount of energy and gives the best economic returns, with a payback period of 6.19 years and internal rate of return of 22.63%. Despite the low yield of vanillin, the abundant supply and low cost of Kraft lignin make the valorization technique able to compete with the commercial process.

Similarly, the overall process mass balance is important in building complete process model for TEA and lifecycle assessment (LCA). In lignin conversion process, most of the mass balance can be separated into two aspects, i.e., (a) mass balance of extraction, depolymerization and separation processes, and (b) mass balance of catalyst synthesis process. For (a), most recent lignin research was focused on depolymerization processes, to some extent, mass balance in lignin extraction and monomer and/or dimer separation were ignored. For example, beech wood lignin was oxidative depolymerized to vanillin and syringaldehyde with high yields, however, the yield of substrates to extracted lignin was not reported, therefore, makes it difficult to understand the economic value (Gu et al., 2012). Moreover, downstream separation and purification processes were frequently ignored in related research, in fact, most of lignin research only reported the monomer and/or dimer yield without further actions in separation and purification (Gu et al., 2012). It is definitely understandable that experimentalist always aims for better performance in depolymerization, but it is also important to include mass balance from the original substrate to final product. For (b), another significant issue is the absence of mass balance for catalyst synthesis. Currently, conventional catalyst like Ru/C was widely used and commercially available, but its cost and environmental impact were unpredictable. Unconventional novel catalysts such as La/SBA-15, Cu-PMO, HZSM-5 and Cu/Mo ZSM-5 have been synthesized, but the monomer yields have not been reported (Gu et al., 2012). From economic perspective, catalyst cost constitutes a considerable amount of operational cost and significantly affect the profitability of the overall process and hence should be included in literatures for future references.

Overall, the economic feasibility and technological maturity of lignin-based processes are critical aspects that need to be considered for successful commercialization. Thus, TEA studies provide valuable insights into the economic potential, cost optimization opportunities, and environmental impacts of lignin valorization, guiding researchers, and industry stakeholders toward sustainable and economically viable lignin-based biorefineries.

6.2 Potential economic value evaluation of lignin monomers from fruit and nutshell

Based on the analysis of lignin monomer yield and the information of global production of all the fruit and nutshell selected in the study (**Chapter 4**), the economic analysis of potential monomer product was conducted. Among the 10 selected fruit and nutshells, peanuts, peaches, and mangoes are the top three fruits/nuts in terms of their highest annual production (96.76, 40.00, and 39.86 million tons/year) (**Figure 6.1a**). Additionally, they also have the highest total quantity of inedible parts (26.39, 15.30, and 5.04 million tons/year) (See **Table 6.1**).

Table 6.1. Annual fruit and nutshell production and the waste produced based on the weight percentage of kernels/shells to fruits and nuts.

Sample	Production* (Mt)	Fruit & Nutshell Weight (%)	Waste Biomass (Mt)
Walnut	4.42(FAOSTAT, 2023)	40-67% (Morales et al., 2021)	2.36
Peach	39.86(FAOSTAT, 2023)	10-15% (Natić et al., 2020)	5.04
Peanut	96.76(FAOSTAT, 2023)	25-30% (Perea-Moreno et al., 2018)	26.39
Mango	40(Mitra, 2014)	30-45% (Ganeshan et al., 2016)	15.3
Date	9.62(FAOSTAT, 2023)	10-15% (Afiq et al., 2013)	1.35
Cherry	2.61(Gençdağ et al., 2022)	12-20% (Lipiński et al., 2018; Pollard & Goldfarb, 2021)	0.43
Candlenut	0.554(Mariana et al., 2022)	66-70% (Tambunan et al., 2014)	0.38
Macadamia	0.0628 (INC, 2021)	35-38% (Richards et al., 2020)	0.02
Pistachio	1.008 (INC, 2021)	35-45% (Barreca et al., 2016)	0.41
Avocado	8.06(Rabobank, 2023)	10-16 % (Ahmad & Danish, 2022)	1.52

* Based on data from year 2019-2021

Although there is a clear demand for some lignin monomers such as guaiacol (M1) and syringol (M2) in the fields of medicine and agriculture(Cáceres et al., 2020; Machovina et al., 2019) , the low annual production and incomplete downstream development of most of the lignin monomers result in limited market demand. Therefore, we estimated the value of lignin monomers in a fully developed market scenario using vanillin, a common aromatic organic compound, as a reference. Meanwhile, the analysis assumed the Ru/C waste employed in industrial-scale production, with a catalyst recovery rate of 98% (Sultan et al., 2019a).

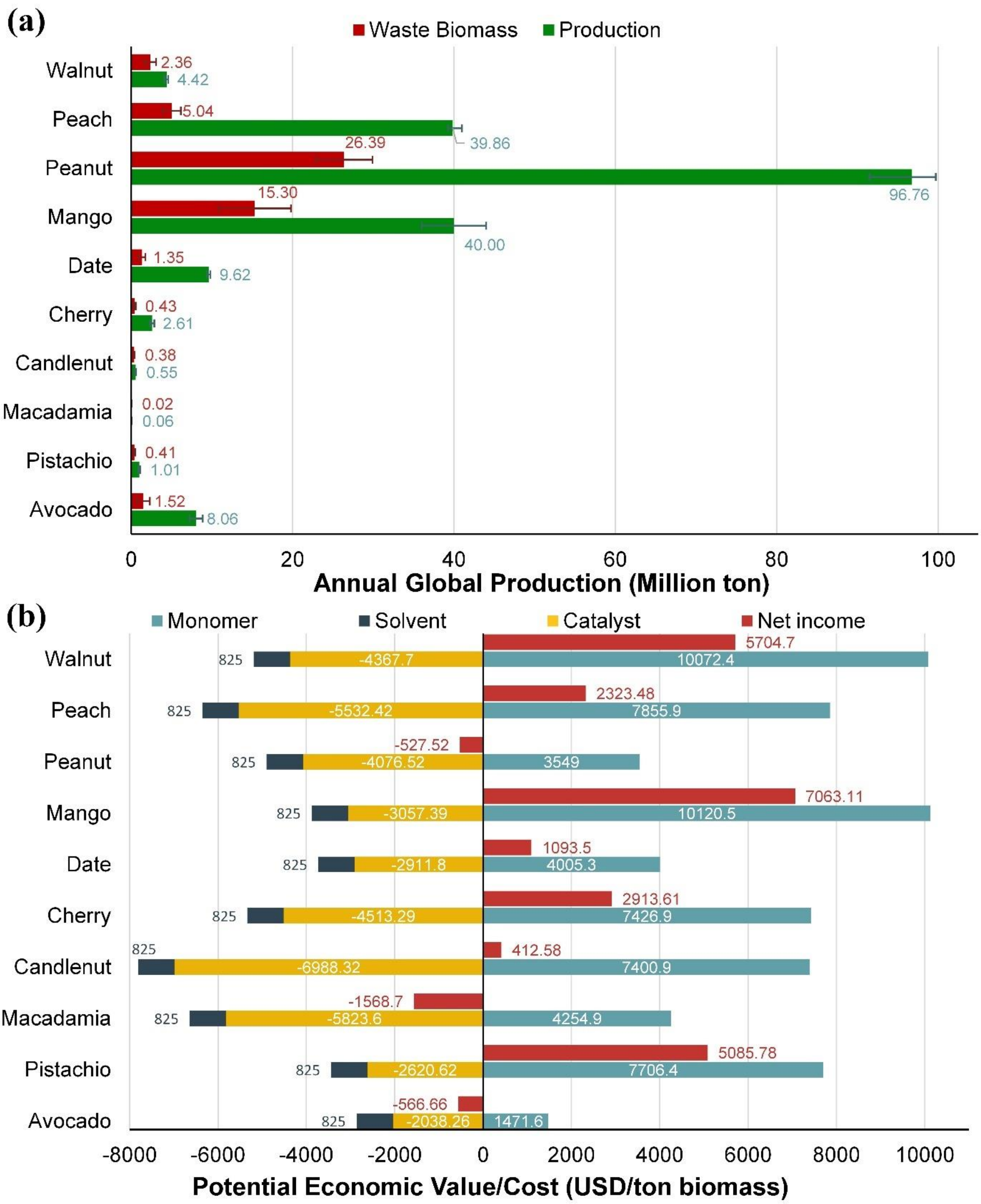

Figure 6.1: Potential economic value evaluation. (a) Annual global production of selected fruit and nutshell (2019-2021); (b) Economic value of potential monomer products. The cost of catalyst was calculated on lignin percentage of biomass with 98% recycling rate of catalyst. The unit price of the monomer is estimated using the market price of vanillin.

For potential monomer, economic benefits of some species turn out to be negative after eliminating costs of solvent and the catalyst (**Figure 6.1b**). Under the set conditions, the recovery of lignin monomers from macadamia, avocado, and peanut is not economically viable. While some species, such as mango, walnut, and pistachio have potential profitability opportunities. The economic evaluation presented in this study provides only a preliminary analysis of the potential value of lignin monomers under relatively ideal conditions. In practical industrial production, numerous factors need to be taken into consideration, such as energy consumption, raw material collection, catalyst development, etc. Some of these factors may increase operating costs, such as the construction of reaction equipment, while others may reduce production costs, such as the use of highly efficient and cost-effective catalysts. Although the results indicate some potential profitability in recovering lignin monomers from waste biomass, further research and on-site analysis are needed to fully explore this potential industry.

6.3 Challenges and future direction

The principal challenge in the lignin research field is to elaborate efficient and scalable approaches for isolating lignin that minimize structural degradation while still reaching high product yields and purity. Despite considerable progress, every isolation method introduces some degree of structural alteration, that can negatively impact succeeding lignin conversion to valuable chemicals. Thus, improving the quality of isolated lignin can be enhanced by considering two fundamental principles. The first principle focuses on minimizing degradation by preserving the original lignin structure and preventing depolymerization. Retaining β–O–4 linkages in lignin is one approach to enhance the potential for subsequent valorization routes. By keeping these bonds intact, the lignin's reactivity and potential for conversion can be maintained. The second theory aims to inhibit lignin’s structural degradation by avoiding the repolymerization of the reactive intermediate compounds. A practical technique to stall the formation of stable C-C bonds is to substantially remove such intermediate compounds from the heating region, typically achieved through continuous flow-through operations instead of batch processes. However, the continuous flow-through systems usually need higher liquid-to-solid ratios or gas-to-solid ratios as compared to the batch systems. While this approach prevents repolymerization, it results in streams that are more diluted, an additional energy-intensive product, and increased rates of solvent utilization, regeneration, and recycling. Hence, it is crucial to further explore and foster lignin isolation methods that strike a balance between high yield and purity while minimizing structural degradation. Additionally, investigating innovative strategies to prevent repolymerization and efficiently remove reactive intermediates will be vital for enhancing lignin conversion processes. These advancements will contribute to the sustainable utilization of lignin and facilitate the development of lignin-based biorefineries.

The current chapter has implied that lignin holds huge potential as a sustainable feedstock for the production of aromatic compounds. Based on the results of TEA, however, lignin based aromatics may hardly be competitive without government subsidies especially when the built of industry needs to developed upon the existing refinery products, such as energy and chemicals. In order to expand the industrial production of lignin, the aspects related to reactor scaling up, cost and risk analysis, supply chain, market assessments and regulatory and policy implications, which forms into significant sizes of needed investments. If the price of oil remains low, the constraints would be more acute and not suitable for local recyclers or departments. The industry may need to associate with (not competing with) conventional refinery before large scale utilization. A conceptual diagram of incorporating biorefinery process in a petroleum refinery, its related products, and instrumental retrofits have been illustrated in **Figure 6.2.** As hydrogenation catalysis and distillation systems are the most critical elements in petroleum refinery and the key unit operations for lignin depolymerization, solvent recovery, and product separation, the combine system may provide useful carbon benefits if some part of the fossil based feedstock can be replaced by biomass carbon.

In addition, one serious barrier in lignin valorization is the lack of rapid and comprehensive approach for lignin structure analysis. Evaluation of lignin depolymerization is currently time-consuming and hence real-time process control is not possible. Most lignin research therefore does not include detailed product information, market values, and potential applications. Furthermore, lignin is chemically and structurally inherently different from the currently used petrochemicals, therefore needs advance and innovative technologies for the one-to-one replacement of petrochemical precursors with lignin. This further indicates the need for adjustment and optimization of the existing formulation process, along with lignin. While significant research efforts have been made in this field, there still remains a gap in synergy and collaborative endeavors. We need to go beyond the "proof-of-concept" stage and to take a deeper dive into the "proof-of-value" stage in order to showcase on a commercial scale that lignin is a superior feedstock for certain chemicals and materials.

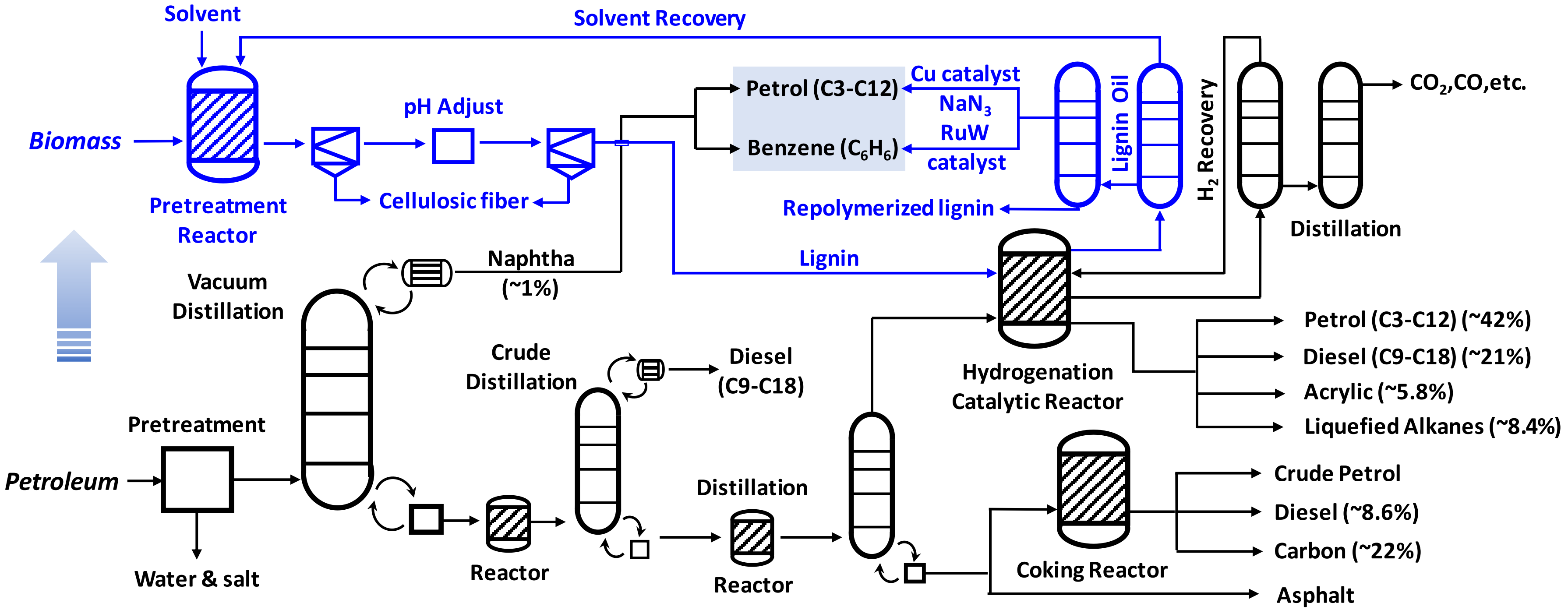

Figure 6.2: Possible retrofit and related aromatic products (marked in blue) in conventional refinery for lignin valorization. Note that distillation units may be replaced with and some products can only be provided by petroleum refinery.

6.4 Summary

The technoeconomic analysis of RCF process highlights the promising potential of lignin monomers in a fully developed market scenario. While there is a demand for specific lignin monomers such as guaiacol and syringol in industries like medicine and agriculture, the overall market for lignin monomers is currently limited due to low production levels and incomplete downstream development. To evaluate the economic feasibility of lignin monomers, the study considered vanillin, as a reference in a fully developed market. The analysis incorporated the use of Ru/C waste as a catalyst, assuming a high catalyst recovery rate of 98% based on industrial-scale production data. By estimating the value of lignin monomers in this scenario, the study provides insights into their potential market competitiveness. However, it also emphasizes the importance of further developing downstream processes for lignin utilization to unlock the full economic potential of lignin monomers. Overall, the technoeconomic analysis of RCF underscores the need for continued research and development efforts to enhance the downstream conversion of lignin monomers and establish a robust market for these valuable bio-based compounds.

Chapter 7. Conclusion and Future Perspective

In this dissertation, the influence of various factors on monomer yields obtained from lignin depolymerization has been investigated. It has been observed that the depolymerization method, lignin isolation method, and lignin source play significant roles in determining the efficiency of depolymerization. Also, the selection of lignin source has a substantial impact on the reactivity and yield of depolymerization products. Another aspect explored in this dissertation is the product selectivity in depolymerization, which was also influenced by the lignin source and the fractionation method employed. More condensed lignins were obtained through severe fractionation treatments. Thus, comparative pretreatment studies using the same lignin substrate were conducted to accurately examine the effect of depolymerization methods on product selectivity. Furthermore, the dissertation has recognized the importance of exploring practical applications for lignin and its derivatives, thereby facilitating the transition of lignin biorefineries towards value-added products. To this end, waste wood lignin has been examined as an additive in ultrafiltration membranes, offering a sustainable and efficient solution for water purification. This investigation has demonstrated the potential of lignin as a renewable resource with broader utilization prospects.

While RCF holds great promise as a sustainable method for the production of aromatic compounds, there are several challenges that need to be addressed. This thesis has shed light on some of these challenges and provided insights into potential solutions. However, there are still areas that require further research and exploration to fully unlock the potential of lignin depolymerization. One of the main challenges is the lack of standardized approaches and comparability among different depolymerization methods. Future research should prioritize standardized comparative studies using similar lignin substrates and analytical approaches to accurately evaluate depolymerization efficiency. This will enable researchers to make meaningful comparisons and identify the most effective depolymerization methods. This approach allows for the decoupling of the influence of structure of lignin from the depolymerization method. Studies should consider lignins obtained through optimized fractionation methods and industrially relevant lignin substrates. It is important to report the isolated lignin yield and consider the trade-off between isolation yield and lignin reactivity. When investigating the depolymerization of isolated lignins, the complete lignin mass balance should be taken into account to maximize the yield of the target product on a native lignin basis. Therefore, methods that enhance isolated yields of lignin products while preserving reactivity should be prioritized. The complexity of the depolymerization product mixture has implications for its valorization. Simple product mixtures can be easily separated and purified into individual compounds, whereas complex mixtures may be suitable for applications requiring specific chemical and physical characteristics. Convergent funneling approaches can also be employed to reduce the complexity of depolymerized lignin.

In conclusion, future research in lignin depolymerization should prioritize standardized comparative studies using similar lignin substrates and analytical approaches to accurately evaluate depolymerization efficiency. Lignin isolation methods that achieve high yields while preserving reactivity should be considered. The complete lignin mass balance and product selectivity based on the lignin source and fractionation method should be carefully examined. By addressing these challenges and implementing the recommended strategies, the development of efficient lignin isolation methods and valorization routes can be advanced, contributing to the utilization of lignin as a valuable resource in sustainable industries.

References

Abbati de Assis, C., Greca, L.G., Ago, M., Balakshin, M.Y., Jameel, H., Gonzalez, R., Rojas, O.J. 2018. Techno-economic assessment, scalability, and applications of aerosol lignin micro- and nanoparticles. *ACS sustainable chemistry & engineering*, **6**(9), 11853-11868.

Abu-Omar, M.M., Barta, K., Beckham, G.T., Luterbacher, J.S., Ralph, J., Rinaldi, R., Román-Leshkov, Y., Samec, J.S., Sels, B.F., Wang, F. 2021. Guidelines for performing lignin-first biorefining. *Energy & Environmental Science*, **14**(1), 262-292.

Achyuthan, K.E., Achyuthan, A.M., Adams, P.D., Dirk, S.M., Harper, J.C., Simmons, B.A., Singh, A.K. 2010. Supramolecular self-assembled chaos: polyphenolic lignin's barrier to cost-effective lignocellulosic biofuels. *Molecules*, **15**(12), 8641-8688.

Afiq, M.A., Rahman, R.A., Man, Y.C., Al-Kahtani, H., Mansor, T. 2013. Date seed and date seed oil. *International Food Research Journal*, **20**(5), 2035.

Ahmad, T., Danish, M. 2022. A review of avocado waste-derived adsorbents: Characterizations, adsorption characteristics, and surface mechanism. *Chemosphere*, **296**, 134036.

Anderson, E.M., Katahira, R., Reed, M., Resch, M.G., Karp, E.M., Beckham, G.T., Román-Leshkov, Y. 2016. Reductive catalytic fractionation of corn stover lignin. *ACS Sustainable Chemistry & Engineering*, **4**(12), 6940-6950.

Anderson, E.M., Stone, M.L., Katahira, R., Reed, M., Beckham, G.T., Román-Leshkov, Y. 2017. Flowthrough Reductive Catalytic Fractionation of Biomass. *Joule*, **1**(3), 613-622.

Ashokkumar, V., Venkatkarthick, R., Jayashree, S., Chuetor, S., Dharmaraj, S., Kumar, G., Chen, W.-H., Ngamcharussrivichai, C. 2022. Recent advances in lignocellulosic biomass for biofuels and value-added bioproducts - A critical review. *Bioresource Technology*, **344**, 126195.

Balasubramanian, S., Venkatachalam, P., N. Gummadi, S. 2023. Chapter 5 - Biofuel production from lignocellulosic biomass waste. in: *Valorization of Wastes for Sustainable Development*, (Eds.) R. Selvasembian, N.I. Wan Azelee, S.R. Shanmugam, P. Venkatachalam, A.K. Mishra, Elsevier, pp. 113-135.

Balat, M., Ayar, G. 2005. Biomass energy in the world, use of biomass and potential trends. *Energy Sources*, **27**(10), 931-940.

Banu, J.R., Kavitha, S., Kannah, R.Y., Devi, T.P., Gunasekaran, M., Kim, S.-H., Kumar, G. 2019. A review on biopolymer production via lignin valorization. *Bioresource technology*, **290**, 121790.

Barana, D., Ali, S.D., Salanti, A., Orlandi, M., Castellani, L., Hanel, T., Zoia, L. 2016. Influence of lignin features on thermal stability and mechanical properties of natural rubber compounds. *ACS Sustainable Chemistry & Engineering*, **4**(10), 5258-5267.

Barreca, D., Laganà, G., Leuzzi, U., Smeriglio, A., Trombetta, D., Bellocco, E. 2016. Evaluation of the nutraceutical, antioxidant and cytoprotective properties of ripe pistachio (Pistacia vera L., variety Bronte) hulls. *Food chemistry*, **196**, 493-502.

Barros, J., Serk, H., Granlund, I., Pesquet, E. 2015. The cell biology of lignification in higher plants. *Ann Bot*, **115**(7), 1053-74.

Barta, K., Warner, G.R., Beach, E.S., Anastas, P.T. 2014. Depolymerization of organosolv lignin to aromatic compounds over Cu-doped porous metal oxides. *Green Chemistry*, **16**(1), 191-196.

Bateman, R.M., Crane, P.R., DiMichele, W.A., Kenrick, P.R., Rowe, N.P., Speck, T., Stein, W.E. 1998. Early evolution of land plants: Phylogeny, physiology, and ecology of the primary terrestrial radiation. *Annual Review of Ecology and Systematics*, **29**(1), 263-292.

Bawareth, B., Di Marino, D., Nijhuis, T.A., Jestel, T., Wessling, M. 2019. Electrochemical Membrane Reactor Modeling for Lignin Depolymerization. *ACS Sustainable Chemistry & Engineering*, **7**(2), 2091-2099.

Bedia, J., Rosas, J.M., Rodríguez-Mirasol, J., Cordero, T. 2010. Pd supported on mesoporous activated carbons with high oxidation resistance as catalysts for toluene oxidation. *Applied Catalysis B: Environmental*, **94**(1), 8-18.

Behaghel de Bueren, J., Héroguel, F., Wegmann, C., Dick, G.R., Buser, R., Luterbacher, J.S. 2020. Aldehyde-assisted fractionation enhances lignin valorization in endocarp waste biomass. *ACS Sustainable Chemistry & Engineering*, **8**(45), 16737-16745.

Ben, H., Huang, F., Li, L., Ragauskas, A.J. 2015. In situ upgrading of whole biomass to biofuel precursors with low average molecular weight and acidity by the use of zeolite mixture. *RSC Advances*, **5**(91), 74821-74827.

Bengtsson, A., Bengtsson, J., Sedin, M., Sjöholm, E. 2019. Carbon fibers from lignin-cellulose precursors: effect of stabilization conditions. *ACS Sustainable Chemistry & Engineering*, **7**(9), 8440-8448.

Berstis, L., Elder, T., Crowley, M., Beckham, G.T. 2016. Radical nature of C-lignin. *ACS Sustainable Chemistry & Engineering*, **4**(10), 5327-5335.

Bjelić, A., Grilc, M., Huš, M., Likozar, B. 2019. Hydrogenation and hydrodeoxygenation of aromatic lignin monomers over Cu/C, Ni/C, Pd/C, Pt/C, Rh/C and Ru/C catalysts: mechanisms, reaction micro-kinetic modelling and quantitative structure-activity relationships. *Chemical Engineering Journal*, **359**, 305-320.

Boerjan, W., Ralph, J., Baucher, M. 2003. Lignin biosynthesis. *Annu Rev Plant Biol*, **54**(1), 519-46.

Boudet, A.-M. 2000. Lignins and lignification: selected issues. *Plant physiology and biochemistry*, **38**(1-2), 81-96.

Brandner, D.G., Kruger, J.S., Thornburg, N.E., Facas, G.G., Kenny, J.K., Dreiling, R.J., Morais, A.R.C., Renders, T., Cleveland, N.S., Happs, R.M. 2021. Flow-through solvolysis enables production of native-like lignin from biomass. *Green Chemistry*, **23**(15), 5437-5441.

Brienza, F., Van Aelst, K., Devred, F., Magnin, D., Sels, B.F., Gerin, P.A., Cybulska, I., Debecker, D.P. 2022. Reductive catalytic fractionation of wheat straw biomass. *ACS Sustainable Chemistry & Engineering*, **10**(34), 11130-11142.

Buchanan, B.B., Gruissem, W., Jones, R.L. 2015. *Biochemistry and molecular biology of plants*. John wiley & sons.

Bugg, T., Ahmad, M., Hardiman, E., Rahman Pour, R. 2011. ChemInform Abstract: Pathways for Degradation of Lignin in Bacteria and Fungi. *Natural product reports*, **28**, 1883-96.

Cabral Almada, C., Kazachenko, A., Fongarland, P., Da Silva Perez, D., Kuznetsov, B.N., Djakovitch, L. 2021. Supported-Metal Catalysts in Upgrading Lignin to Aromatics by Oxidative Depolymerization. *Catalysts*, **11**(4).

Cáceres, M., Guzmán, E., Alvarez-Costa, A., Ortega, F., G. Rubio, R., Coviella, C., Santo Orihuela, P.L., Vassena, C.V., Lucia, A. 2020. Surfactantless Emulsions Containing Eugenol for Imidacloprid Solubilization: Physicochemical Characterization and Toxicity against Insecticide-Resistant Cimex lectularius. *Molecules*, **25**(10), 2290.

Cai, C., Zhan, X., Zeng, M., Lou, H., Pang, Y., Yang, J., Yang, D., Qiu, X. 2017. Using recyclable pH-responsive lignin amphoteric surfactant to enhance the enzymatic hydrolysis of lignocelluloses. *Green Chemistry*, **19**(22), 5479-5487.

Cai, P., Fan, H., Cao, S., Qi, J., Zhang, S., Li, G. 2018. Electrochemical conversion of corn stover lignin to biomass-based chemicals between Cu/NiMoCo cathode and Pb/PbO2 anode in alkali solution. *Electrochimica Acta*, **264**, 128-139.

Cai, Z., Long, J., Li, Y., Ye, L., Yin, B., France, L.J., Dong, J., Zheng, L., He, H., Liu, S. 2019a. Selective production of diethyl maleate via oxidative cleavage of lignin aromatic unit. *Chem*, **5**(9), 2365-2377.

Cai, Z., Long, J., Li, Y., Ye, L., Yin, B., France, L.J., Dong, J., Zheng, L., He, H., Liu, S., Tsang, S.C.E., Li, X. 2019b. Selective Production of Diethyl Maleate via Oxidative Cleavage of Lignin Aromatic Unit. *Chem*, **5**(9), 2365-2377.

Chakraborty, M.S., Lali, A.M. 2021. Separation and catalytic depolymerization of empty palm fruit bunch lignin. *Industrial Crops and Products*, **174**, 114183.

Chaleawlert-umpon, S., Liedel, C. 2017. More sustainable energy storage: lignin based electrodes with glyoxal crosslinking. *Journal of Materials Chemistry A*, **5**(46), 24344-24352.

Chen, F., Tobimatsu, Y., Havkin-Frenkel, D., Dixon, R.A., Ralph, J. 2012. A polymer of caffeyl alcohol in plant seeds. *Proc Natl Acad Sci U S A*, **109**(5), 1772-7.

Chen, H. 2015. 3 - Lignocellulose biorefinery feedstock engineering. in: *Lignocellulose Biorefinery Engineering*, (Ed.) H. Chen, Woodhead Publishing, pp. 37-86.

Chen, X., Sun, S., Wang, X., Wen, J., Wang, Y., Cao, X., Yuan, T., Wang, S., Shi, Q., Sun, R. 2020. One-pot preparation and characterization of lignin-based cation exchange resin and its utilization in Pb (II) removal. *Bioresource Technology*, **295**, 122297.

Chesi, C., de Castro, I.B., Clough, M.T., Ferrini, P., Rinaldi, R. 2016. The influence of hemicellulose sugars on product distribution of early-stage conversion of lignin oligomers catalysed by Raney nickel. *ChemCatChem*, **8**(12), 2079-2088.

Chundawat, S.P.S., Sousa, L.d.C., Roy, S., Yang, Z., Gupta, S., Pal, R., Zhao, C., Liu, S.-H., Petridis, L., O'Neill, H., Pingali, S.V. 2020. Ammonia-salt solvent promotes cellulosic biomass deconstruction under ambient pretreatment conditions to enable rapid soluble sugar production at ultra-low enzyme loadings. *Green Chemistry*, **22**(1), 204-218.

Cooreman, E., Vangeel, T., Van Aelst, K., Van Aelst, J., Lauwaert, J., Thybaut, J.W., Van den Bosch, S., Sels, B.F. 2020. Perspective on overcoming scale-up hurdles for the reductive catalytic fractionation of lignocellulose biomass. *Industrial & Engineering Chemistry Research*, **59**(39), 17035-17045.

Dai, L., Ma, M., Xu, J., Si, C., Wang, X., Liu, Z., Ni, Y. 2020. All-lignin-based hydrogel with fast pH-stimuli responsiveness for mechanical switching and actuation. *Chemistry of Materials*, **32**(10), 4324-4330.

Das, L., Xu, S., Shi, J. 2017. Catalytic Oxidation and Depolymerization of Lignin in Aqueous Ionic Liquid. *Frontiers in Energy Research*, **5**, 21.

Demuner, I., Colodette, J., Demuner, A., Jardim, C. 2019. Biorefinery review: Wide-reaching products through kraft lignin. *BioResources*, **14**, 7543-7581.

Deuss, P.J., Scott, M., Tran, F., Westwood, N.J., de Vries, J.G., Barta, K. 2015. Aromatic monomers by in situ conversion of reactive intermediates in the acid-catalyzed depolymerization of lignin. *Journal of the American Chemical Society*, **137**(23), 7456-7467.

Diaz-Baca, J.A., Fatehi, P. 2021. Process development for tall oil lignin production. *Bioresource Technology*, **329**, 124891.

Dier, T.K.F., Rauber, D., Durneata, D., Hempelmann, R., Volmer, D.A. 2017. Sustainable Electrochemical Depolymerization of Lignin in Reusable Ionic Liquids. *Scientific Reports*, **7**(1), 5041.

Domínguez-Robles, J., Cárcamo-Martínez, Á., Stewart, S.A., Donnelly, R.F., Larrañeta, E., Borrega, M. 2020. Lignin for pharmaceutical and biomedical applications–Could this become a reality? *Sustainable Chemistry and Pharmacy*, **18**, 100320.

Dong, C., Meng, X., Yeung, C.S., TSE, H.-Y., Ragauskas, A.J., Leu, S.-Y. 2019. Diol pretreatment to fractionate a reactive lignin in lignocellulosic biomass biorefineries. *Green Chemistry*, **21**(10), 2788-2800.

Emmanouilidou, E., Mitkidou, S., Agapiou, A., Kokkinos, N.C. 2023. Solid waste biomass as a potential feedstock for producing sustainable aviation fuel: A systematic review. *Renewable Energy*, **206**, 897-907.

Fan, H., Chang, X., Wang, J., Zhang, Z. 2020. Catalytic pyrolysis of agricultural and forestry wastes in a fixed-bed reactor using K2CO3 as the catalyst. *Waste Management & Research*, **38**(1), 78-87.

FAOSTAT, C.D. 2023. Production—Crops and Livestock Products in 2020.

Fengel, D., Wegener, G. 2011. *Wood: chemistry, ultrastructure, reactions*. Walter de Gruyter.

Figueiredo, P., Lintinen, K., Hirvonen, J.T., Kostiainen, M.A., Santos, H.A. 2018. Properties and chemical modifications of lignin: Towards lignin-based nanomaterials for biomedical applications. *Progress in Materials Science*, **93**, 233-269.

Gan, L., Lyu, L., Shen, T., Wang, S. 2019. Sulfonated lignin-derived ordered mesoporous carbon with highly selective and recyclable catalysis for the conversion of fructose into 5-hydroxymethylfurfural. *Applied Catalysis A: General*, **574**, 132-143.

Ganeshan, G., Shadangi, K.P., Mohanty, K. 2016. Thermo-chemical conversion of mango seed kernel and shell to value added products. *Journal of Analytical and Applied Pyrolysis*, **121**, 403-408.

Gao, F., Webb, J.D., Hartwig, J.F. 2016. Chemo-and Regioselective Hydrogenolysis of Diaryl Ether C− O Bonds by a Robust Heterogeneous Ni/C Catalyst: Applications to the Cleavage of Complex Lignin-Related Fragments. *Angewandte Chemie*, **128**(4), 1496-1500.

García-Mateos, F.J., Cordero-Lanzac, T., Berenguer, R., Morallón, E., Cazorla-Amorós, D., Rodríguez-Mirasol, J., Cordero, T. 2017. Lignin-derived Pt supported carbon (submicron)fiber electrocatalysts for alcohol electro-oxidation. *Applied Catalysis B: Environmental*, **211**, 18-30.

Garedew, M., Lam, C.H., Petitjean, L., Huang, S., Song, B., Lin, F., Jackson, J.E., Saffron, C.M., Anastas, P.T. 2021. Electrochemical upgrading of depolymerized lignin: a review of model compound studies. *Green Chemistry*, **23**(8), 2868-2899.

Garedew, M., Young-Farhat, D., Jackson, J.E., Saffron, C.M. 2019. Electrocatalytic Upgrading of Phenolic Compounds Observed after Lignin Pyrolysis. *ACS Sustainable Chemistry & Engineering*, **7**(9), 8375-8386.

Garlapati, V.K., Chandel, A.K., Kumar, S.P.J., Sharma, S., Sevda, S., Ingle, A.P., Pant, D. 2020. Circular economy aspects of lignin: Towards a lignocellulose biorefinery. *Renewable and Sustainable Energy Reviews*, **130**, 109977.

Gellerstedt, G. 2015. Softwood kraft lignin: Raw material for the future. *Industrial Crops and Products*, **77**, 845-854.

Gençdağ, E., Görgüç, A., Yılmaz, F.M. 2022. Valorization of Sweet Cherry (Prunus avium) Wastes as a Source of Advanced Bioactive Compounds. in: *Mediterranean Fruits Bio-wastes: Chemistry, Functionality and Technological Applications*, Springer, pp. 559-579.

Gerardy, R., Debecker, D.P., Estager, J., Luis, P., Monbaliu, J.-C.M. 2020. Continuous flow upgrading of selected C2–C6 platform chemicals derived from biomass. *Chemical Reviews*, **120**(15), 7219-7347.

Ghazali, S.A.I.S.M., Fatimah, I., Zamil, Z.N., Zulkifli, N.N., Adam, N. 2023. Graphene quantum dots: A comprehensive overview. *Open Chemistry*, **21**(1).

Gomes, E., Rodrigues, A. 2020. Crystallization of vanillin from kraft lignin oxidation. *Separation and Purification Technology*, **247**, 116977.

Gomes, E., Rodrigues, A. 2019. Lignin biorefinery: Separation of vanillin, vanillic acid and acetovanillone by adsorption. *Separation and Purification Technology*, **216**, 92-101.

Gordobil, O., Herrera, R., Yahyaoui, M., İlk, S., Kaya, M., Labidi, J. 2018. Potential use of kraft and organosolv lignins as a natural additive for healthcare products. *RSC advances*, **8**(43), 24525-24533.

Gu, X., Kanghua, C., Ming, H., Shi, Y., Li, Z. 2012. La-modified SBA-15/H2O2 systems for the microwave assisted oxidation of organosolv beech wood lignin. *Maderas. Ciencia y tecnología*, **14**(1), 31-41.

Guan, J.Y., Zhuang, H.C., Lau, C.Y., Leng, L., Yeung, C.S., Vuppaladadiyam, A.K., Wang, H.M., Tse, H.Y., Leu, S.Y. 2022. Energy and carbon footprint analysis of municipal wastewater treatment process integrated with food waste disposer. *Journal of Cleaner Production*, **375**, 134063.

Guo, D., Hu, M., Chen, Z., Cui, B., Zhang, Q., Liu, Y., Luo, S., Ruan, R., Liu, Y. 2020. Catalytic Pyrolysis of rain tree biomass with nano nickel oxide synthetized from nickel plating slag: A green path for treating waste by waste. *Bioresource Technology*, **315**, 123831.

Guo, H., Chen, Y., Yang, S., Li, R., Zhang, X., Dong, Q., Li, X., Ma, X. 2021. Lignin-based adsorbent-catalyst with high capacity and stability for polychlorinated aromatics removal. *Bioresource Technology*, **337**, 125453.

Guo, L., Dou, R., Wu, Y., Zhang, R., Wang, L., Wang, Y., Gong, Z., Chen, J., Wu, X. 2019. From lignin waste to efficient catalyst: Illuminating the impact of lignin structure on catalytic activity of cycloaddition reaction. *ACS Sustainable Chemistry & Engineering*, **7**(19), 16585-16594.

Hendry, A., Åhlén, M., Fernandes, T., Cheung, O., Sanna, A. 2020. Catalytic cracking of Etek lignin with zirconia supported metal-oxides for alkyl and alkoxy phenols recovery. *Bioresource Technology*, **317**, 124008.

Henrique, M.A., Silvério, H.A., Neto, W.P.F., Pasquini, D. 2013. Valorization of an agro-industrial waste, mango seed, by the extraction and characterization of its cellulose nanocrystals. *Journal of environmental management*, **121**, 202-209.

Hodásová, Ľ., Jablonsky, M., Butor Skulcova, A., Haz, A. 2015. Lignin, potential products and their market value. *Wood research*, **60**, 973-986.

Hu, J., Zhang, Q., Lee, D.-J. 2018. Kraft lignin biorefinery: A perspective. *Bioresource Technology*, **247**, 1181-1183.

Hu, J., Zhang, S., Xiao, R., Jiang, X., Wang, Y., Sun, Y., Lu, P. 2019. Catalytic transfer hydrogenolysis of lignin into monophenols over platinum-rhenium supported on titanium dioxide using isopropanol as in situ hydrogen source. *Bioresource technology*, **279**, 228-233.

Huang, H. 2021. linkET: Everything is Linkable. 0.0.3 ed. GitHub, pp. R package.

Huang, K., Fasahati, P., Maravelias, C.T. 2020. System-Level Analysis of Lignin Valorization in Lignocellulosic Biorefineries. *iScience*, **23**(1), 100751.

Huang, X., Gonzalez, O.M.M., Zhu, J., Korányi, T.I., Boot, M.D., Hensen, E.J. 2017. Reductive fractionation of woody biomass into lignin monomers and cellulose by tandem metal triflate and Pd/C catalysis. *Green Chemistry*, **19**(1), 175-187.

Huang, X., Zhu, J., Korányi, T.I., Boot, M.D., Hensen, E.J. 2016. Effective release of lignin fragments from lignocellulose by Lewis acid metal triflates in the lignin-first approach. *ChemSusChem*, **9**(23), 3262-3267.

INC. 2021. Nuts & Dried Fruits Statistical Yearbook 2020/2021. The International Nut and Dried Fruit Council Foundation (INC).

Islam, M.K., Rehman, S., Guan, J., Lau, C.-Y., Tse, H.-Y., Yeung, C.S., Leu, S.-Y. 2021. Biphasic pretreatment for energy and carbon efficient conversion of lignocellulose into bioenergy and reactive lignin. *Applied Energy*, **303**, 117653.

Islam, M.K., Wang, H., Rehman, S., Dong, C., Hsu, H.-Y., Lin, C.S.K., Leu, S.-Y. 2020. Sustainability metrics of pretreatment processes in a waste derived lignocellulosic biomass biorefinery. *Bioresource technology*, **298**, 122558.

Ji, H., Lv, P. 2020. Mechanistic insights into the lignin dissolution behaviors of a recyclable acid hydrotrope, deep eutectic solvent (DES), and ionic liquid (IL). *Green Chemistry*, **22**(4), 1378-1387.

Ji, Q., Yu, X., Wu, P., Yagoub, A.E.-G.A., Chen, L., Taiye, M.A., Zhou, C. 2021. Pretreatment of sugarcane bagasse with deep eutectic solvents affect the structure and morphology of lignin. *Industrial Crops and Products*, **173**, 114108.

Jiang, B., Chen, C., Liang, Z., He, S., Kuang, Y., Song, J., Mi, R., Chen, G., Jiao, M., Hu, L. 2020. Lignin as a wood-inspired binder enabled strong, water stable, and biodegradable paper for plastic replacement. *Advanced Functional Materials*, **30**(4), 1906307.

Jin, J., Ding, J., Klett, A., Thies, M.C., Ogale, A.A. 2018. Carbon Fibers Derived from Fractionated–Solvated Lignin Precursors for Enhanced Mechanical Performance. *ACS Sustainable Chemistry & Engineering*, **6**(11), 14135-14142.

Jindal, M., Kumar, A., Rawat, S., Yang, B., Thallada, B. 2023a. Reductive catalytic cracking of industrial phenolics mixture to selective cyclohexanols. *Applied Catalysis A: General*, **653**, 119068.

Jindal, M., Uniyal, P., Thallada, B. 2023b. Reductive catalytic fractionation as a novel pretreatment/lignin-first approach for lignocellulosic biomass valorization: A review. *Bioresource Technology*, **385**, 129396.

Jönsson, A.S. 2016. 5 - Membranes for lignin and hemicellulose recovery in pulp mills. in: *Membrane Technologies for Biorefining*, (Eds.) A. Figoli, A. Cassano, A. Basile, Woodhead Publishing, pp. 105-133.

Jõul, P., Järvik, O., Lees, H., Kallavus, U., Koel, M., Lukk, T. 2024. Preparation and characterization of lignin-derived carbon aerogels. *Frontiers in Chemistry*, **11**.

Kai, D., Tan, M.J., Chee, P.L., Chua, Y.K., Yap, Y.L., Loh, X.J. 2016. Towards lignin-based functional materials in a sustainable world. *Green Chemistry*, **18**(5), 1175-1200.

Kaur, R., Bhardwaj, S.K., Chandna, S., Kim, K.-H., Bhaumik, J. 2021. Lignin-based metal oxide nanocomposites for UV protection applications: A review. *Journal of Cleaner Production*, **317**, 128300.

Kazachenko, A.S., Tarabanko, V.E., Miroshnikova, A.V., Sychev, V.V., Skripnikov, A.M., Malyar, Y.N., Mikhlin, Y.L., Baryshnikov, S.V., Taran, O.P. 2020. Reductive catalytic fractionation of flax shive over Ru/C catalysts. *Catalysts*, **11**(1), 42.

Khan, R.J., Guan, J., Lau, C.Y., Zhuang, H., Rehman, S., Leu, S.Y. 2023. Monolignol Potential and Insights into Direct Depolymerization of Fruit and Nutshell Remains for High Value Sustainable Aromatics. *ChemSusChem*, e202301306.

Khan, R.J., Lau, C.Y., Farid, M.U., Islam, M.K., An, A.K., Yi, J., Leu, S.-Y. 2024. Woody biomass derived nano lignin-enabled membrane with high structural stability for efficient wastewater treatment. *Process Safety and Environmental Protection*, **182**, 595-607.

Khan, R.J., Lau, C.Y., Guan, J., Lam, C.H., Zhao, J., Ji, Y., Wang, H., Xu, J., Lee, D.-J., Leu, S.-Y. 2022. Recent advances of lignin valorization techniques toward sustainable aromatics and potential benchmarks to fossil refinery products. *Bioresource Technology*, **346**, 126419.

Khwanjaisakun, N., Amornraksa, S., Simasatitkul, L., Charoensuppanimit, P., Assabumrungrat, S. 2020. Techno-economic analysis of vanillin production from Kraft lignin: Feasibility study of lignin valorization. *Bioresource Technology*, **299**, 122559.

Kim, J.-Y., Moon, J., Lee, J.H., Jin, X., Choi, J.W. 2020. Conversion of phenol intermediates into aromatic hydrocarbons over various zeolites during lignin pyrolysis. *Fuel*, **279**, 118484.

Kishimoto, T., Sano, Y. 2002. Delignification Mechanism during High-Boiling Solvent Pulping. Part 2. Homolysis of Guaiacylglycerol-β-Guaiacyl Ether. **56**(6), 623-631.

Klinger, G.E., Zhou, Y., Foote, J.A., Wester, A.M., Cui, Y., Alherech, M., Stahl, S.S., Jackson, J.E., Hegg, E.L. 2020. Nucleophilic Thiols Reductively Cleave Ether Linkages in Lignin Model Polymers and Lignin. *ChemSusChem*, **n/a**(n/a).

Koelewijn, S.F., Cooreman, C., Renders, T., Andecochea Saiz, C., Van den Bosch, S., Schutyser, W., De Leger, W., Smet, M., Van Puyvelde, P., Witters, H., Van der Bruggen, B., Sels, B.F. 2018. Promising bulk production of a potentially benign bisphenol A replacement from a hardwood lignin platform. *Green Chemistry*, **20**(5), 1050-1058.

Kouris, P.D., Huang, X., Boot, M.D., Hensen, E.J.M. 2018. Scaling-Up Catalytic Depolymerisation of Lignin: Performance Criteria for Industrial Operation. *Topics in Catalysis*, **61**(18), 1901-1911.

Kramarenko, A., Etit, D., Laudadio, G., D'Angelo, F.N. 2021. β-Zeolite-Assisted Lignin-First Fractionation in a Flow-Through Reactor. *ChemSusChem*, **14**(18), 3838-3849.

Kumaniaev, I., Subbotina, E., Sävmarker, J., Larhed, M., Galkin, M.V., Samec, J.S. 2017. Lignin depolymerization to monophenolic compounds in a flow-through system. *Green Chemistry*, **19**(24), 5767-5771.

Kumar, A., Biswas, B., Bhaskar, T. 2020. Effect of cobalt on titania, ceria and zirconia oxide supported catalysts on the oxidative depolymerization of prot and alkali lignin. *Bioresource technology*, **299**, 122589.

Lam, C.H., Deng, W., Lang, L., Jin, X., Hu, X., Wang, Y. 2020. Minireview on Bio-Oil Upgrading via Electrocatalytic Hydrogenation: Connecting Biofuel Production with Renewable Power. *Energy & Fuels*.

Lee, D.-W., Jin, M.-H., Park, J.-H., Lee, Y.-J., Choi, Y.-C. 2018. Flexible Synthetic Strategies for Lignin-Derived Hierarchically Porous Carbon Materials. *ACS Sustainable Chemistry & Engineering*, **6**(8), 10454-10462.

Li, C., Zheng, M., Wang, A., Zhang, T. 2012. One-pot catalytic hydrocracking of raw woody biomass into chemicals over supported carbide catalysts: simultaneous conversion of cellulose, hemicellulose and lignin. *Energy & Environmental Science*, **5**(4), 6383-6390.

Li, M., Yuan, Y., Zhu, Y., Jiang, B., Wu, W., Wu, S., Jin, Y. 2021. Comparison of sulfomethylated lignin from poplar and masson pine on cellulase adsorption and the enzymatic hydrolysis of wheat straw. *Bioresource Technology*, 126142.

Li, M., Zhang, Q., Luo, B., Chen, C., Wang, S., Min, D. 2020. Lignin-based carbon solid acid catalyst prepared for selectively converting fructose to 5-hydroxymethylfurfural. *Industrial Crops and Products*, **145**, 111920.

Li, Q., Serem, W.K., Dai, W., Yue, Y., Naik, M.T., Xie, S., Karki, P., Liu, L., Sue, H.-J., Liang, H., Zhou, F., Yuan, J.S. 2017a. Molecular weight and uniformity define the mechanical performance of lignin-based carbon fiber. *Journal of Materials Chemistry A*, **5**(25), 12740-12746.

Li, T., Lin, H., Ouyang, X., Qiu, X., Wan, Z. 2019a. In situ preparation of Ru@ N-doped carbon catalyst for the hydrogenolysis of lignin to produce aromatic monomers. *ACS Catalysis*, **9**(7), 5828-5836.

Li, W., Amos, K., Li, M., Pu, Y., Debolt, S., Ragauskas, A.J., Shi, J. 2018a. Fractionation and characterization of lignin streams from unique high-lignin content endocarp feedstocks. *Biotechnol Biofuels*, **11**, 304.

Li, Y., Demir, B., Ramos, L.M.V., Chen, M., Dumesic, J.A., Ralph, J. 2019b. Kinetic and mechanistic insights into hydrogenolysis of lignin to monomers in a continuous flow reactor. *Green chemistry*, **21**(13), 3561-3572.

Li, Y., Qiu, X., Qian, Y., Xiong, W., Yang, D. 2017b. pH-responsive lignin-based complex micelles: Preparation, characterization and application in oral drug delivery. *Chemical Engineering Journal*, **327**, 1176-1183.

Li, Y., Shuai, L., Kim, H., Motagamwala, A.H., Mobley, J.K., Yue, F., Tobimatsu, Y., Havkin-Frenkel, D., Chen, F., Dixon, R.A. 2018b. An “ideal lignin” facilitates full biomass utilization. *Science advances*, **4**(9), eaau2968.

Li, Y., Yang, D., Lu, S., Lao, S., Qiu, X. 2018c. Modified lignin with anionic surfactant and its application in controlled release of avermectin. *Journal of agricultural and food chemistry*, **66**(13), 3457-3464.

Liao, Y., Koelewijn, S.-F., Van den Bossche, G., Van Aelst, J., Van den Bosch, S., Renders, T., Navare, K., Nicolaï, T., Van Aelst, K., Maesen, M. 2020. A sustainable wood biorefinery for low–carbon footprint chemicals production. *Science*, **367**(6484), 1385-1390.

Lipiński, A.J., Lipiński, S., Kowalkowski, P. 2018. Utilization of post-production waste from fruit processing for energetic purposes: analysis of Polish potential and case study. *Journal of Material Cycles and Waste Management*, **20**, 1878-1883.

Liu, B., Abu-Omar, M.M. 2021. Chapter Five - Lignin extraction and valorization using heterogeneous transition metal catalysts. in: *Advances in Inorganic Chemistry*, (Eds.) P.C. Ford, R. van Eldik, Vol. 77, Academic Press, pp. 137-174.

Liu, C., Wang, S., Wang, B., Song, G. 2021a. Catalytic hydrogenolysis of castor seeds C-lignin in deep eutectic solvents. *Industrial Crops and Products*, **169**, 113666.

Liu, F., Wang, Q., Zhai, G., Xiang, H., Zhou, J., Jia, C., Zhu, L., Wu, Q., Zhu, M. 2022a. Continuously processing waste lignin into high-value carbon nanotube fibers. *Nature Communications*, **13**(1), 5755.

Liu, H., Sun, J., Leu, S.Y., Chen, S. 2016. Toward a fundamental understanding of cellulase-lignin interactions in the whole slurry enzymatic saccharification process. *Biofuels, Bioproducts and Biorefining*, **10**(5), 648-663.

Liu, J., Li, X., Li, M., Zheng, Y. 2022b. Chapter Six - Lignin biorefinery: Lignin source, isolation, characterization, and bioconversion. in: *Advances in Bioenergy*, (Eds.) Y. Li, Y. Zhou, Vol. 7, Elsevier, pp. 211-270.

Liu, S., Das, L., Blauch, D.N., Veronee, C., Dou, C., Gladden, J., Sun, N., Socha, A.M. 2020. Statistical design of experiments for production and purification of vanillin and aminophenols from commercial lignin. *Green Chemistry*, **22**(12), 3917-3926.

Liu, Y., Chen, L., Wang, T., Zhang, Q., Wang, C., Yan, J., Ma, L. 2015. One-pot catalytic conversion of raw lignocellulosic biomass into gasoline alkanes and chemicals over LiTaMoO6 and Ru/C in aqueous phosphoric acid. *ACS Sustainable Chemistry & Engineering*, **3**(8), 1745-1755.

Liu, Y., Deak, N., Wang, Z., Yu, H., Hameleers, L., Jurak, E., Deuss, P.J., Barta, K. 2021b. Tunable and functional deep eutectic solvents for lignocellulose valorization. *Nature communications*, **12**(1), 5424.

Liu, Z., Li, H., Gao, X., Guo, X., Wang, S., Fang, Y., Song, G. 2022c. Rational highly dispersed ruthenium for reductive catalytic fractionation of lignocellulose. *Nature Communications*, **13**(1), 4716.

Luo, C., Du, L., Wu, W., Xu, H., Zhang, G., Li, S., Wang, C., Lu, Z., Deng, Y. 2018. Novel Lignin-Derived Water-Soluble Binder for Micro Silicon Anode in Lithium-Ion Batteries. *ACS Sustainable Chemistry & Engineering*, **6**(10), 12621-12629.

Ma, Z., Ghosh, A., Asthana, N., van Bokhoven, J. 2017. Optimization of the reaction conditions for catalytic fast pyrolysis of pretreated lignin over zeolite for the production of phenol. *ChemCatChem*, **9**(6), 954-961.

Macfarlane, A.L., Mai, M., Kadla, J.F. 2014. 20 - Bio-based chemicals from biorefining: lignin conversion and utilisation. in: *Advances in Biorefineries*, (Ed.) K. Waldron, Woodhead Publishing, pp. 659-692.

Machovina, M.M., Mallinson, S.J.B., Knott, B.C., Meyers, A.W., Garcia-Borras, M., Bu, L., Gado, J.E., Oliver, A., Schmidt, G.P., Hinchen, D.J., Crowley, M.F., Johnson, C.W., Neidle, E.L., Payne, C.M., Houk, K.N., Beckham, G.T., McGeehan, J.E., DuBois, J.L. 2019. Enabling microbial syringol conversion through structure-guided protein engineering. *Proc Natl Acad Sci U S A*, **116**(28), 13970-13976.

Mandeep, Kumar Gupta, G., Shukla, P. 2020. Insights into the resources generation from pulp and paper industry wastes: Challenges, perspectives and innovations. *Bioresource Technology*, **297**, 122496.

Mariana, M., Mistar, E.M., Syabriyana, M., Zulkipli, A.S., Aswita, D., Alfatah, T. 2022. Properties and adsorptive performance of candlenut shell and its porous charcoals for aqueous mercury (II) removal. *Bioresource Technology Reports*, **19**, 101182.

Martinez-Hernandez, E., Cui, X., Scown, C.D., Amezcua-Allieri, M.A., Aburto, J., Simmons, B.A. 2019. Techno-economic and greenhouse gas analyses of lignin valorization to eugenol and phenolic products in integrated ethanol biorefineries. *Biofuels, Bioproducts and Biorefining*, **13**(4), 978-993.

Matson, T.D., Barta, K., Iretskii, A.V., Ford, P.C. 2011. One-pot catalytic conversion of cellulose and of woody biomass solids to liquid fuels. *Journal of the American Chemical Society*, **133**(35), 14090-14097.

McCann, M.C., Carpita, N.C. 2015. Biomass recalcitrance: a multi-scale, multi-factor, and conversion-specific property. *Journal of Experimental Botany*, **66**(14), 4109-4118.

Mendu, V., Shearin, T., Campbell, J.E., Jr., Stork, J., Jae, J., Crocker, M., Huber, G., DeBolt, S. 2012. Global bioenergy potential from high-lignin agricultural residue. *Proc Natl Acad Sci U S A*, **109**(10), 4014-9.

Meng, X., Parikh, A., Seemala, B., Kumar, R., Pu, Y., Wyman, C.E., Cai, C.M., Ragauskas, A.J. 2019. Characterization of fractional cuts of co-solvent enhanced lignocellulosic fractionation lignin isolated by sequential precipitation. *Bioresour Technol*, **272**, 202-208.

Mitra, S. 2014. Mango production in the world–present situation and future prospect. *XXIX International Horticultural Congress on Horticulture: Sustaining Lives, Livelihoods and Landscapes (IHC2014): IV 1111*. pp. 287-296.

Morales, A., Labidi, J., Gullón, P. 2021. Hydrothermal treatments of walnut shells: a potential pretreatment for subsequent product obtaining. *Science of The Total Environment*, **764**, 142800.

Mosier, N., Wyman, C., Dale, B., Elander, R., Lee, Y., Holtzapple, M., Ladisch, M. 2005. Features of promising technologies for pretreatment of lignocellulosic biomass. *Bioresource technology*, **96**(6), 673-686.

Mottiar, Y., Vanholme, R., Boerjan, W., Ralph, J., Mansfield, S.D. 2016. Designer lignins: harnessing the plasticity of lignification. *Current Opinion in Biotechnology*, **37**, 190-200.

Muangmeesri, S., Li, N., Georgouvelas, D., Ouagne, P., Placet, V., Mathew, A.P., Samec, J.S. 2021. Holistic valorization of hemp through reductive catalytic fractionation. *ACS Sustainable Chemistry & Engineering*, **9**(51), 17207-17213.

Mukundan, S., Chowdari, R.K., Beltramini, J. 2021. External Solvent-Free Catalytic Hydrodeoxygenation of Softwood Lignin to Aromatics over Carbon–ZrO2 Supported Ni/MoS2 Catalysts. *Advanced Sustainable Systems*, **5**(3), 2000243.

Nakashima, J., Chen, F., Jackson, L., Shadle, G., Dixon, R.A. 2008. Multi-site genetic modification of monolignol biosynthesis in alfalfa (Medicago sativa): effects on lignin composition in specific cell types. *New Phytol*, **179**(3), 738-750.

Nasrollahzadeh, M., Issaabadi, Z., Varma, R.S. 2019. Magnetic Lignosulfonate-Supported Pd Complex: Renewable Resource-Derived Catalyst for Aqueous Suzuki–Miyaura Reaction. *ACS Omega*, **4**(10), 14234-14241.

Natić, M., Zagorac, D.D., Ćirić, I., Meland, M., Rabrenović, B., Akšić, M.F. 2020. Cold pressed oils from genus Prunus. in: *Cold pressed oils*, Elsevier, pp. 637-658.

Neeraj, M., Aurélie, C., François, R., Stéphane, G., Fabine, S., Giulio, M., Jin-Ping, G. 2018. An Overview on the Use of Lignin and Its Derivatives in Fire Retardant Polymer Systems. in: *Lignin*, (Ed.) P. Matheus, IntechOpen. Rijeka, pp. Ch. 9.

Nguyen, N.A., Barnes, S.H., Bowland, C.C., Meek, K.M., Littrell, K.C., Keum, J.K., Naskar, A.K. 2018. A path for lignin valorization via additive manufacturing of high-performance sustainable composites with enhanced 3D printability. *Science Advances*, **4**(12), eaat4967.

Nunes Ferraz Junior, A.D., Etchebehere, C., Perecin, D., Teixeira, S., Woods, J. 2022. Advancing anaerobic digestion of sugarcane vinasse: Current development, struggles and future trends on production and end-uses of biogas in Brazil. *Renewable and Sustainable Energy Reviews*, **157**, 112045.

Otromke, M., Shuttleworth, P.S., Sauer, J., White, R.J. 2019. Hydrothermal base catalysed treatment of Kraft lignin - time dependent analysis and a techno-economic evaluation for carbon fibre applications. *Bioresource Technology Reports*, **6**, 241-250.

Pang, S. 2019. Advances in thermochemical conversion of woody biomass to energy, fuels and chemicals. *Biotechnology advances*, **37**(4), 589-597.

Panovic, I., Montgomery, J.R., Lancefield, C.S., Puri, D., Lebl, T., Westwood, N.J. 2017. Grafting of technical lignins through regioselective triazole formation on β-O-4 linkages. *ACS Sustainable Chemistry & Engineering*, **5**(11), 10640-10648.

Parchami, M., Agnihotri, S., Taherzadeh, M.J. 2022. Aqueous ethanol organosolv process for the valorization of Brewer's spent grain (BSG). *Bioresource Technology*, **362**, 127764.

Parsell, T., Yohe, S., Degenstein, J., Jarrell, T., Klein, I., Gencer, E., Hewetson, B., Hurt, M., Kim, J.I., Choudhari, H., Saha, B., Meilan, R., Mosier, N., Ribeiro, F., Delgass, W.N., Chapple, C., Kenttämaa, H.I., Agrawal, R., Abu-Omar, M.M. 2015. A synergistic biorefinery based on catalytic conversion of lignin prior to cellulose starting from lignocellulosic biomass. *Green Chemistry*, **17**(3), 1492-1499.

Patel, A.K., Singhania, R.R., Sim, S.J., Pandey, A. 2019. Thermostable cellulases: current status and perspectives. *Bioresource technology*, **279**, 385-392.

Patil, S.A., Chigome, S., Hägerhäll, C., Torto, N., Gorton, L. 2013. Electrospun carbon nanofibers from polyacrylonitrile blended with activated or graphitized carbonaceous materials for improving anodic bioelectrocatalysis. *Bioresource Technology*, **132**, 121-126.

Patria, R.D., Rehman, S., Vuppaladadiyam, A.K., Wang, H., Lin, C.S.K., Antunes, E., Leu, S.-Y. 2022. Bioconversion of food and lignocellulosic wastes employing sugar platform: A review of enzymatic hydrolysis and kinetics. *Bioresource Technology*, 127083.

Patria, R.D., Rehman, S., Yuen, C.-B., Lee, D.-J., Vuppaladadiyam, A.K., Leu, S.-Y. 2024. Energy-environment-economic (3E) hub for sustainable plastic management – Upgraded recycling, chemical valorization, and bioplastics. *Applied Energy*, **357**, 122543.

Pepper, J., Lee, Y. 1969. Lignin and related compounds. I. A comparative study of catalysts for lignin hydrogenolysis. *Canadian Journal of Chemistry*, **47**(5), 723-727.

Perea-Moreno, M.-A., Manzano-Agugliaro, F., Hernandez-Escobedo, Q., Perea-Moreno, A.-J. 2018. Peanut shell for energy: properties and its potential to respect the environment. *Sustainability*, **10**(9), 3254.

Phongpreecha, T., Hool, N.C., Stoklosa, R.J., Klett, A.S., Foster, C.E., Bhalla, A., Holmes, D., Thies, M.C., Hodge, D.B. 2017. Predicting lignin depolymerization yields from quantifiable properties using fractionated biorefinery lignins. *Green Chemistry*, **19**(21), 5131-5143.

Piccinino, D., Capecchi, E., Tomaino, E., Gabellone, S., Gigli, V., Avitabile, D., Saladino, R. 2021. Nano-Structured Lignin as Green Antioxidant and UV Shielding Ingredient for Sunscreen Applications. *Antioxidants*, **10**(2), 274.

Pollard, Z.A., Goldfarb, J.L. 2021. Valorization of cherry pits: Great Lakes agro-industrial waste to mediate Great Lakes water quality. *Environmental Pollution*, **270**, 116073.

Polo, C.C., Pereira, L., Mazzafera, P., Flores-Borges, D.N., Mayer, J.L., Guizar-Sicairos, M., Holler, M., Barsi-Andreeta, M., Westfahl, H., Meneau, F. 2020. Correlations between lignin content and structural robustness in plants revealed by X-ray ptychography. *Scientific reports*, **10**(1), 1-11.

Prieur, B., Meub, M., Wittemann, M., Klein, R., Bellayer, S., Fontaine, G., Bourbigot, S. 2017. Phosphorylation of lignin: characterization and investigation of the thermal decomposition. *RSC advances*, **7**(27), 16866-16877.

Qin, Y., Yang, D., Qiu, X. 2015. Hydroxypropyl Sulfonated Lignin as Dye Dispersant: Effect of Average Molecular Weight. *ACS Sustainable Chemistry & Engineering*, **3**(12), 3239-3244.

Questell-Santiago, Y.M., Galkin, M.V., Barta, K., Luterbacher, J.S. 2020. Stabilization strategies in biomass depolymerization using chemical functionalization. *Nat Rev Chem*, **4**(6), 311-330.

Rabobank. 2023. World Avocado Map 2023: Global Growth Far From Over.

Ragauskas, A.J., Beckham, G.T., Biddy, M.J., Chandra, R., Chen, F., Davis, M.F., Davison, B.H., Dixon, R.A., Gilna, P., Keller, M. 2014. Lignin valorization: improving lignin processing in the biorefinery. *science*, **344**(6185), 1246843.

Rahzani, B., Saidi, M., Rahimpour, H.R., Gates, B.C., Rahimpour, M.R. 2017. Experimental investigation of upgrading of lignin-derived bio-oil component anisole catalyzed by carbon nanotube-supported molybdenum. *RSC Advances*, **7**(17), 10545-10556.

Raj, T., Chandrasekhar, K., Banu, R., Yoon, J.-J., Kumar, G., Kim, S.-H. 2021. Synthesis of γ-valerolactone (GVL) and their applications for lignocellulosic deconstruction for sustainable green biorefineries. *Fuel*, **303**, 121333.

Rajesh Banu, J., Kavitha, S., Yukesh Kannah, R., Poornima Devi, T., Gunasekaran, M., Kim, S.-H., Kumar, G. 2019. A review on biopolymer production via lignin valorization. *Bioresource Technology*, **290**, 121790.

Rehman, S., Yang, Y.S., Patria, R.D., Zulfiqar, T., Khanzada, N.K., Khan, R.J., Lin, C.S.K., Lee, D.-J., Leu, S.-Y. 2023. Substrate-related factors and kinetic studies of Carbohydrate-Rich food wastes on enzymatic saccharification. *Bioresource Technology*, **390**, 129858.

Renders, T., Cooreman, E., Van den Bosch, S., Schutyser, W., Koelewijn, S.-F., Vangeel, T., Deneyer, A., Van den Bossche, G., Courtin, C., Sels, B. 2018. Catalytic lignocellulose biorefining in n-butanol/water: a one-pot approach toward phenolics, polyols, and cellulose. *Green Chemistry*, **20**(20), 4607-4619.

Renders, T., Van den Bosch, S., Koelewijn, S.F., Schutyser, W., Sels, B.F. 2017. Lignin-first biomass fractionation: the advent of active stabilisation strategies. *Energy & Environmental Science*, **10**(7), 1551-1557.

Renders, T., Van den Bosch, S., Vangeel, T., Ennaert, T., Koelewijn, S.-F., Van den Bossche, G., Courtin, C.M., Schutyser, W., Sels, B.F. 2016. Synergetic effects of alcohol/water mixing on the catalytic reductive fractionation of poplar wood. *ACS Sustainable Chemistry & Engineering*, **4**(12), 6894-6904.

Renders, T., Van den Bossche, G., Vangeel, T., Van Aelst, K., Sels, B. 2019. Reductive catalytic fractionation: state of the art of the lignin-first biorefinery. *Current Opinion in Biotechnology*, **56**, 193-201.

Richards, T.E., Kämper, W., Trueman, S.J., Wallace, H.M., Ogbourne, S.M., Brooks, P.R., Nichols, J., Hosseini Bai, S. 2020. Relationships between nut size, kernel quality, nutritional composition and levels of outcrossing in three macadamia cultivars. *Plants*, **9**(2), 228.

Rinaldi, R., Jastrzebski, R., Clough, M.T., Ralph, J., Kennema, M., Bruijnincx, P.C., Weckhuysen, B.M. 2016a. Paving the way for lignin valorisation: recent advances in bioengineering, biorefining and catalysis. *Angewandte Chemie International Edition*, **55**(29), 8164-8215.

Rinaldi, R., Jastrzebski, R., Clough, M.T., Ralph, J., Kennema, M., Bruijnincx, P.C.A., Weckhuysen, B.M. 2016b. Paving the Way for Lignin Valorisation: Recent Advances in Bioengineering, Biorefining and Catalysis. *Angewandte Chemie International Edition*, **55**(29), 8164-8215.

Rivas, S., López, L., Vila, C., Parajó, J. 2021. Organosolv processing of vine shoots: Fractionation and conversion of hemicellulosic sugars into platform chemicals by microwave irradiation. *Bioresource Technology*, **342**, 125967.

Rodriguez, G., Lama, A., Rodriguez, R., Jimenez, A., Guillen, R., Fernandez-Bolanos, J. 2008. Olive stone an attractive source of bioactive and valuable compounds. *Bioresour Technol*, **99**(13), 5261-9.

Rumpf, J., Do, X.T., Burger, R., Monakhova, Y., Schulze, M. 2021. Chapter 4 - Types of lignin, properties, and structural characterization techniques. in: *Lignin-Based Materials for Biomedical Applications*, (Eds.) H. Santos, P. Figueiredo, Elsevier, pp. 105-158.

Schneider, W.D.H., Fontana, R.C., Baudel, H.M., de Siqueira, F.G., Rencoret, J., Gutiérrez, A., de Eugenio, L.I., Prieto, A., Martínez, M.J., Martínez, A.T., Dillon, A.J.P., Camassola, M. 2020. Lignin degradation and detoxification of eucalyptus wastes by on-site manufacturing fungal enzymes to enhance second-generation ethanol yield. *Applied Energy*, **262**, 114493.

Schutyser, W., Renders, T., Van den Bosch, S., Koelewijn, S.F., Beckham, G.T., Sels, B.F. 2018. Chemicals from lignin: an interplay of lignocellulose fractionation, depolymerisation, and upgrading. *Chemical Society Reviews*, **47**(3), 852-908.

Schutyser, W., Van den Bosch, S., Renders, T., De Boe, T., Koelewijn, S.-F., Dewaele, A., Ennaert, T., Verkinderen, O., Goderis, B., Courtin, C. 2015. Influence of bio-based solvents on the catalytic reductive fractionation of birch wood. *Green Chemistry*, **17**(11), 5035-5045.

Shrotri, A., Kobayashi, H., Fukuoka, A. 2017. Chapter Two - Catalytic Conversion of Structural Carbohydrates and Lignin to Chemicals. in: *Advances in Catalysis*, (Ed.) C. Song, Vol. 60, Academic Press, pp. 59-123.

Shuai, L., Amiri, M.T., Questell-Santiago, Y.M., Héroguel, F., Li, Y., Kim, H., Meilan, R., Chapple, C., Ralph, J., Luterbacher, J.S. 2016. Formaldehyde stabilization facilitates lignin monomer production during biomass depolymerization. *Science*, **354**(6310), 329-333.

Si, X., Chen, J., Lu, F., Liu, X., Ren, Y., Lu, R., Jiang, H., Liu, H., Miao, S., Zhu, Y. 2019. Immobilized Ni Clusters in Mesoporous Aluminum Silica Nanospheres for Catalytic Hydrogenolysis of Lignin. *ACS Sustainable Chemistry & Engineering*, **7**(23), 19034-19041.

Sluiter, A., Hames, B., Ruiz, R., Scarlata, C., Sluiter, J., Templeton, D., Crocker, D. 2008. Determination of structural carbohydrates and lignin in biomass. *Laboratory analytical procedure*, **1617**(1), 1-16.

Song, B., Lin, R., Lam, C.H., Wu, H., Tsui, T.-H., Yu, Y. 2021. Recent advances and challenges of inter-disciplinary biomass valorization by integrating hydrothermal and biological techniques. *Renewable and Sustainable Energy Reviews*, **135**, 110370.

Song, W., Du, Q., Li, X., Wang, S., Song, G. 2022. Sustainable Production of Bioactive Molecules from C-Lignin-Derived Propenylcatechol. *ChemSusChem*, **15**(14), e202200646.

Stewart, W.N., Rothwell, G.W. 1993. *Paleobotany and the evolution of plants*. Cambridge University Press.

Stone, M.L., Anderson, E.M., Meek, K.M., Reed, M., Katahira, R., Chen, F., Dixon, R.A., Beckham, G.T., Román-Leshkov, Y. 2018. Reductive catalytic fractionation of C-lignin. *ACS Sustainable Chemistry & Engineering*, **6**(9), 11211-11218.

Sultan, Z., Graca, I., Li, Y., Lima, S., Peeva, L.G., Kim, D., Ebrahim, M.A., Rinaldi, R., Livingston, A.G. 2019a. Membrane Fractionation of Liquors from Lignin-First Biorefining. *ChemSusChem*, **12**(6), 1203-1212.

Sultan, Z., Graça, I., Li, Y., Lima, S., Peeva, L.G., Kim, D., Ebrahim, M.A., Rinaldi, R., Livingston, A.G. 2019b. Membrane Fractionation of Liquors from Lignin-First Biorefining. *ChemSusChem*, **12**(6), 1203-1212.

Sun, Q., Khunsupat, R., Akato, K., Tao, J., Labbé, N., Gallego, N.C., Bozell, J.J., Rials, T.G., Tuskan, G.A., Tschaplinski, T.J., Naskar, A.K., Pu, Y., Ragauskas, A.J. 2016. A study of poplar organosolv lignin after melt rheology treatment as carbon fiber precursors. *Green Chemistry*, **18**(18), 5015-5024.

Sun, Z., Bottari, G., Afanasenko, A., Stuart, M.C.A., Deuss, P.J., Fridrich, B., Barta, K. 2018a. Complete lignocellulose conversion with integrated catalyst recycling yielding valuable aromatics and fuels. *Nature Catalysis*, **1**(1), 82-92.

Sun, Z., Cheng, J., Wang, D., Yuan, T.-Q., Song, G., Barta, K. 2020a. Downstream Processing Strategies for Lignin-First Biorefinery. *ChemSusChem*, **13**(19), 5199-5212.

Sun, Z., Cheng, J., Wang, D., Yuan, T.Q., Song, G., Barta, K. 2020b. Downstream processing strategies for lignin-first biorefinery. *ChemSusChem*, **13**(19), 5199-5212.

Sun, Z., Fridrich, B., De Santi, A., Elangovan, S., Barta, K. 2018b. Bright side of lignin depolymerization: toward new platform chemicals. *Chemical reviews*, **118**(2), 614-678.

Supanchaiyamat, N., Jetsrisuparb, K., Knijnenburg, J.T.N., Tsang, D.C.W., Hunt, A.J. 2019. Lignin materials for adsorption: Current trend, perspectives and opportunities. *Bioresource Technology*, **272**, 570-581.

Taleb, F., Ammar, M., ben Mosbah, M., ben Salem, R., Moussaoui, Y. 2020. Chemical modification of lignin derived from spent coffee grounds for methylene blue adsorption. *Scientific Reports*, **10**(1), 1-13.

Tambunan, B., Saptoadi, H., Syamsiro, M. 2014. A Preliminary Study on Use of Candlenut Shell as a Renewable Source of Energy, Min Indonesia. *Journal of Ocean, Mechanical and Aerospace*, **9**.

Tedeschi, G., Guzman-Puyol, S., Ceseracciu, L., Paul, U.C., Picone, P., Di Carlo, M., Athanassiou, A., Heredia-Guerrero, J.A. 2020. Multifunctional Bioplastics Inspired by Wood Composition: Effect of Hydrolyzed Lignin Addition to Xylan-Cellulose Matrices. *Biomacromolecules*, **21**(2), 910-920.

Thakur, S., Govender, P.P., Mamo, M.A., Tamulevicius, S., Mishra, Y.K., Thakur, V.K. 2017. Progress in lignin hydrogels and nanocomposites for water purification: Future perspectives. *Vacuum*, **146**, 342-355.

Tobimatsu, Y., Chen, F., Nakashima, J., Escamilla-Trevino, L.L., Jackson, L., Dixon, R.A., Ralph, J. 2013. Coexistence but independent biosynthesis of catechyl and guaiacyl/syringyl lignin polymers in seed coats. *Plant Cell*, **25**(7), 2587-600.

Tolbert, A., Akinosho, H., Khunsupat, R., Naskar, A.K., Ragauskas, A.J. 2014. Characterization and analysis of the molecular weight of lignin for biorefining studies. *Biofuels, Bioproducts and Biorefining*, **8**(6), 836-856.

Tse, H.-Y., Yeung, C.S., Lau, C.Y., Cheung, M.Y., Guan, J., Islam, M.K., Anastas, P.T., Leu, S.-Y. 2022. One-pot synthesis to prepare lignin/photoacid nanohybrids for multifunctional biosensors and photo-triggered singlet oxygen generation. *Green Chemistry*, **24**(7), 2904-2918.

Tu, Q., Parvatker, A., Garedew, M., Harris, C., Eckelman, M., Zimmerman, J.B., Anastas, P.T., Lam, C.H. 2021. Electrocatalysis for Chemical and Fuel Production: Investigating Climate Change Mitigation Potential and Economic Feasibility. *Environmental Science & Technology*.

Ubando, A.T., Felix, C.B., Chen, W.-H. 2020. Biorefineries in circular bioeconomy: A comprehensive review. *Bioresource technology*, **299**, 122585.

Usmani, Z., Sharma, M., Awasthi, A.K., Lukk, T., Tuohy, M.G., Gong, L., Nguyen-Tri, P., Goddard, A.D., Bill, R.M., Nayak, S.C., Gupta, V.K. 2021. Lignocellulosic biorefineries: The current state of challenges and strategies for efficient commercialization. *Renewable and Sustainable Energy Reviews*, **148**, 111258.

Van, d.B.S., Koelewijn, S.F., Renders, T., Van, d.B.G., Vangeel, T., Schutyser, W., Sels, B.F. 2018. Catalytic Strategies Towards Lignin-Derived Chemicals. *Top Curr Chem (Cham)*, **376**(5), 36.

Van den Bosch, S., Renders, T., Kennis, S., Koelewijn, S.-F., Van den Bossche, G., Vangeel, T., Deneyer, A., Depuydt, D., Courtin, C., Thevelein, J. 2017a. Integrating lignin valorization and bio-ethanol production: on the role of Ni-Al 2 O 3 catalyst pellets during lignin-first fractionation. *Green Chemistry*, **19**(14), 3313-3326.

Van Den Bosch, S., Renders, T., Kennis, S., Koelewijn, S.F., Van Den Bossche, G., Vangeel, T., Deneyer, A., Depuydt, D., Courtin, C.M., Thevelein, J.M., Schutyser, W., Sels, B.F. 2017b. Integrating lignin valorization and bio-ethanol production: On the role of Ni-Al2O3 catalyst pellets during lignin-first fractionation. *Green Chemistry*, **19**(14), 3313-3326.

Van den Bosch, S., Schutyser, W., Koelewijn, S.F., Renders, T., Courtin, C.M., Sels, B.F. 2015a. Tuning the lignin oil OH-content with Ru and Pd catalysts during lignin hydrogenolysis on birch wood. *Chem Commun (Camb)*, **51**(67), 13158-61.

Van den Bosch, S., Schutyser, W., Vanholme, R., Driessen, T., Koelewijn, S.-F., Renders, T., De Meester, B., Huijgen, W., Dehaen, W., Courtin, C. 2015b. Reductive lignocellulose fractionation into soluble lignin-derived phenolic monomers and dimers and processable carbohydrate pulps. *Energy & environmental science*, **8**(6), 1748-1763.

Vangeel, T., Renders, T., Van Aetst, K., Cooreman, E., Van den Bosch, S., Van den Bossche, G., Koelewijn, S.F., Courtin, C.M., Sels, B.F. 2019. Reductive catalytic fractionation of black locust bark. *Green Chemistry*, **21**(21), 5841-5851.

Vanholme, R., Morreel, K., Darrah, C., Oyarce, P., Grabber, J.H., Ralph, J., Boerjan, W. 2012. Metabolic engineering of novel lignin in biomass crops. *New Phytologist*, **196**(4), 978-1000.

Vincent, S., Prado, R., Kuzmina, O., Potter, K., Bhardwaj, J., Wanasekara, N.D., Harniman, R.L., Koutsomitopoulou, A., Eichhorn, S.J., Welton, T., Rahatekar, S.S. 2018. Regenerated Cellulose and Willow Lignin Blends as Potential Renewable Precursors for Carbon Fibers. *ACS Sustainable Chemistry & Engineering*, **6**(5), 5903-5910.

Vuppaladadiyam, A.K., Vuppaladadiyam, S.S.V., Sikarwar, V.S., Ahmad, E., Pant, K.K., Murugavelh, S., Pandey, A., Bhattacharya, S., Sarmah, A., Leu, S.-Y. 2023. A critical review on biomass pyrolysis: Reaction mechanisms, process modeling and potential challenges. *Journal of the Energy Institute*, 101236.

Walch, F., Abdelaziz, O.Y., Meier, S., Bjelić, S., Hulteberg, C.P., Riisager, A. 2021. Oxidative depolymerization of Kraft lignin to high-value aromatics using a homogeneous vanadium–copper catalyst. *Catalysis Science & Technology*, **11**(5), 1843-1853.

Wang, B., Ran, M., Fang, G., Wu, T., Ni, Y. 2020a. Biochars from Lignin-rich Residue of Furfural Manufacturing Process for Heavy Metal Ions Remediation. *Materials*, **13**(5), 1037.

Wang, H.M., Wang, B., Wen, J.L., Yuan, T.Q., Sun, R.C. 2017. Structural Characteristics of Lignin Macromolecules from Different

Species. *Acs Sustainable Chemistry & Engineering*, **5**(12), 11618-11627.

Wang, J., Xu, Y., Meng, X., Pu, Y., Ragauskas, A., Zhang, J. 2021a. Production of xylo-oligosaccharides from poplar by acetic acid pretreatment and its impact on inhibitory effect of poplar lignin. *Bioresource Technology*, **323**, 124593.

Wang, S., Shuai, L., Saha, B., Vlachos, D.G., Epps, T.H., III. 2018a. From Tree to Tape: Direct Synthesis of Pressure Sensitive Adhesives from Depolymerized Raw Lignocellulosic Biomass. *ACS Central Science*, **4**(6), 701-708.

Wang, S., Zhang, K., Li, H., Xiao, L.-P., Song, G. 2021b. Selective hydrogenolysis of catechyl lignin into propenylcatechol over an atomically dispersed ruthenium catalyst. *Nature Communications*, **12**(1), 416.

Wang, S.Z., Li, W.X., Yang, Y.Q., Chen, X.H., Ma, J.L., Chen, C.Z., Xiao, L.P., Sun, R.C. 2020b. Unlocking Structure-Reactivity Relationships for Catalytic Hydrogenolysis of Lignin into Phenolic Monomers. *Chemsuschem*, **13**(17), 4548-4556.

Wang, T., Li, H., Diao, X., Lu, X., Ma, D., Ji, N. 2023a. Lignin to dispersants, adsorbents, flocculants and adhesives: A critical review on industrial applications of lignin. *Industrial Crops and Products*, **199**, 116715.

Wang, T., Liu, Z., Li, P., Wei, H., Wei, K., Chen, X. 2023b. Lignin-derived carbon aerogels with high surface area for supercapacitor applications. *Chemical Engineering Journal*, **466**, 143118.

Wang, W., Li, X., Ye, D., Cai, L., Shi, S.Q. 2018b. Catalytic pyrolysis of larch sawdust for phenol-rich bio-oil using different catalysts. *Renewable Energy*, **121**, 146-152.

Wang, Y.-Y., Sengupta, P., Scheidemantle, B., Pu, Y., Wyman, C.E., Cai, C.M., Ragauskas, A.J. 2020c. Effects of CELF pretreatment severity on lignin structure and the lignin-based polyurethane properties. *Frontiers in Energy Research*, **8**, 149.

Wang, Z., Deuss, P.J. 2021. Catalytic hydrogenolysis of lignin: The influence of minor units and saccharides. *ChemSusChem*, **14**(23), 5186-5198.

Weerasai, K., Laosiripojana, N., Imman, S., Kreetachat, T., Suriyachai, N. 2021. Reusable alkaline catalyzed organosolv pretreatment and delignification of bagasse for sugar platform biorefinery. *Biomass Conversion and Biorefinery*, 1-11.

Wei, C., Zhu, X., Peng, H., Chen, J., Zhang, F., Zhao, Q. 2019. Facile preparation of lignin-based underwater adhesives with improved performances. *ACS Sustainable Chemistry & Engineering*, **7**(4), 4508-4514.

Wei, W., Wang, B., Wang, X., Ling, R., Jin, Y. 2021. Comparison of acid and alkali catalyzed ethylene glycol organosolv pretreatment for sugar production from bagasse. *Bioresource Technology*, **320**, 124293.

Weng, J.K., Akiyama, T., Bonawitz, N.D., Li, X., Ralph, J., Chapple, C. 2010. Convergent evolution of syringyl lignin biosynthesis via distinct pathways in the lycophyte Selaginella and flowering plants. *Plant Cell*, **22**(4), 1033-45.

Wickham, H. 2016. *ggplot2: Elegant Graphics for Data Analysis*. Springer-Verlag New York.

Wong, S.S., Shu, R., Zhang, J., Liu, H., Yan, N. 2020. Downstream processing of lignin derived feedstock into end products. *Chemical Society Reviews*, **49**(15), 5510-5560.

Xia, Q., Chen, Z., Shao, Y., Gong, X., Wang, H., Liu, X., Parker, S.F., Han, X., Yang, S., Wang, Y. 2016. Direct hydrodeoxygenation of raw woody biomass into liquid alkanes. *Nature communications*, **7**(1), 11162.

Xu, C., Zhang, J., Zhang, Y., Guo, Y., Xu, H., Xu, J., Wang, Z. 2019. Enhancement of high-solids enzymatic hydrolysis efficiency of alkali pretreated sugarcane bagasse at low cellulase dosage by fed-batch strategy based on optimized accessory enzymes and additives. *Bioresource technology*, **292**, 121993.

Xu, L., Mao, W., Huang, J., Li, S., Huang, K., Li, M., Xia, J., Chen, Q. 2016. Economical, green route to highly fluorescence intensity carbon materials based on ligninsulfonate/graphene quantum dots composites: Application as excellent fluorescent sensing platform for detection of Fe3+ ions. *Sensors and Actuators B: Chemical*, **230**, 54-60.

Xu, L., Zhang, J., Zong, Q.-J., Wang, L., Xu, T., Gong, J., Liu, Z.-H., Li, B.-Z., Yuan, Y.-J. 2022. High-solid ethylenediamine pretreatment to fractionate new lignin streams from lignocellulosic biomass. *Chemical Engineering Journal*, **427**, 130962.

Yadav, P., Athanassiadis, D., Antonopoulou, I., Rova, U., Christakopoulos, P., Tysklind, M., Matsakas, L. 2021. Environmental impact and cost assessment of a novel lignin production method. *Journal of Cleaner Production*, **279**.

Yang, W., Liang, J., Ding, Y., Bian, H., Han, J., Dai, H. 2023. A strategy for generating value-added aromatic monomers and lignocellulosic nanofibrils simultaneously from lignocellulosic biomass via polyoxometalate-mediated oxidative fractionation. *Industrial Crops and Products*, **193**, 116215.

Yang, Z., Gleisner, R., H Mann, D., Xu, J., Jiang, J., Zhu, J. 2020. Lignin Based Activated Carbon Using H3PO4 Activation. *Polymers*, **12**(12), 2829.

Yin, L., Leng, E., Fang, Y., Liu, T., Gong, X., Zhou, J. 2020. Effects of KCl, KOH and K2CO3 on the pyrolysis of Cβ-O type lignin-related polymers. *Journal of Analytical and Applied Pyrolysis*, **147**, 104809.

Youssefian, S., Rahbar, N. 2015. Molecular origin of strength and stiffness in bamboo fibrils. *Scientific reports*, **5**(1), 1-13.

Yun, S.I., Kim, S.H., Kim, D.W., Kim, Y.A., Kim, B.-H. 2019. Facile preparation and capacitive properties of low-cost carbon nanofibers with ZnO derived from lignin and pitch as supercapacitor electrodes. *Carbon*, **149**, 637-645.

Zhang, D., Wang, L., Zeng, H., Rhimi, B., Wang, C. 2020. Novel polyethyleneimine functionalized chitosan–lignin composite sponge with nanowall-network structures for fast and efficient removal of Hg (ii) ions from aqueous solution. *Environmental Science: Nano*, **7**(3), 793-802.

Zhang, H., Chen, F., Liu, X., Fu, S. 2018a. Micromorphology influence on the color performance of lignin and its application in guiding the preparation of light-colored lignin sunscreen. *ACS Sustainable Chemistry & Engineering*, **6**(9), 12532-12540.

Zhang, J., Su, Z., Wu, Z., Wang, P., Xiao, F.-S. 2021a. Basic carrier promoted Pt-catalyzed hydrogenolysis of alkaline lignin. *Catalysis Today*, **365**, 193-198.

Zhang, L., Song, Y., Wang, Q., Zhang, X. 2021b. Culturing rhodotorula glutinis in fermentation-friendly deep eutectic solvent extraction liquor of lignin for producing microbial lipid. *Bioresource Technology*, **337**, 125475.

Zhang, N., Tao, P., Lu, Y., Nie, S. 2019a. Effect of lignin on the thermal stability of cellulose nanofibrils produced from bagasse pulp. *Cellulose*, **26**(13), 7823-7835.

Zhang, R., Du, Q., Wang, L., Zheng, Z., Guo, L., Zhang, X., Yang, X., Yu, H. 2019b. Unlocking the response of lignin structure for improved carbon fiber production and mechanical strength. *Green Chemistry*, **21**(18), 4981-4987.

Zhang, S., Zhang, H., Liu, X., Zhu, S., Hu, L., Zhang, Q. 2018b. Upgrading of bio-oil from catalytic pyrolysis of pretreated rice husk over Fe-modified ZSM-5 zeolite catalyst. *Fuel Processing Technology*, **175**, 17-25.

Zhang, Y., Zhao, Q., Li, L., Yan, R., Zhang, J., Duan, J., Liu, B., Sun, Z., Zhang, M., Hu, W. 2018c. Synthesis of a lignin-based phosphorus-containing flame retardant and its application in polyurethane. *RSC advances*, **8**(56), 32252-32261.

Zhang, Z., Harrison, M.D., Rackemann, D.W., Doherty, W.O., O'Hara, I.M. 2016. Organosolv pretreatment of plant biomass for enhanced enzymatic saccharification. *Green chemistry*, **18**(2), 360-381.

Zhang, Z., Song, J., Han, B. 2017. Catalytic Transformation of Lignocellulose into Chemicals and Fuel Products in Ionic Liquids. *Chemical Reviews*, **117**(10), 6834-6880.

Zhang, Z., Terrasson, V., Guénin, E. 2021c. Lignin Nanoparticles and Their Nanocomposites. *Nanomaterials*, **11**(5), 1336.

Zhao, J., Yao, F., Hu, C. 2022. Enhancing enzymatic hydrolysis efficiency of crop straws via tetrahydrofuran/water co-solvent pretreatment. *Bioresource technology*, **358**, 127428.

Zhong, L., Xu, M., Wang, C., Shao, L., Mao, J., Jiang, W., Ji, X., Yang, G., Chen, J., Lyu, G. 2020. Pretreatment of willow using the alkaline-catalyzed sulfolane/water solution for high-purity and antioxidative lignin production. *International journal of biological macromolecules*, **159**, 287-294.

Zijlstra, D.S., Lahive, C.W., Analbers, C.A., Figueirêdo, M.B., Wang, Z., Lancefield, C.S., Deuss, P.J. 2020. Mild organosolv lignin extraction with alcohols: the importance of benzylic alkoxylation. *ACS sustainable chemistry & engineering*, **8**(13), 5119-5131.